Transcriptomics and Immune Profiles of Asymptomatic Filarial-Infected Individuals

Dissertation

zur

Elangung des Doktorgrades (Dr. rer. nat.)

der

Mathematisch-Naturwissenschaftlichen Fakultät

der

Rheinischen Friedrich-Wilhelms-Universität Bonn

vorgelegt von

Alexander Kwarteng

aus

Kumasi, Ghana

Bonn, August 2015

Angefertigt mit Genehmigung der Mathematisch-Naturwissenschaftlichen Fakultät

der Rheinischen Friedrich-Wilhelms-Universität Bonn

Promotionskomitee:

1. Gutachter: PD Dr. rer. nat. Sabine Specht

2. Gutachter: Prof. Dr. Sven Burgdorf

Tag der Promotion: 30.10.2015
Erscheinungsjahr: 2015

Summary

Filarial infections caused by *Wuchereria bancrofti* and *Brugia* species (lymphatic filariasis (LF)) and *Onchocerca volvulus* (onchocerciasis) affect almost 200 million individuals worldwide and pose major public health challenges in endemic regions. Indeed, the collective DALYs (disability-adjusted life years) for both infections is 3.3 million. Infections with these thread-like nematodes are chronic and although most individuals develop a regulated state, a portion develop severe forms of pathology. Mass drug administration (MDA) programmes on endemic populations focus on reducing prevalence levels of people with microfilariae (MF), the worm's offspring in the blood to less than 1%. Although this has been successful in some areas, studies show that MDA will be required for longer than initially conceived. Thus, there is still a requirement for better drugs or vaccines. *W. bancrofti*-infected individuals without pathology (asymptomatic) can be subdivided into two groups that are patent (MF+) or latent (MF-). Patent infections are associated with an immunologically tolerant phenotype state that favours worm survival and in addition does not provoke overt pathology in the host. Latent infections are characterized by the lack of MF in the periphery, despite the presence of adult worms, and their immune profiles show markers of immune-mediated MF control. In *O. volvulus* infection however, the majority of individuals have dermal-residing MF and amicrofilaridermic (a-MF) individuals appear to be the consequences of repeated MDA treatment. Interestingly, recent research revealed that *O. volvulus* endemic areas, with a lowered infection pressure due to MDA, appear to influence bystander responses to *Plasmodium*-derived antigens in community members even if they have not regularly participated in the therapy. Pathology that arises in either filarial infection is associated with dampened regulatory T cell responses (Treg) and IL-10 but elevated Th17 responses. Thus, identifying immune determinants that drive these different infection states has the potential to guide the development of improved anti-filarial drugs and vaccines. In this study, microarray and cellular profiling approaches were used to evaluate gene expression patterns and to reveal genetic pathways specific to *W. bancrofti* or *O. volvulus* infection. Individuals with latent LF infections showed an enhanced gene expression profile, including genes involved in Actin Nucleation by ARP-WASP Complex, Rac signaling, Cdc42 signaling, RhoGD1 signaling, eosinophil effector functions and CD28 signaling in T helper cell pathways. Interestingly, the *Charcot-Leyden crystal/galectin-10* (*CLC/Gal-10*), an immunosuppressive molecule, was among the top commonly expressed genes in both infections and elevated levels were also detected in plasma. Moreover, compared to healthy volunteers, T cells recovered from *W. bancrofti*-infected individuals secreted higher levels of CLC/Gal-10 and were even higher in MF+ individuals: by complementing their elevated Treg responses (Foxp3/IL-10). Latent *W. bancrofti*-infected individuals on the other hand had pronounced Th1, Th2 and Th17 responses. With regards to filarial-specific antibody responses, IgG4, IgE and IgA in plasma were associated with MF+, MF- and endemic normals, respectively. Overall, the transcriptome profiling revealed overlapping genes in both infections: *CLC/Gal-10, ribonuclease RNase A family, 2* (*RNASE2)* and *ribosomal protein S4, y-linked 1* (*RPS4Y1).* Thus, the study offers insight into filarial-specific genes, signaling pathways and

immune determinants, which may be central targets towards the development of new anti-filarial interventions.

Zusammenfassung

Infektionen, die durch die Filarien *Wuchereria bancrofti* und *Brugia* Spezies (Lymphatische Filariose, LF) und durch *Onchocerca volvulus* (Onchozerkose) hervorgerufen werden, beeinträchtigen weltweit nahezu 200 Millionen Menschen. Diese Erkrankungen stellen für die betroffenen endemischen Regionen eine große Herausforderung ihres Gesundheitssystems dar, da insgesamt für beide Erkrankungen zusammen die Anzahl der DALYs (disability-adjusted life years) 3,3 Millionen beträgt. Infektionen mit diesen Fadenwürmern sind chronisch und obwohl die meisten Individuen eine moderate Form der Erkrankung entwickeln, weist doch eine erhebliche Anzahl eine schwerwiegende Pathologie auf. Massentherapiebehandlungen (Mass drug administration, MDA) in Endemiegebieten konzentrieren sich auf eine Reduzierung der Wurmnachkommen, der sogenannten Mikrofilarien (MF), unter ein Transmissionsniveau von 1%. Obwohl die MDA Programme bereits in einigen Gebieten erfolgreich waren, haben Studien gezeigt, dass diese Programme für längere Zeit durchgeführt werden müssen als ursprünglich geplant war. Demzufolge besteht immer noch ein Bedarf an wirksameren Medikamenten oder Impfungen. *Wuchereria bancrofti* infizierte Individuen ohne Pathologie (asymptomatischer Verlauf) können in Abhängigkeit von der Anwesenheit der MF in zwei Gruppen unterteilt werden: patent (MF+) und latent (MF-) infizierte Patienten. Patente Infektionen sind mit einem immunologisch toleranten Phänotyp assoziiert, welcher das Überleben der Würmer begünstigt und zusätzlich eine sichtbare Pathologie des Wirtes verhindert. Latente Infektionen sind trotz der Präsenz adulter Würmer durch ein Fehlen peripherer MF charakterisiert. Latent infizierte Individuen weisen zudem immunologische Marker auf, die mit einer Suppression der Filarientransmission verbunden sind. Im Gegensatz dazu verfügt die Mehrheit der *O. volvulus* infizierten Individuen über MF, die sich in der Haut befinden, während amikrofilaridermische (a-MF) Individuen das Ergebnis wiederholter MDA Behandlungen zu sein scheinen. Interessanterweise haben kürzlich publizierte Forschungsarbeiten gezeigt, dass in *O. volvulus* Endemiegebieten, die einen niedrigeren Infektionsdruck aufgrund wiederholter MDA aufweisen, die Immunantworten gegen *Plasmodium* Antigene beeinflusst werden und zwar auch in Gemeindemitgliedern, die nicht regelmäßig an der Therapie teilgenommen haben. In beiden Filarieninfektionen ist eine Pathologie mit einer verminderten Antwort regulatorischer T-Zellen (Treg) und herabgesetzten IL-10 Spiegeln verbunden, gleichzeitig aber auch mit einer erhöhten Th17 Antwort. Eine Identifizierung immunologischer Faktoren, welche diese unterschiedlichen Infektionszustände bedingen, bietet die Möglichkeit verbesserte Medikamente und Impfungen gegen Filarieninfektionen zu entwickeln. In der vorliegenden Arbeit wurde mit Hilfe von Microarrays und Zellprofilanalyse spezifische Genexpressionsmuster evaluiert, um *W. bancrofti* und *O. volvulus* spezifische Gensignalwege aufzudecken. Individuen mit einer latenten LF Infektion zeigten verstärkte Genexpressionsprofile, darunter Gene, die an der Aktin Nukleation durch den ARP-WASP Komplex beteiligt waren sowie am Signalweg von Rac, Cdc42, RhoGD1, an Effektorfunktionen von Eosinophilen und am Signalweg von CD28 in T-Helferzellen. Interessanterweise war in beiden Infektionen das immunsuppressive *Charcot-Leyden crystal/galectin-10* (*CLC/Gal-10*) Molekül unter den am stärksten exprimierten Genen und dessen erhöhte Spiegel wurden auch im Patientenplasma detektiert. Darüber hinaus konnte gezeigt werden, dass T-Zellen von *W. bancrofti* infizierten Individuen im Vergleich zu denen von gesunden Freiwilligen höhere Mengen von *CLC/Gal-10* sezernierten. Besonders hoch waren

diese Spiegel in MF+ Individuen, was deren erhöhte Treg Antworten (Foxp3/IL-10) ergänzte. Im Gegensatz dazu wiesen latent infizierte *W. bancrofti* Individuen ausgeprägte Th1, Th2 und Th17 Antworten auf. Im Hinblick auf filarienspezifische Antikörperantworten waren MF+ Individuen mit IgG4, MF- Individuen mit IgE und Endemisch Normale mit IgA assoziiert. Ingesamt konnte in beiden Infektionen mit Hilfe der Transkriptomsanalyse folgende überlappende Gene detektiert werden: *CLC/Gal-10, Ribonuclease, RNase A Familie, 2* (*RNASE2)* und *Ribosomales Protein S4, y-linked 1* (*RPS4Y1)*. Somit konnte die vorliegende Studie Einblicke in filarienspezifische Gene, Signalwege und immunologische Faktoren aufzeigen, die zukünftig als zentrale Zielmoleküle bei der Entwicklung neuer Interventionen gegen Filarieninfektionen dienen könnten.

This Thesis is Based on the Following Original Publications and Presentations

Kwarteng A. *et al.,* Patently filarial-infected individuals are characterised with elevated T cell exhaustion markers (*manuscript in preparation*)

Kwarteng A, *et al.,* Transcriptomics in human filariasis reveal increased gene expression in individuals with latent infection (*manuscript in preparation*)

Arndts K, Specht S, Debrah AY, Tamarozzi F, Schulz K, Mand S, Batsa L, **Kwarteng A**, Taylor M, Adjei O, Martin C, Layland L, and Hoerauf A (**2014**): Immuno-epidemiological Profiling of Onchocerciasis Patients Reveals Associations with Microfilaria Loads and Ivermectin Intake on Both Individual and Community Levels *Plos Neglected Tropical Disease* 10.1371/journal.pntd.0002679.

Arndts K, Deininger S, Specht S, Klarmann U, Mand S, Adjobimey T, Debrah AY, Batsa L, **Kwarteng A**, Epp C, Taylor M, Adjei O, Layland LE, and Hoerauf A (**2012**): Elevated Adaptive Immune Responses Are Associated with Latent Infections of *Wuchereria bancrofti*. *Plos Neglected Tropical Disease* 10.1371/journal.pntd.0001611.

Kwarteng A, Debrah, AY, Adjobimey T, Taylor D, Hoerauf A, and Specht S (**2014**): Differential regulation of CLC/Galectin-10 gene and protein in human filarial infections (ImmunoSensation Cluster Conference: poster presentation, Bonn, Germany).

Kwarteng A, Debrah, AY, Taylor D, Hoerauf A, and Specht S (**2014**): Transcriptomics in human filariasis reveal increased gene expression in individuals with latent infection (International Filariasis Meeting: oral presentation, Paris, France).

Kwarteng A, Debrah, AY, Taylor D, Hoerauf A, and Specht S (**2013**): Transcriptomics analysis of human filarial infections (Filarial Immunity Meeting: oral presentation, Paris, France).

Kwarteng A, Debrah, AY, Taylor D, Hoerauf A, and Specht S (**2012**): Protective Immunity in Human Filariasis (Helminths Immunity: poster presentation, Paris, France).

Other Publications & Presentations

Debrah AY, Specht S, Klarmann-Schulz U, Batsa L, Mand S, Marfo-Debrekyei Y, Fimmers R, Dubben B, **Kwarteng A**, Osei-Atweneboana M, Boakye D, Ricchiuto A, Büttner M, Ohene Adjei, Mackenzie C, Hoerauf A (**2015**). Doxycycline leads to sterility and enhanced killing of female *Onchocerca volvulus* worms in an area with persistent microfilaridermia after repeated ivermectin treatment - a randomized placebo controlled double-blind trial. Clin Infect Dis. 61(4):517-26. doi: 10.1093/cid/civ363.

Katawa G, Layland L, Debrah AY, von Horn, Batsa L, **Kwarteng A,** Arriens S, Taylor WD**,** Specht S, Hoerauf A, and Adjobimey T (**2015**): Hyperreactive onchocerciasis is characterised by a combination of Th17/Th2 and reduced regulatory responses. *Plos Neglected Tropical Disease*: 10.1371/journal.pntd.0003414.

Mand S, Debrah AY, Klarman U, Batsa L, Marfo-Debrekyei, **Kwarteng A,** Specht S, Belda-Domene A, Fimmers R, Tayor M, Adjei O, Hoerauf A (**2012**): Doxycycline Improves Filarial Lymphedema Independent of Active Filarial Infection: A Randomized Controlled Trial. Clin Infect Dis. 55(5):621-30. doi: 10.1093/cid/cis486.

Mand S, Debrah AY, Klarmann U, **Kwarteng A**, Specht S, Batsa L, Mante S, Adjei O, Hoerauf A (**2010**): The role of ultrasonography in the differentiation of the various types of filaricele due to bancroftian filariasis *Acta Trop*. Sep; 120 Suppl. 1:S23-32.

Kwarteng A, Debrah AY, Mand S, Batsa L, Marfo-Debrekyei, Specht S, Taylor M, Adjei O, and Hoerauf A (**2011**): Effect of Anti-*Wolbachia* treatment in the pathogenesis of lymphedema development (VW Summer School, oral presentation, KCCR, Kumasi).

List of Abbreviations

Ab	antibody
αCD3/αCD28	anti-CD3/anti-CD28
adj.	adjusted
a-MF	amicrofilaridermia
ALB	albendazole
APC	allophycocyanin
APCs	antigen presenting cells
AW	Ahanta West
BmAg	*Brugia malayi* antigen
BSA	bovine serum albumin
CD	cluster of differentiation
CD107a	lysosomal-associated membrane protein 107a
cDNA	complementary DNA
CFA	circulating filarial antigen
CLC	charcot leyden crystal
cRNA	complementary RNA
CTLA-4	cytotoxic T lymphocytes antigen-4
DALYs	daily adjusted life years
DEC	diethlycarbamazine
DMSO	dimethyl sulfoxide
DNA	deoxyribonucleic acid
EDTA	ethylene diaminetetraacetic acid
ELISA	enzyme linked immunosorbent assay
EN	endemic normal
EPIAF	Enhanced Protective Immunity Against Filariasis
EOMES	eomesodermin
FACS	fluorescence activated cell sorting
FC	fold change
FCS	fetal calf serum
FITC	fluorescein isothiocyanate
FOXP3	forkhead box protein-3
FR3	Filariasis Reagent Research Resource
GATA-3	GATA binding protein-3
Gal-10	galectin-10
GEO	generalised onchocerciasis
GITR	glucocorticoid-induced tumour-necrosis factor receptor
GITRL	glucocorticoid-induced tumour-necrosis factor receptor ligand
GZMA	granzyme A
GZMB	granzyme B
H_2SO4	tetrahydorsulphuric acid

HO	hyperreactive onchocerciasis
HRP	horseradish peroxidase
ICT	immunochromatography test
Ig	immunoglobulin
IgG	immunoglobulin gamma
IFN-γ	interferon gamma
IPA	igenuity pathway analysis
IVM	ivermectin
L3	larvae 3
LAL	limulus amoebocyte lysate
LE	lymphedema
LF	lymphatic filariasis
LPS	lipopolysaccharide
MDA	mass drug administration
mRNA	messenger RNA
MF	microfilariae
mAb	monoclonal antibodies
NaCl	sodium chloride
NE	Nzema East
NEC	non-endemic control
NK	natural killer cells
OD	optical density
OvAg	*Onchocerca volvulus* antigen
Ov	*Onchocerca volvulus*
PBMCs	peripheral blood mononuclear cells
PBS	phosphate buffered saline
PCR	polymerase chain reaction
PD-1	programmed death-1
PE	phycoerythrin
PE-Cy7	phycoerythrin-cyanine 7
PMA	phorbol 12-myristate 13-acetate
RNA	ribonucleic acid
RNASE 2/3	ribonuclease 2/3
RPMI	Roswell Park Memorial Institute
RORC2	retinoic acid receptor-related orphan receptor c2
sCD8	soluble CD8
Spp	species
T-bet	T-box transcription factor
TCR	T cell receptor
TGF-β	transforming growth factor beta
Th1	T helper type 1
Th2	T helper type 2
Th17	T helper type 17

TLRs	toll-like receptors
TMB	3,3'5,5' tetramethybendizine
TNF-α	tumor necrosis factor alpha
TPE	tropical pulmonary eosinophilia
Tr1	regulatory type 1 cells
Tregs	regulatory T cells
VEGFs	vascular endothelial growth factors
VEGFR	vascular endothelial growth factor receptor
Wb	*Wuchereria bancrofti*
WHO	World Health Organisation
°C	degree celsius
g	relative centrifugal force
hr	hour
μg	microgram
mg	milligram
ml	milliliter
ng	nanogram
nm	nanometer
pg	picogram
rpm	revolutions per minute
rt	room temperature
vs	versus

TABLE OF CONTENTS Page

List of Figures

List of Tables

1   INTRODUCTION

1.1   Background

Clinically important filarial nematodes in humans include blood-dwelling *Wuchereria bancrofti*, *Brugia malayi* and *Brugia timori* that elicit lymphatic filariasis (LF), and the tissue-dwelling nematodes *Onchocerca volvulus* and *Loa loa* that induce onchocerciasis and loaisis. In addition, individuals can be infected with Mansonella species, which do not provoke any overt pathological symptoms, reviewed in [1]. Filarial infections present a diverse array of clinical manifestations ranging from asymptomatic conditions to chronic states of severe pathology. Aside from causing debilitating chronic pathologies in some individuals, human filariasis presents a huge economic burden to endemic countries of which the majority are in the developing world [2].

1.2   Epidemiology and distribution of lymphatic filariasis and onchocerciasis

Lymphatic filariasis caused by *W. bancrofti* and *Brugia* spp. is the second largest cause of disability in the world. Depending on the species, disease morbidity may range from transient fevers or immobilizing edema of the limbs (lymphedema) and (hydrocele). Globally, over 1.4 million individuals are at risk of infection (WHO, 2015). In LF, adult worms inhabit lymphatic vessels or scrotal areas and produce their offspring, microfilariae (MF), which are defined as the larval stage, in peripheral blood. LF has recently been estimated to infect 67.88 million individuals living in 73 endemic countries in Africa, Asia, and South America [3]. Current estimates suggest that 36.45 million individuals carry MF+, whilst the same estimates apply to MF- since asymptomatic groups are reported to be 50:50. Individuals presenting chronic pathologies such as lymphedema (dilation of the lymphatic vessels and extravasation of lymph fluid in the surrounding tissues) and/or hydrocele (accumulation of lymph fluid in the tunica vaginalis) affect 16.68 and 19.43 million individuals, respectively [1]. About 90% of lymphatic filariasis cases are caused by *W. bancrofti* with the widest geographical distribution in Africa, while the remaining cases are caused by *Brugia* spp. in Asia. Approximately, 40% of the global disease burden of lymphatic filariasis occurs in Africa, and the global target for the elimination of LF is set for 2020.

Human onchocerciasis caused by *Onchocerca volvulus*, is found exclusively in man. In onchocerciasis, adult worms inhabit subcutaneous regions called nodules and release MF into dermal layers, leading to varying forms of dermal pathology. In addition, infection can lead to

blindness and in the 37 million infected individuals worldwide, over 460,000 lose their vision every year [4] with an estimated burden of about 1 million daily disability adjusted annual life years (DALYs) [5]. Hence, onchocerciasis is noted as the second-leading cause of blindness. About 99% of cases occur in Africa with a few pockets of endemic areas in South America. The disease has been targeted for elimination by 2025. Recently, onchocercal infections have been further implicated in promoting epileptic seizures [6], increasing the repute of the already associated stigma in most endemic regions [7]. The different disease forms are discussed further in the following sections. Areas endemic for onchocerciasis are close to fast flowing rivers or forests depending on the vector host. The pattern of infection may vary between savannah and forest regions. For instance, in most savannah regions, ocular onchocerciasis leads to blindness, whereas in forest areas onchocercal skin diseases predominate. In West Africa, vectors prefer biting lower limbs, resulting in high nodule (made up of connective tissues in which female adult worms aggregate) density and MF load [8]. Both filarial diseases are distributed throughout tropical and subtropical regions with ambient temperatures, which promote breeding of transmission vectors. In most parts of Africa and South America, lymphatic filariasis and onchocerciasis are co-endemic (Figure 1.1). The majority of these infections are found in sub-Saharan Africa.
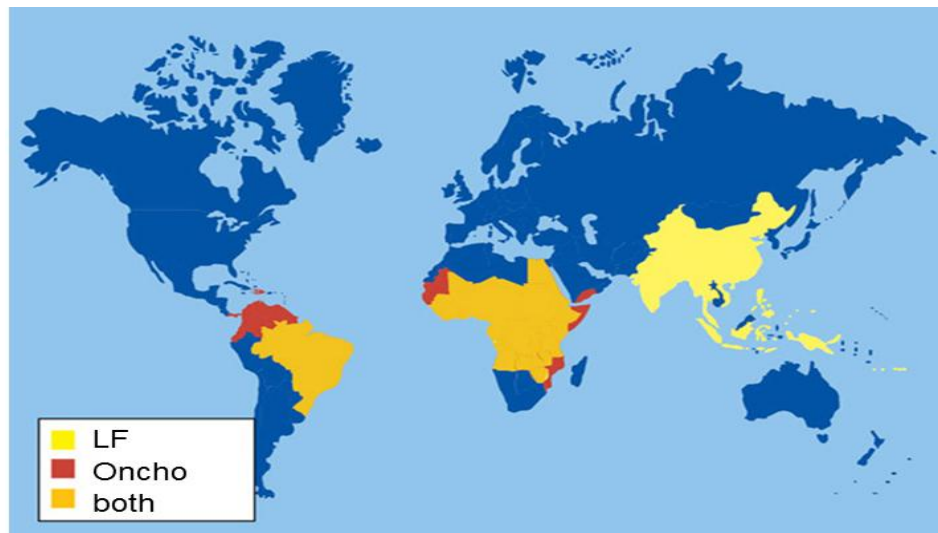
Figure 1.1: Global distribution of lymphatic filariasis and onchocerciasis (Adapted from WHO. http:/who.int/dr/).

1.3 Life-cycle of filarial parasites (*W. bancrofti and O. volvulus*)

The life-cycles of filarial parasites are relatively complex with several distinct morphological stages in both vector and mammalian hosts. The life-cycle begins when an infected female vector takes a blood meal from a human host simultaneously injecting the infective larvae (known as L3) into the dermis (Figure 1.2). The vectors for LF and *O. volvulus* are mosquitoes and black flies, respectively. The vector penetrates the superficial layers of the skin with its proboscis, after which the released larvae begin to migrate and develop into further larval stages and eventually adult worms in the body over a period of 6-12 months. In individuals with LF, mature worms reside in the afferent lymphatic vessels, scrotal regions in men or breast areas of females. In *O. volvulus*-infected patients, worms remain in the dermal regions and form nodules, termed onchocercomas.
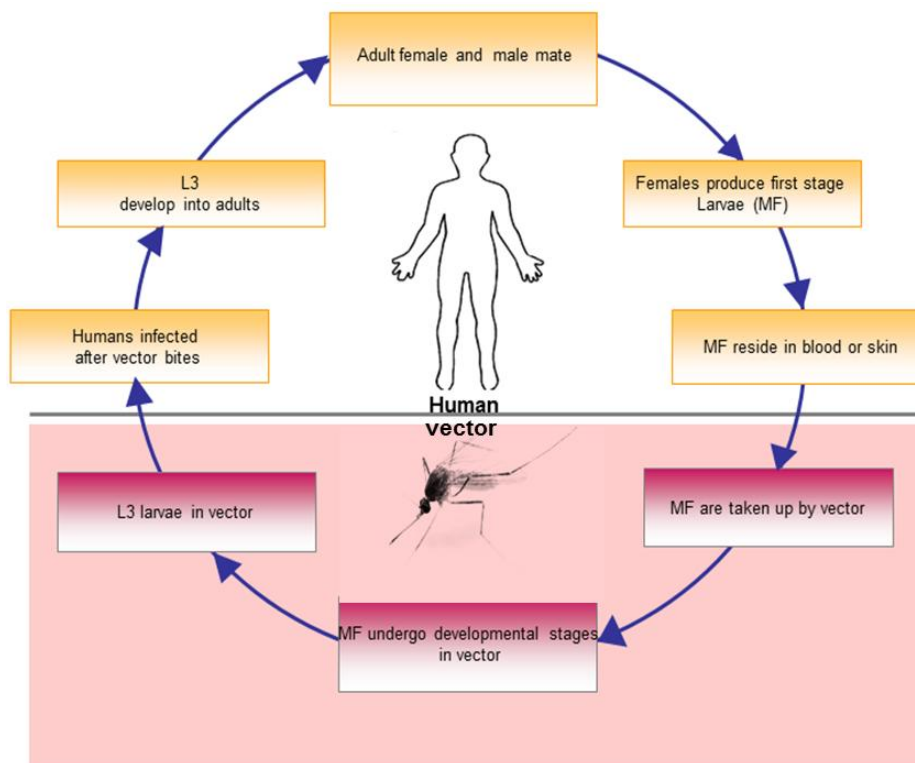
Figure 1.2: Schematic representation of the life-cycle of filarial parasites:
During a blood meal, infective larvae (L3) are transmitted by vectors to the human host. L3 migrate to specific locations (lymphatic vessels, scrotal regions or dermis) and develop into adult male and female worms within 12 months. After mating, females produce first stage larvae (MF), which are released into blood or skin depending on the filarial species and are subsequently ingested, and undergo several developmental stages in the vector (Kwarteng A., University of Bonn, 2015).

In both cases, fertilized female worms produce first stage larvae, termed MF, which have an average lifespan of 1.5 years. On subsequent biting, the specific vector ingests MF, which enters the stomach (10-12 days), where most of them are digested and destroyed. Surviving MF moult twice to become infective larvae [1]. These latter forms migrate to the mouthparts and are transmitted to a human host during a subsequent blood meal. Regarding transmission, circulating MF are the key life-cycle stage of the parasite, therefore identifying strategies that successfully reduce MF levels has the potential to reduce transmission of filarial infections in endemic regions. MF in LF [9] have a periodic state but not in onchocerciasis. Later sections of this chapter focus on current treatment regimens.

1.4   Infection phenotypes in lymphatic filariasis

In endemic regions of LF, only a small portion of infected individuals develop severe clinical conditions, suggesting a differential response to the parasitic nematode. Infection phenotypes range from asymptomatic infections to chronic pathology [10]. Asymptomatic infections can be further categorized into patent (MF+) and latent (MF-) states with the former presenting high levels of circulating MF, whilst the latter are positive for adult worms but amicrofilaremic. These asymptomatic states represent the majority of infected individuals and are associated with an immune permissive state that favours the survival of adult worms to produce MF in an immunologically tolerant host [11]. The presence of peripheral MF and circulating filarial antigen (CFA) in infected individuals defines a patent state. However, the drivers of patent infection are currently unknown and appear to be promoted by several factors; given that predisposition to infection and susceptibility to disease is mediated by genetics [12]. Latent infections on the other hand are a disease phenotype that inhibits productive transmission of the disease and hence represents a dead end for the parasite [13]. However, the mechanism behind this latter phenotype remains unclear including whether female worms are simply infertile or whether the MF are eliminated from the host.

Indeed, these two groups appear in equal proportions in endemic regions, and even after several years of follow-up do not develop severe pathological manifestations [14]. The two populations were distinguished from one another by the development of the CFA test. Recently, Arndts *et al* showed some differences at the cellular level between the two groups [13]. However, much remains to be studied regarding the regulation of the immune responses, particularly at the gene expression level. Individuals presenting pathology, i.e. lymphedema (Figure 1.3 A), elephantiasis (Figure 1.3 B) and hydrocele (Figure 1.3 C) in the extremities are

usually MF negative and have eradicated the worms and the etiological reasons behind the development of these groups are also unclear [15].

In addition to infected persons, there are individuals who fail to show parasitological or pathological manifestations despite prolonged exposure to infections (lack MF and antigenaemia): these are known as endemic normals. Why these individuals fail to acquire filarial infection, despite having lived in endemic regions, suggests a display of protective immunity. Indeed, this subset of individuals is crucial towards understanding the immune disposition of the host. However, the immune mediators and pathways, which drive the different infection states, require further characterization.

(A)   (B)   (C)

Figure 1.3: Developing pathologies in lymphatic filariasis
(A) early stages of LE (B) advanced LE and (C) advanced hydrocele caused by *W. bancrofti*. Images (courtesy of Prof. D.W. Buttner).

1.5   Infection phenotypes in onchocerciasis

In onchocerciasis, two main forms of infection have been categorized: generalized onchocerciasis (GEO) (Figure 1.4 A) and hyperreactive onchocerciasis (HO) (Figure 1.4 B). Individuals with generalized onchocerciasis harbour high worm and MF loads and are associated with a regulatory immune phenotype resulting in the suppression of proinflammatory responses [16]. On the other hand, individuals with hyperreactive forms have dominant inflammatory immune responses [17]. However, between the two polar forms, is another group, without MF, i.e. amicrofilaridermic (a-MF). This phenotype in onchocerciasis may be either from a) pre-patent infection b) no longer fertile worms or c) ivermectin treatment [18].

In onchocerciasis endemic areas, heavy skin MF burdens may induce skin irritations with intense itching and associated dermatitis, as shown in (Figure 1.4 B). In a few individuals, a unilateral dermal pathology can occur which is referred to as sowda. Biopsies from sowda patients show an increased presence of cellular infiltrates believed to mediate MF killing and

clearance. In subjects with a high MF load, MF can invade the conjunctiva, the cornea and posterior regions of the eye. Increasing numbers of degenerating MF in the eye lead to the release of multiple antigens that can induce inflammatory responses through a breakdown of the so-called immune privilege, normally preventing inflammation in the eye [5]. Heavy MF degeneration in the conjunctiva may result in the release of *Wolbachia*, which induces strong immune responses and cellular infiltration leading to visual impairment (Figure 1.4 C) [19]. Chronic inflammation and vascularization eventually results in the opacification of the cornea, hence the colloquial term of infection "river-blindness". As in LF, individuals in *O. volvulus* endemic regions can remain infection free, despite continued exposure to the bites of black flies that may carry the infection: these are also referred to as putative immune.

(A)   (B)   (C)
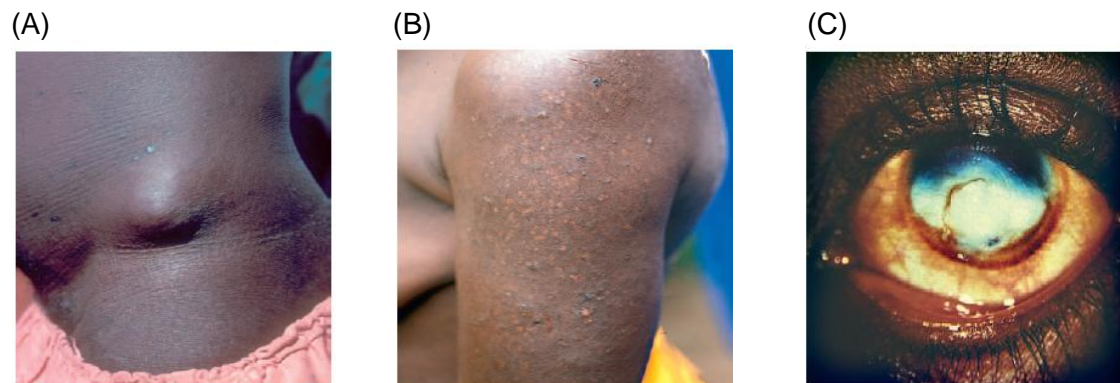
Figure 1.4: Differing forms of pathology in onchocerciasis
(A) *O. volvulus* nodule (GEO)   **(B)** Papular skin lesions (HO)   **(C)** Advanced sclerosing keratitis.
Images (courtesy of Prof. D. W. Buttner).

1.6   Pathogenesis and clinical presentations in lymphatic filariasis and onchocerciasis

In LF, two pathological pathways have been suggested to lead to the development of pathology. The first pathway emphasizes dilatation of lymphatic vessels as the key lesion that precedes the development of clinically evident filariasis [1]. Filarial worms appear to be capable of inducing endothelial cell proliferation and lymphatic dilatation via mechanisms that do not involve lymphatic obstruction. Dilatation may result from host proteins such as vascular endothelial growth factors, angiopoietin and matrix metalloproteinase [20]. In the second pathway, products released from dead or dying adult worms and *Wolbachia* have been shown to trigger innate immune response of the host, resulting in the release of proinflammatory determinants that promote chronic disease [5, 21]. Persistent proinflammatory responses may lead to dilation of

lymphatic vessels, lymphatic obstruction as well as enhanced trafficking of immune cells leading to granuloma formation. In cases where such responses are not regulated, the integrity of the lymphatic vessels may be altered resulting in the accumulation of lymph fluid and extravasation of fluid from neighbouring tissues leading to lymphedema (LE) and/or hydrocele development [15]. The development of lymphedema may take many years and is often characterised with acute dermatolymphangioadenitis (ADLA) due to skin injuries and bacterial infections [22]. According to Dreyer, LE of the limbs can be graded as follows: (1) swelling is reversible overnight, (2) swelling is not reversible overnight, (3) shallow skin folds are reversible, (4) appearance of knobs, (5) knobs and deep skin folds are present, (6) presence of lesions, and (7) patients are unable to perform daily tasks [23]. In contrast to hydrocele patients, LE-affected individuals are more vulnerable to opportunistic microorganisms that may enter the lymphatics through smaller wounds [15]. With regard to hydrocele, grading of dilation is described by Debrah *et al* [24]. Figure 1.3 shows some clinical presentations of LF caused by *W. bancrofti*, which include lymphedema (LE) (A), elephantiasis (advanced LE) (B) and hydrocele (C).

In onchocerciasis, pathology appears in several forms, i.e., skin (dermatitis) and ocular pathology. Grading of dermatitis is described by Murdoch *et al* [25]. While clinically significant onchocerciasis is caused by inflammatory responses to MF in the skin and eye, adult worms initiate nodule formation but these may not induce overt response [1]. Skin pathology normally arises when the host reacts vigorously to MF. Not only are individuals with hyperreactive onchocerciasis characterized by low numbers of parasites but also this infection phenotype has reduced frequencies of nodules. Since structural deformities associated with filarial infections are often not easily reversible, elucidating the mechanisms that promote protective immunity is important.

1.7   Diagnosis of lymphatic filariasis and onchocerciasis

Diagnosis of human filariasis consists of physical examinations and parasitological tests. In endemic areas of LF, knowledge on the periodicity of MF in blood is required for correct sampling. MF are detected in blood smears following standard Giemsa staining after filtering blood to concentrate the MF. To determine the presence of adult worms, CFA tests are used in *W. bancrofti* infection [26] or specific enzyme linked immunosorbent assay ELISA (Og4C3) are performed [27]. CFA tests have shown that in *W. bancrofti* endemic communities there are almost equal proportions of MF+ and MF- individuals and due to the absence of overt clinical manifestations, the latter group remained largely undetected and were excluded from most

previous studies. In infections caused by *Brugia* spp., anti-filarial IgG4-specific ELISA tests are used [28]. Furthermore, the advent of high sensitive ultrasonography (USG) technology has allowed the detection of moving filarial worms, i.e. filarial dance sign (FDS) [29, 30]. The FDS in the scrotal regions of male hosts detects worm nests since the worms remain in the same area for long periods of time [29]. Moreover, Mand *et al* showed that USG is imperative in diagnosing early stages of hydrocele [31]. In recent times, polymerase chain reaction (PCR) assays have become a mainstay diagnostic parameter to detect filarial DNA in blood samples [32]. Recently, computer-based approaches for assessing the motility of larger nematode stages have been developed. This technique works by converting the motion of nematodes through a light-scattering system into an electrical waveform, for the estimation of the number of nematode worms of different forms and sizes [33].

In onchocerciasis, the primary method of diagnosis remains the presence of nodules in the skin. In addition, MF are detected from skin snips and the site of infection for a skin snip depends primarily on geographical area as mentioned in (section 1.2). For example, skin snips are obtained from the iliac crests of patients in Africa [1]. Another diagnostic parameter in detecting *Onchocerca* infection is a diethlycarbamazine (DEC) patch test or Mazzotti reaction [34], which although less invasive, is not very specific compared to the skin skip. Moreover, it can be life-threatening so current applications use topical administrations of DEC that result in locally contained acute dermatitis [35]. Additionally, anti-filarial tests have been developed to detect IgG4 antibodies against recombinant *O. volvulus*; yet it remains to be produced on a commercial scale. Furthermore, qPCR based assays with increased sensitivity and specificity have been developed to detect *O. volvulus* adult worm DNA and skin MF [36].

1.8   *Wolbachia* endosymbionts

Knowledge of the symbiosis between *Wolbachia* and filarial nematodes has grown rapidly in recent years. Phylogenetic analyses, which highlight a co-evolutionary pattern for filarial nematodes and their *Wolbachia*, and molecular evolutionary analyses [37], are both in line with the notion that *Wolbachia* has evolved a mutualistic association with its hosts [38]. Filarial nematodes, which elicit LF and onchocerciasis, live in symbiosis with *Wolbachia* endobacteria that belong to the order Rickettsiales. While in most arthropod-*Wolbachia* interactions, *Wolbachia* have parasitic habits, the endosymbiosis of *W. bancrofti, B. malayi, B. timori* and *O. volvulus* with *Wolbachia* is obligate, suggesting an indispensable role of the endobacteria for fertility, reproduction, larval moulting and the survival of the helminths [39]. *Wolbachia* reside

intracellularly, within host-derived vacuoles, throughout the syncytial hypodermal cord cells [40]; and are transmitted vertically by adult females. They can be detected in ovarian tissues, oogonia, oocytes and developing embryos within the uterus [41]. Several studies have demonstrated that these endosymbionts are a strong inducer of innate immune responses through the activation of macrophages as well as the recruitment of neutrophils. *Wolbachia* achieve this fate through activation of the Toll like receptor 2 (TLR-2) pathway on these innate immune cells and result in increased production of pro-inflammatory cytokines such as IL-6, IL-1β and TNF-α [42, 43]. Elevated levels of these cytokines on the other hand are believed to activate the vascular endothelial growth factor pathways (VEGFs), which have been implicated in filarial pathologies as reviewed in [15]. Interestingly, depletion of *Wolbachia* from all infected filarial nematodes with tetracyclines remarkably precludes or blocks the development of larval and embryonic stages with long term effects on adult worm fertility and viability [44]. This suggests that the nematodes have evolved to become dependent on the bacteria for a diverse range of biological processes.

1.9   Treatment options in lymphatic filariasis and onchocerciasis

In accordance with current mass drug administration (MDA) programs, the mainstay chemotherapy against lymphatic filariasis and onchocerciasis are combinations of ivermectin (IVM), diethlycarbamazine (DEC) with Albendazole (ALB) for LF and IVM for onchocerciasis. The activity of these drugs is seen in their profound ability to kill MF as well as late embryonic stages inside the adult female worms. However, these therapies have little effect on adult worms themselves and therefore, the aim of MDA is to break transmission [1].

Ivermectin is a macrocyclic lactone with broad spectrum activity on parasites. The drug interacts with postsynaptic glutamate-gated chloride channels (GluCl) which results in paralysis of the MF. These targeted proteins (GluCl) are encoded exclusively in genome of Nematoda and Arthropoda, restricting the effects of this IVM to these organisms [45]. In filarial infections, IVM exhibits profound microfilaricidal effects, i.e. it kills MF in the human body [46]. However, observations in *in vitro* settings of *Acanthocheilonema viteae* model system with IVM show a weaker activity compared to the potent killing patterns in parasite infected hosts [46], emphasizing the role of host immune responses in controlling the parasite. Albendazole (ALB) is a carbamate benzimidazole, broad-spectrum anthelminthic drug against flatworms, nematodes and cestodes that inhibits the polymerization of worm β-tubulin and microtubule formation [47].

Whether ALB has demonstrable antifilarial effects is still unclear [48]. But it has been reported to increase compliance of MDA program because of its direct effect on other gastrointestinal helminths.

Finally, DEC is a piperazine derivative, which attacks all life-cycle stages of the filarial parasites, but till date, the exact mechanism of DEC remains to be elucidated. Elsewhere, DEC has been shown to inhibit the cyclooxygenase pathway of parasites resulting in MF death and when administered to infected subjects results in a sharp decline in MF loads and an estimated adulticidal effect of 40% [49]. However, due to its severe adverse effects, DEC is not recommended as MDA in onchocerciasis endemic areas where it may induce local inflammation in subjects with ocular MF [50].

Given the unique activities of each of the above mentioned drugs, specific combination therapies are used in filarial endemic regions. As mentioned above, to treat lymphatic filariasis, IVM or DEC in combination with ALB is used by the global program to eliminate LF (GPELF), whereas IVM is primarily used to treat onchocerciasis. Surprisingly, despite the microfilaricidal effects of these classical antifilarial drugs, they show minimal macrofilaricidal effects [51]. While IVM rapidly eliminates MF, this transmission life-stage has been reported in some endemic communities to reappear after 3 months [52], suggesting that several rounds of treatment are required to bring the MF threshold to a level below which transmission can be successfully interrupted.

As mentioned in section 1.8, *Wolbachia* is essential for the growth and survival of most filarial worms. This endosymbiotic relationship has become the focus of alternative therapy; the application of tetracycline antibiotics from field studies has shown that 200 mg of doxycycline therapy for 4-6 weeks eliminates adult worms [53, 54]. Doxycycline is the first and, so far, only macrofilaricidal drug against onchocerciasis. Recent studies have also shown that rifampicin exhibits macrofilaricidal activities [55]. More importantly, Mand *et al* have observed that doxycycline has an additive effect in patients without active infection since it demonstrated exceptional anti-proliferative activity leading to improved pathology conditions [24, 56]. This suggests the use of this drug as an effective tool for individuals drug treatment in filarial endemic areas [57, 58]. While doxycycline application in field studies has shown macrofilaricidal effects compared to the conventional antifilarial drugs [54], it is obstructed by contraindications since it is not suitable for pregnant women or children under 9 nine years. This coupled with current reports of IVM resistance in some endemic communities [59] calls for the development

of new and effective antifilarial drugs or vaccines if the goal to eliminate LF and onchocerciasis is to be achieved by 2020 and 2025, respectively. Infections of filarial nematodes are successful because they have the ability to initiate regulatory pathways. Bypassing this regulation may be key to developing an effective vaccine for filarial control. This will require a complete appreciation of how the parasite induces regulation and identification of the targets and processes that mediate protective responses. Such an approach could in the first place protect individuals since proteins that are expressed during infection may represent the most likely protective vaccine components [60]. In the following section, the different immune profiles in *W. bancrofti*- and *O. volvulus*-infected individuals are reviewed.

1.10 Immune profiles in filarial infected individuals

The immune response against filarial nematodes involves a remarkable range of innate and adaptive pathways. In fact, persons living in LF and onchocerciasis endemic areas are challenged with persistent exposure to incoming larvae, filarial derived products from both living and dead worms as well as to *Wolbachia* endosymbionts. While these factors induce innate immune responses, which proceed to activate and shape adaptive immunity, the intensity of the host's reactivity has been associated with the infection phenotype.

As with many infections, dendritic cells and macrophages serve as the first line of defence and react strongly to filarial nematodes as well as their derived products in order to activate the appropriate adaptive immune responses to clear invading parasites. The activation of innate cells is provoked by pathogen receptor recognition through an array of different receptor such as the Toll-like receptor (TLR) or C-type lectin families. Previous studies have demonstrated that filarial extracts trigger TLR-2 and TLR-6 [61], which results in the secretion of cytokines, such as IL-6 and TNF-α by macrophages. Alternatively, macrophages that are activated by IL-4 and IL-13 may develop an alternative phenotype characterized by the production of arginase-1. The catalytic properties of arginase-1 promotes the repair of tissues damaged by helminths and coincides with the immunoregulatory state exhibited in MF+ individuals [62].

Innate immunity comprises several other cell types including natural killer cells, neutrophils and eosinophils. Natural killer cells are large lymphocytes that are principally cytotoxic but have a high immunomodulatory capacity as well since they secrete mediators that influence immune responses when activated. NK cells play an important role during infection, especially toward intracellular microorganisms. Although a recent study has shown that both CD16^{bright} and

11

CD56^{dim} and CD16^{dim} and CD56^{bright} NK cell populations are higher in EN when compared to individuals with generalized onchocerciasis and hypereactive groups [17], their characterisation in other filarial infections and their function requires further study. Granulocytes are generated from hematopoietic stems cells and subsequently differentiate into myeloid progenitor lineages. In fact, in circulating leucocytes of healthy humans, granulocytes consist of approximately 50% neutrophils, whereas eosinophils and basophils make up 2-5% and 1%, respectively. Largely these cells are considered as friends or foes of helminths because they are normally induced during helminth infections [63]. The role of granulocytes in filariasis appears to be diverse. They are believed to either promote protective immunity or even facilitate parasite establishment. Interestingly, eosinophils are not only associated with helminth infections but are hallmarks of allergic responses, asthma and viral infections too. Peripheral eosinophil counts may reach up to 75% during filarial infections and can induce tropical pulmonary eosinophil (TPE) in *W. bancrofti*- and *B. malayi*-infected individuals. Eosinophils contribute to the destruction of helminths by antibody-dependent cytotoxicity [64]. Activated eosinophils release granule proteins, such as ribonuclease (RNAS2 and RNASE3), Eosinophil Cationic Protein (ECP), Major Basic Protein (MBP) and Eosinophil Peroxidase (EPO). Studies in EPO and MBP knockout mice have demonstrated that, through their granule contents, eosinophils facilitate *Litomosoides sigmodontis* larval clearance since in their absence worms develop faster [65]. Others have suggested that eosinophils are essential for early worm development [66].

In addition to the above granules, activated eosinophils release the carbohydrate binding proteins called galectins. Galectins are β-galactoside-binding animal lectins, and are characterized by conserved amino acid sequences in the carbohydrate recognition domain (CRD) with high affinity for β-galactosides [67]. Currently, 15 galectins have been characterised and although primarily localized in the cytoplasm or extracellular space [67], under certain physiological conditions, they can translocate into the nucleus or associate with intracellular vesicles. While galectins may not have specific individual receptors, each can bind to a set of cell-surface glycoproteins containing suitable oligosaccharides through lectin-carbohydrate interactions [68]. Galectins are commonly produced by eosinophils, however, recent studies have demonstrated that the Charcot Leyden crystal protein also referred to as galectin-10 (CLC/Gal-10) is highly expressed in human CD25^{+} Treg cells, indicating that the expression of this protein is involved in regulatory T cell functions [69].

In *O. volvulus* infection, eosinophil infiltration in nodules is dependent on MF released from adults worms [70] and has been shown to target skin-residing MF, which possibly reflects their

functional role in host defence strategy [71]. As with most infections, neutrophils are among the first cells to be recruited during filarial infections. Similar to eosinophils, studies in BALB/c laboratory mice have shown that neutrophils control filarial nematodes in an IL-5 dependent manner: *L. sigmodontis* infections in mice with an impaired capacity to activate neutrophils exhibited diminished parasite clearance [72]. In onchocerciasis, neutrophils are recruited to the site of infection and are influenced by the presence of *Wolbachia* endosymbionts [45]. In that study, neutrophils were found to accumulate around nodules obtained from placebo treated subjects compared to doxycycline treated counterparts. Basophils are a key cell type in the initiation of Th2 immune response since they produce IL-4. Studies in mice with *L. sigmodontis* infection showed that IL-4 is produced by basophils and that depletion of basophils resulted in drastic reduction in eosinophils and CD4$^+$ T cell proliferation [73].

Since filarial infections are chronic, much research has focused on adaptive immune responses (T and B cell responses). CD4$^+$ helper T cells form the majority of T lymphocyte responses and following activation differentiate into effector Th1, Th2, Th17 and regulatory T cell subsets depending on the source of antigen and surrounding cytokine milieu as reviewed in [74]. These T helper cell lineages are regulated by T-bet (Th1), GATA-3 (Th2), RORC2 (Th17) and FOXP3 (Tregs), respectively. These distinct effector T cell subsets play diverse roles in mediating immune responses through the secretion of cytokines and interactions with different cell types.
In LF, the immune response of MF+ individuals are characterised by T cell hypo-responsiveness which is accompanied by diminished production of IFN-γ and IL-2 [75]. In addition, when compared to individuals with chronic pathology, associations have been observed regarding the reduced frequencies of parasite-specific T and B cells and an overall immune suppression [76]. This hypo-responsiveness in MF+ persons is mediated by factors, such as IL-10, TGF-β as well as increased regulatory T cells. In fact, PBMCs from MF+ individuals spontaneously release antigen-specific IL-10 compared to pathology patients [77]. When comparing MF+ and MF- individuals in bancroftian filariasis, our recent studies showed that MF- individuals presented elevated adaptive immune responses, such as TNF-α and IL-17 production compared to MF+ subjects [13]. Further studies in *O. volvulus* infection showed that MF+ individuals or generalized onchocerciasis (GEO) exhibit mild skin dermatitis [5] with increased IL-10 levels compared to a-MF individuals [18]. Indeed, CD4$^+$ T cells have been shown to be the main source of IL-10 in onchocerciasis [78]. Additionally, the promoter haplotype of IL-10 has been shown to influence filarial-specific proliferative capacity [56]. Furthermore, Korten *et al* described that a-MF individuals present a somewhat low hypo-

responsiveness state as reflected in the diminished production of TGF-β accompanied with moderate Th2 responses [79] and that repeated ivermectin treatment in a-MF subjects was unable to restore the Th1-Th2 balance [80].

While immune responses in individuals with asymptomatic infections may be somewhat regulated (albeit with mild disease), chronic pathology patients are characterised by heightened proinflammatory responses [81]. Previous studies showed that higher frequencies of Th1 and Th17 cells were associated with lymphedema patients, alongside reduced MF load and a dampened regulatory T cell phenotype [82]. The apparent sustained proinflammatory condition in pathology patients is believed to be exacerbated by the presence of *Wolbachia*, (see section 1.8) which are potent activators of innate immune responses via TLR activation [83]. Indeed these endosymbionts promote increased production of proinflammatory cytokines that can further instigate the induction of vascular endothelial growth factors and their receptors (VEGFs/VEGFR); factors known to be linked with lymphangiogenesis and vascular permeability leading to filarial pathology [20, 56, 84].

In *O. volvulus* infection, sowda patients appear to have a very effective defence mechanism which is able to kill the worms albeit at the expense of the host's immune system. Therefore, while this approach is necessary, future investigations underlying such scenarios are warranted. More recently, studies in onchocerciasis showed a strong association of Th2 and Th17 responses in individuals presenting hyper-reactive onchocerciasis (HO) [17]. In that study, HO patients presented a reduced regulatory phenotype when compared to GEO individuals, and it was shown that in comparison to infected individuals, EN exhibited a pronounced Th1 phenotype since the frequency of IFN-γ producing CD4$^+$ T cells and released IFN-γ upon filarial-specific re-stimulation of PBMCs were both elevated. As mentioned above, this group remains infection-free, despite permanent exposure to biting vectors.

T helper cell responses are controlled by regulatory T cells and the induction of helminth-specific Treg responses has been the focus of many filarial studies in man and mouse [85, 86]. Almost a decade ago a major stride was made in the field of filarial regulatory T cell biology when Satoguina *et al* demonstrated that Tr1 clones in *O. volvulus*-infected subjects produced elevated amounts of IL-10 and TGF-β when stimulated with filarial-specific antigens [87]. Regulatory T cell subsets can modulate responses through a number of different mechanisms such as cell-cell contact, through increased expression of glucocorticoid-induced tumour-necrosis factor receptor-related protein (GITR) or cytotoxic T lymphocyte antigen 4 (CTLA-4) or

via the secretion of regulatory cytokines (like IL-10 and TGF-β) [88]. Further *in vitro* studies from Satoguina *et al* found that GITR-GITRL interactions between B cells and Tregs were necessary to stimulate IgG4 production from B cells, which was also dependent on TGF-β, suggesting that the amount of circulating IgG4 in MF+ persons may reflect enhanced Treg function [89]. Interestingly, the contents of nodules from GEO individuals also reflects this pattern since immunohistochemistry showed increased IL-10, TGF-β, FOXP3 and IgG4 expression[90]. Interestingly, nodules from sowda individuals had very little FOXP3 and regulatory cytokines showing that within the nodules themselves the peripheral regulatory profiles in the different *O. volvulus*-infected groups are in play. [55]. Therefore, in MF+ individuals the induction of IgG4, elevated IL-10 and a skewed balance between Th1 and Th2 immunity and regulatory T-cell networks represent the major mechanisms used by filarial parasites to evade destruction and prevent the onset of severe pathology [89], and in doing so, the host tolerates high worm burden.

Tregs may also mediate cellular responses through the release of granzymes. Granzymes are serine proteases found in the granules of NK cells and T lymphocytes in addition to regulatory T cells and are associated with important immune functions and surveillance. There are five granzymes in humans, among which, granzyme A (GZMA) and granzyme B (GZMB) are the most abundant and well-characterized [91]. Conventionally, GZMA and GZMB kill cells via the activation of cell death pathways during viral or other intracellular infections [92]. Studies have shown that other immune cells, such as macrophages [93] and regulatory T cells [94] secrete GZMA/GZMB. In fact, GZMB-producing Tregs have been found to suppress antigen-specific CD8$^+$ T cells in viral infection [95]. Whether a similar suppression of CD8$^+$ T cells by Treg exists in filarial models remains unclear although recent studies in *L. sigmodontis*-infected laboratory mice have also shown that GZMB enhanced susceptibility, whilst GZMA promoted resistance to infection [96].

Aside from T helper cells and B cells, cytotoxic CD8$^+$ T cells are also vital members of adaptive immunity. Prominent in cases of infection by intracellular pathogens, the role of CD8$^+$ T cells in promoting protective immunity is well established in protozoan infection as reviewed in [97]. However, paucity of information exists on the functions of CD8$^+$ T cells during multicellular parasites, such as filarial nematodes. Previous work has documented a lower proportion of CD8$^+$ T cells in PBMCs of patently-infected LF individuals when compared to chronically infected individuals [98]. Furthermore, increased levels of CD8$^+$ T cells have been found in limb biopsies of patients suffering from chronic LF infection when compared to asymptomatic

individuals [99]. In onchocerciasis, elevated frequencies of CD8^{+} T cells were observed in EN individuals when compared to those presenting GEO [17]. Chronic infections are known to induce exhaustion on CD8^{+} T cells, thus impairing their effector activity. For example, chronic viral infections have been shown to impair viral specific-CD8^{+} T cell responses because of increased expression of inhibitory markers, such as programmed death cell, PD-1 [100, 101]. While the phenotypic characterization of CD8^{+} T cell subtypes is highly advanced, little is known about their activity in filarial infections. It is also unclear whether filarial infections also give rise to CD8^{+} T cell exhaustion given the general ability of helminths to suppress host immune responses in order to promote their survival. Alternatively, CD8^{+} T cell responses could be suppressed by the regulatory responses induced by the helminth. In schistosomiasis, a chronic helminth infection that affects the liver, co-infection with hepatitis C virus leads to exaggerated pathology and elevated viral titres. Recent findings have also shown that this cohort has elevated Granzyme B suppressing cells and perhaps this stronger activation of Treg suppresses essential CD8 responses that are required for controlling the infection [102].

As mentioned above, B cell responses are the other important branch of the adaptive immune system. In addition to cytokine production and antigen presentation, B cells can differentiate into educated plasma cells and produce immunoglobulins (Igs). Elevated levels of IgE is a hallmark of helminth infections and since IgG4 and IgE respond through the same receptor, studying the ratio of these two Igs in human filarial infections revealed that IgG4 is predominant in asymptomatic LF infected MF+ persons when compared to latent individuals [103]. This scenario also reflected studying GEO and HO group [89, 104]. Thus, alongside IL-10 and regulatory T cells, the production of IgG4 is linked to a regulated immune response in filarial-infected patients [89]. In LF, individuals with pathology have elevated levels of filarial-specific IgG1 antibodies, whilst the levels of IgG2 and IgG3 were lowly expressed in MF+ subjects [105]. In endemic normals, while increased levels of plasma IgG1 and IgG2 have been observed, the amount of IgG4 was reduced when compared to MF+ individuals [106]. Recently, studies in India have associated filarial-specific IgA, (an Ig associated with mucosal immunology) expression with protective immunity since higher levels were measured in EN when compared to individuals with asymptomatic LF infection [107]. However, the mechanisms underlying the function of IgA in filarial infection remain to be understood.

1.10.1 Immunomodulation in filarial infections

Filarial nematodes have an inherent ability to induce Th2 responses characterised by IL-4, IL-5 IL-19, IL-10 and IL-13, increased eosinophilia, elevated IgE and IgG4 [103]. Apart from the fact that Th2 responses elicited by nematode parasites is a stereotypic response of the host, the initiation, progression and maintenance of this response requires interaction with many other immune cells, such as antigen presenting cells, lymphocytes and granulocytes [108]. More interestingly, host-parasite interactions may eventually result in a myriad of modulated immune responses such as the expansion of Tregs, regulatory B cells, alternatively activated macrophages and other suppressive subsets such as myeloid suppressive dendritic cells [109, 110]. Additionally, filarial nematodes have been shown to suppress dendritic cell maturation and function [75] such as the down-regulation of Toll-like receptors on APCs and T cells [111]. This modulation of immune responses by filarial nematodes seems to have several benefits for individuals living in endemic areas, since many infected persons are protected from developing allergy and asthma [112] giving credence to the hygiene hypothesis. Similarly, in experimental models, mice exposed to nematode parasites were less likely to develop Th1 mediated diseases as reviewed in [113]. However, since filarial infections induce a state of unresponsiveness, this potentially impacts immune responses to non-filarial antigens, i.e. bystander antigens and research has shown that this modulation occurs in an IL-10 and TGF-β dependent manner [114]. This scenario therefore, may pose a challenge for the effectiveness of vaccination programs in helminth endemic regions.

1.11 Genetic associations in filarial infections

Heterogeneity characterizes filarial infections and disease states. Such phenomenon appears to be driven by several factors, amongst which is host immunogenetics. There are only a limited number of reports that correlate host genetics with a predisposition of filarial infections and/or disease. Studies in human onchocerciasis by Hoerauf *et al*, for example showed that the IL-13 variant, Arg110GIn was significantly associated with sowda patients, whilst the frequency of the variant was remarkably reduced in individuals with GEO [115]. In that study, IL-13 was established as an essential player in Th2-like immune reactions in *O. volvulus* infection. Furthermore, a significant association has been revealed between VEGF-A gene promoter polymorphism and increased susceptibility for hydrocele development [24]. In individuals with *W. bancrofti* infection, Debrah *et al* showed that, compared with asymptomatic individuals, chronic pathology patients possessed different single nucleotide polymorphism (SNPs) for TGF-

β, indicating that genetic traits may also be responsible for these excessive reactions observed in patients with pathology [116]. Recently, significant associations were revealed in soluble plasma levels of tumour necrosis factor receptor II (TNFR-II) and endothelia-1 (ET-1) with lymphedema and hydrocele cases, respectively [117]. In that study, polymorphism at codon 196 of the TNFR-II resulted in an amino acid change of methionine to arginine. While in general, immunological responses are genetically mediated [118] and fairly established in individuals with filarial pathology, the contribution of host genetics, i.e. nature and pattern of gene regulation and expression that lead to the development of patent and latent infection phenotypes are yet to be characterized.

1.11.1 Transcriptomics

Blood serves as an integrative tissue whereby its cells and associated signaling and cytokine networks relay or enhance the contribution made by sites of infection or tissue damage, to effect protection or cell injury repair responses. Infections not only elicit but also modify, in a pathogen specific manner, immune inflammatory responses at both the infected cell and the systemic host response level. Systemic responses can be seen in altered cytokine levels, specific lymphocyte responses and alterations in host RNA phenotype in response to infection. Such biological pathways provide a central level of physiological organization.

The transcriptome is the total set of RNA species, including coding and non-coding RNAs (ncRNAs), that are transcribed in a given cell type, tissue or organ at any given time under normal physiological or pathological conditions. The study of the transcriptome, termed transcriptomics [112], represents a promising technique for elucidating and interpreting the mechanistic role of host gene expression in the pathogenesis of infectious diseases. The approach, based on the large-scale measurement of mRNA, has become the method of choice among the emerging technologies of so-called "functional genomics", primarily because this method offers a more comprehensive view of what is really happening in the cell [120]. The mRNA transcriptome diversity and the abundance of the transcripts, then characterizes a cell at a particular time or under a particular condition. Thus, by comparing transcriptomes under different conditions, i.e. infected vs control, differences in the abundance of transcripts may become associated with changes in disease phenotype. Moreover, such studies may reveal the functional roles of these transcripts, thereby providing more insights into molecular mechanisms of infection and allowing identification of distinct gene expression profiles associated with the outcome of infection.

Gene expression is the process by which genomic information is turned into proteins [121] and is divided into two main steps: transcription and translation. In transcription, portions of DNA sequences are copied into molecules of messenger-RNA (mRNA) (Figure 1.5). RNA polymerase and transcription factors are the main players leading this process. The next step is translation into protein, which occurs on ribosomes, macromolecular complexes composed of proteins and RNA. Thereafter, the mRNA sequence is read by the ribosome, codon by codon, in order to produce polypeptide chains. When the translation is completed, the mature protein is released by the ribosome. Translation of mRNAs is regulated by these regions, thus making them particularly important.
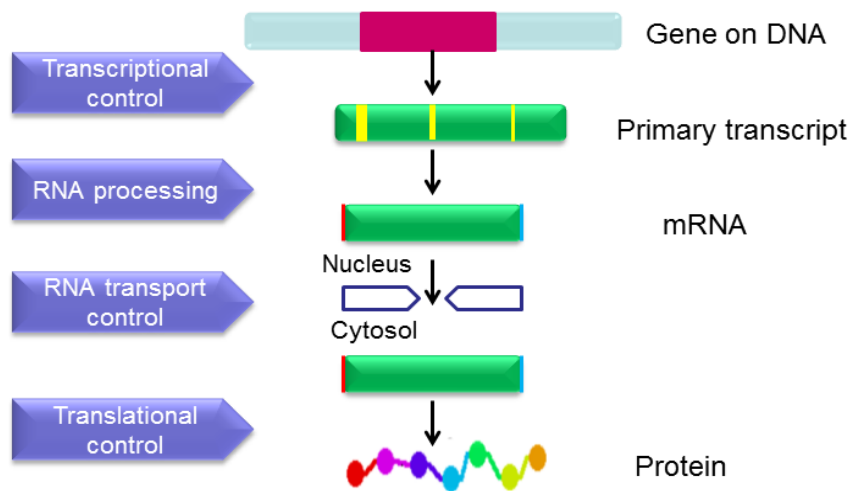
Figure 1.5: Gene expression of eukaryotic DNA
This occurs when an RNA polymerase II unwinds the double stranded DNA helix to generate primary transcripts. This is further processed via splicing into mRNA species, which finally translocates to the cytosol where protein synthesis occurs (Kwarteng. A, University of Bonn, 2015).

Microarray technology is a system used to evaluate genomic expression. This technique offers a snapshot of the entire genome with a resolution that would have been inconceivable some years ago. Microarrays have identified several disease associated biomarkers and hidden underlying networks as observed in bacterial [122] and viral infections [123]. In terms of human filarial infections, large scale microarray surveys have not been performed. A study on individuals infected with *Loa loa* revealed that CD4^{+} and CD8^{+} T cells-associated networks and molecules are highly regulated in chronic infected individuals compared to subjects without

chronic infection [124]. To date, no survey on *W. bancrofti* or *O. volvulus* patients have been performed and as described in the section below, was a primary focus of this thesis work.

1.12 Aims and objectives of the study

Lymphatic filariasis and onchocerciasis pose major public health concerns and socioeconomic problems across the tropics, despite considerable effort to reduce disease burden or regionally eliminate the infection. Presently, abundant evidence shows the existence of immunity in hyper-endemic areas where a proportion of individuals live for many years with constant exposure to filarial infection yet never present either clinical or parasitological signs of infection or even when infected are able to induce an immune response that kills the transmission stage of the parasite (MF). However, knowledge that points to such protective immune responses is still elementary and for the past years has depended heavily on by-products of serological studies. Indeed, several studies have focused mainly on the association between immunology and the induction of pathology [20], but whether there are differences in host gene expression associated with filarial infections and/or as to what extent the differences in gene expression fall into distinct biological categories remains to be delineated. Thus, the molecular determinants at the transcriptome level that drive latent and patent filarial infection states are elusive and remain to be studied. Therefore, there is a need for a comprehensive investigation of the host-parasite interactions at the genomic level, alongside profiling the cellular immune responses of individuals presenting the various filarial infection phenotypes. Hence, this study investigated differentially expressed genes that point to protective immunity during *W. bancrofti* and *O. volvulus* infections. Additionally, it examined immune signaling pathways measured in whole blood at the mRNA level to distinguish different infection phenotypes. These studies complemented studies on immunological characteristics of peripheral blood mononuclear cells (PBMCs) from MF+ and MF- individuals as well as endemic normals under *in vitro* conditions. The study further investigated *in vitro* T cell subpopulations (CD4$^+$ and CD8$^+$ T cells) from MF+ and MF- *W. bancrofti*-infected individuals as well as uninfected controls. Further, a characterization of GZMA and GZMB expressing CD4$^+$ and CD8$^+$ T cells in *W. bancrofti*-infected was performed since previous studies in the murine filarial model have highlighted their potential to influence filarial infection outcome. In addition, the study assessed the total and filarial-specific immunoglobulin responses in *W. bancrofti* individuals in order to establish which antibody contribute to protection or immunosuppression. Collectively, using comprehensive transcriptomics in specimens from individuals exposed to filariae but protected from chronic

pathology might provide information that can be mined to identify new vaccine candidates. Additionally, the study would give a hint which immune determinants or molecules are important in supporting latency as well as which molecules could be key targets for future studies with regards to the development of new therapeutic strategies as well as control interventions.

2 MATERIALS AND METHODS

2.1 Patients, Materials and Methods

2.1.1 Ethical clearance

Informed consent was obtained from all study participants after a careful explanation of study procedures and purposes in their local dialect (Akan). Ethical clearance for this study was given by the Committee on Human Research, Publication and Ethics of The Kwame Nkrumah University of Science and Technology (KNUST), Ghana; the Ethics Commission at the Rheinische Friedrich-Wilhelms-University of Bonn, Germany; and the University of Edinburgh, UK. Permission to conduct studies in the selected communities of LF and onchocerciasis endemic areas were sought from the Districts Health Directorate of Ahanta West and Nzema East in the Western Region, Ghana as well as the Adansi South and North of the Ashanti Region, Ghana. Individuals recruited for this study entitled "Enhanced Protective Immunity Against Filariasis (EPIAF)", (http://www.filaria.eu/projects/projects/epiaf.html) included adult men and women of age (18-55). Exclusion criteria for both studies were abnormal levels of renal and hepatic profiles (creatinine>1.2mg/100ml; gamma glutamyltransferase >28U/l; and alanine aminotransferase >30 U/l) measured by dip-stick chemistry (Reflotron, Roche Diagnostics, Mannheim, Germany). In addition, individuals were not recruited into the study if they were pregnant, breastfeeding, on chronic medication, alcohol or drug abuse or showed signs of chronic filarial pathology, such as lymphedema and hydrocele (LF) or dermal pathologies (onchocerciasis).

2.2 Patients:

2.2.1 Lymphatic filariasis: sample collection and patients allocation

One hundred and eighty-four (184) individuals were recruited from 25 endemic communities for lymphatic filariasis within the Ahanta West and Nzema East districts in the Western Region of Ghana [125]. Dunyo *et al* previously identified these communities with MF prevalence ranging from 5 to 20% in average of 500-800 of the population [125]. Since MF have a periodic cycle night, aliquots of blood (9ml x1 and 2.5ml x1) were collected from each individual between 9:00 pm and midnight. The 9ml aliquot of blood was collected in EDTA tubes (Sarstedt, Numbrecht, Germany), whilst 2.5ml aliquot was collected in a pre-filled stabilizer PAXgene™ blood RNA

tube (PreAnalytiX, Cat No. 762165 from BD Biosciences) that was subsequently used for microarray studies.

Infections with *W. bancrofti* were first screened using an immunochromatography assay (ICT). The levels of circulating filarial antigen (CFA) in blood was qualitatively assessed using ICT, BinaxNOW® Filariasis, (Alere, Sinnamon Park, Australia) according to the manufacturer's specification [26]. Briefly, 100µL of blood was collected from each volunteer by finger prick into a calibrated capillary tube coated with an anticoagulant, EDTA. The blood sample was added slowly to the white portion of the sample pad and firmly closed after removing the adhesive liner. Test samples were incubated for 10 min at room temperature before analysis. Samples were positive when both control and test lines appeared pink.

To distinguish MF+ from MF- patients, 100µl of each patient's blood was diluted in 900µl of 3% acetic acid and counted in a Sedgewick counting chamber for MF load expressed as MF/ml of blood [53]. As confirmation, 100µl or 1000µl (depending on the Sedgewick count) of blood was diluted in distilled water and filtered through a Whatman Nucleopore filter (5 µm pores; Karl Roth, Karlsruhe, Germany) to retain the MF. MF were stained using the standard Giemsa methods and were counted using a microscope (Leica Microsystems GmbH, Wetzlar, Germany). Geometric mean of MF/ml is shown in Table 3.1.1. Study subjects were grouped as patently infected: (CFA+/MF+), latently infected: (CFA+/MF-) and endemic Normals (EN): (CFA-/MF-).

2.2.2   Onchocerciasis: sample collection and patients allocation

For the study on onchocerciasis, 224 individuals were recruited in 23 endemic communities in the Central Region of Ghana (Upper-and Lower Denkyira Districts, Dunkwa-on-Offin; Amansie Central and Adansi South Districts, Ashanti Region). Blood sampling was the same as described in section 2.2.1 except that here, samples were obtained during the day from patients infected with *O. volvulus*. Infection is characterized by the presence of palpable nodules in the skin, therefore palpation of nodules is one of the most common diagnostic practices to ascertain *O. volvulus* infection [126]. In order to determine the MF load in these individuals, two skin snips (1-2mg) were taken from the iliac crest of each buttock with a corneoscleral (Holth) punch (Koch, Hamburg, Germany). Skin snips were placed in individual wells of a 96-well microtitre plates (U-shaped, Greiner Bio-one Frickenhausen, Germany) and incubated in 100µl 0.9% NaCl at RT. The MF migrate out of the skin and were counted 24 hrs at 63-fold magnification using a microscope (Leica Microsystems GmbH, Wetzlar, Germany). In order to estimate the skin

MF/mg, each skin snip was weighed using an analytical balance (Sartorius electronic balance, Göttingen, Germany) and MF load calculated per mg of skin [18] as shown in Table 3.1.1. Study participants were grouped into nodule+/MF+ and nodule+/MF-, i.e., amicrofilaridermic (a-MF). All participants selected for the onchocerciasis study had at least one palpable nodule. For comparison, *O. volvulus* infection free subjects (absence of palpable nodules and dermal MF) living in the same endemic communities for 10 years or more were also recruited.

2.2.3   Determination of parasitic co-infections

To determine whether recruited subjects were co-infected with intestinal helminths or protozoa, fresh stool and urine samples from all participants were screened using standard methods. Additional, helminth infections were determined by screening for eggs via Kato-Katz concentration methods. Of the 184 individuals recruited for LF, 30 were co-infected with other helminth infections after performing stool and urine analysis. In the onchocerciasis cohort, 10 patients had further gastro-intestinal parasites. For active plasmodium infection (NADAL Medical test, nal von minden Moers, Germany), 8 and 30 were positive in the LF and onchocerciasis cohort, respectively.

2.3   Materials

2.3.1   Plastic and glassware

Unless otherwise stated, all plastic and glassware equipment were supplied by one of the following companies: Eppendorf (Hamburg, Germany), Becton Dickinson (Heidelberg, Germany), Nunc (Roskilde, Denmark) or Greiner (Frickenhausen, Germany).

2.3.2   Antibodies and microbeads

Human T-cell activator, anti-human CD3 and anti-human CD28 monoclonal antibody microbeads (αCD3/αCD28) were obtained from Invitrogen (Carlsbad, USA). FACS staining antibodies: anti-human CD4-APC, CD4-PECy7, CD8-APC, CD8-PECy-7, CD25-APC, CD25-PE, CD107A-FITC, CD244-APC, FOXP3-APC, Foxp3-FITC, T-bet-PE, GATA3-PE, RORC2-PE, EOMES-FITC, IFN-γ-FITC, IL-4-FITC, IL-10-PE and IL-17-FITC, were purchased from (eBioscience, USA) and immunoTools (Friesoythe, Germany). In addition, anti-human GZMA-FITC, anti-human GZMB-PE (R&D Systems, UK), goat anti-human galectin-10 (primary

antibody) and donkey anti-goat IgG (H+L) carboxfluorescein (secondary antibody) were obtained from R&D Systems (USA).

2.3.3   *Brugia malayi* **extract preparation (B.m. extract)**

Since *W. bancrofti* infections are not viable in rodent hosts and cannot be easily obtained from humans, *B. malayi* worms were used as alternative source, given that both worm species are closely related. Adult worms of the human filarial parasite *B. malayi* were isolated from infected jirds (*Meriones unguiculatus*). *B. malayi* worms were obtained from NAID Filariasis Research Reagent Resource, FR3 (University of Georgia, Athens, GA). To prepare soluble *B. malayi* extract, frozen adult worms were thawed and transferred to a Petri dish pre-filled with sterile PBS. Following several washes in 1x PBS (PAA Laboratories GmbH, Pasching, Austria), worms were then placed inside a glass mortar (VWR, Langenfeld, Germany). Based on the amount of worms, 3-5 ml of medium (RPMI 1640 without supplements) was added and worms were crushed until the dispersion was homogenous. The extract was then centrifuged for 10 minutes at 300 x g (4°C) in order to remove larger insoluble material and the supernatant was carefully transferred into a new tube. The protein concentration was determined and aliquots of the extract were stored at -80°C until use. All procedures were conducted on ice. To determine the optimal concentration of the *B. malayi* antigen for *in vitro* assays, titration experiments were performed using PBMCs from infected patients.

2.4   **Methods**

2.4.1   **Microarray**

2.4.1.1   **Microarray platform and method of analysis**

One hundred and eighty four (184) whole blood samples from the lymphatic filariasis cohort (filarial infected plus endemic normals) and 167 samples from the *O. volvulus* study were added to PAX gene blood RNA tubes (PreAnalytiX BD, Biosciences) directly in the field. After shipping to Edinburgh, RNA was extracted and hybridized to Illumina arrays. The arrays used in the experiment were Human HT-12 version 4 Expression Bead Chips (Illumina, San Diego, CA), which comprised of 46,862 genes for LF, and 46,698 features for onchocerciasis. In short, 100ng total RNA was transcribed into double-stranded cDNA, followed by an amplification step (*in vitro* transcription) to generate labeled cRNA, using the Ambion Illumina TotalPrep-96 RNA Amplification Kit. This resulted in a pool of biotin-labeled cRNA corresponding to the polyadenylated (mRNA) fraction. The cRNA was quantified using OD (nanodrop), normalized

and hybridized onto the Illumina HT-12 arrays for 14-20 hours at 58°C. The unhybridized and non-specifically hybridized cRNA was washed and staining with Cy3-Streptavidin was subsequently performed to bind to the analytical probes that had been hybridized to the array. This allowed for the differential detection of signals when the arrays were scanned. The Illumina IScan scanner is a two-colour laser (532 nm/658 nm) fluorescent scanner with a 0.53 µm spatial resolution capable of exciting the fluorophores generated during the staining step of the protocol. Light emissions from these fluorophores were recorded in high-resolution images of the Array sections. The intensities of the images were extracted using Genome Studio (2010.3) Gene Expression Module (1.8.0) software.

2.4.1.2   Analysis of microarray data

The 184 and 167 array studied from both infections were analyzed using the array Quality Metrics package using R and Bio-conductor. The raw data were transformed using a variance stabilizing transformation (VST) method [127], log-transformed and normalised using the robust spline normalisation (RSN) method. Pairwise comparisons were made using a linear fitting model. Empirical Bayesian analysis was then applied (including vertical (within a given comparison)) and p-values were adjusted for multiple testing to control for false discovery rate. For each comparison, the null hypothesis was that there was no difference between the groups being compared at adjusted $p<0.05$. The Bio-conductor package limma was used to identify statistically significant fold-changes between groups.

2.4.1.3   Determination of gene expression fold change in study subjects

To identify differentially regulated genes of interest in a transcriptome data set, several approaches can be used. These include a fold-change or statistical tests or both [128]. Fold change is the ratio of the mean of the log control sample to the mean infected sample. In the present study, two strategies were employed in analyzing differentially expressed genes. First, the study employed fold change expression and statistical significance i.e. ((FC) ≥1. 3; adj. p-value <0.05) to select transcripts with biological relevance. However, it was realized that most genes were below the cut-off (Fold change (FC) ≥1. 3; adj. p-value <0.05) after multiple correction methods. Hence, a second analysis strategy was used where all genes exceeding the expression greater than or equal to 1.3 fold were considered without adjusted p-values as described elsewhere [129, 130].

2.4.2   Isolation of peripheral blood mononuclear cells (PBMC)

After venous blood collection as described by Arndts *et al* [13] samples were quickly transported to the field lab and peripheral blood mononuclear cells (PBMC) were isolated using the ficoll-based density gradient separation method. To increase cell viability, the entire isolation procedure was performed on ice. In short about 7 ml, of patient blood was poured into the leucosep tubes (Greiner Frickenhausen, Germany) and centrifuged for 20 minutes, 800 x g at 4°C. Plasma was removed from the upper phase of the gradient, first stored at -20°C in 1.8 ml cryo-tubes (Nunc, Roskilde, Denmark) and then transferred to liquid nitrogen. The interphase containing the PBMCs was also collected and transferred into a new 15 ml falcon tube. In order to remove residual traces of ficoll, cell suspensions were washed with complete medium for 8 minutes at 400 x g and 4°C. The supernatant was discarded and the washing step repeated after which the cells were re-suspended in 10 ml cell culture medium. Cell concentration was estimated and isolated PBMCs were immediately used or cryo-preserved. Refer to section 2.4.2.2 for detailed description. Cryo-processed samples and plasma were shipped back to Germany for further analysis.

2.4.2.1   Determining cell viability and concentration

To determine the number of viable cells, the trypan blue (Sigma-Aldrich, Munich, Germany) exclusion method was used. Cells were diluted 1:5 or 1:10 with 0.4% trypan blue. 10µl of diluted samples was then transferred to a haemocytometer (LO Laboroptik GmbH, Bad Homburg, Germany). Viable cells (unstained) were estimated and expressed as cell number per ml.

2.4.2.2   Freezing of cells/cryopreservation

After determining the cell concentration, cells were carefully prepared for freezing. All steps were carried out on ice under a sterile hood. Freezing medium containing 80% fetal calf serum, FCS (PAA) plus 20% DMSO (Sigma-Aldrich GmbH, Munich, Germany) was freshly prepared and 1 ml added drop-wise to 1 ml of cells. Next, cell suspensions were gently mixed and 2 ml of cell suspensions were quickly pipetted into labeled Cryo tubes and optimally frozen at -80°C but on the field, samples were first frozen at -20°C for 24hrs and then transferred to liquid nitrogen (N2).

2.4.2.3   Cell thawing process

In order to thaw frozen cells successfully, cryo-tubes containing frozen cells were collected from the liquid nitrogen and gently moved between the palms until re-thawed. Thawed cell suspensions were transferred into 15 ml falcon tubes (Greiner, Frickenhausen, Germany) and then filled up slowly with 10 ml of pre-cooled complete medium under frequent mixing. RPMI 1640 medium (PAA GmbH, Pasching, Austria) was supplemented with 10% FCS and 50µg/ml of gentamycin (PAA), penicillin/streptomycin (50µg/ml, PAA) and L-glutamine (292.3 µg/ml, PAA). After centrifuging for 8 minutes at 400 x g (4°C), the cells were re-washed to remove residual freezing medium, which is toxic to the cells. The final resulting supernatant was discarded and cells were re-suspended in 1 ml of complete cell culture medium, counted and used for further experiments.

2.4.3   Preparation of patient blood smears for white blood cell counts

To determine the differential cell count (white blood cells) of the study participants, smears were prepared from fresh blood in EDTA tubes (Sarstedt). In brief, 2µL of well mixed blood was pipetted into a centre of the labeled specimen slide. A clean spreader slide was held at a 45° and used to spread the drop of blood along the entire width of the specimen slide. Slides were then dried for at least 1hr at RT and then stained as described in the following section.

2.4.4   May-Grünwald-Giemsa staining and determination of absolute cell counts

To estimate the total leukocyte count in the smears, specimen slides were first fixed in methanol (Merck, Darmstadt, Germany) for 5min, after which they were stained for 10 min in a 1:2 pre-diluted solution of 1x PBS, (PAA Laboratories GmbH, Pasching, Austria) and May-Grünwald solution (Carl Roth, Karlsruhe, Germany). The slides were then dipped in a 1:10 pre-diluted mixture of (1x PBS) and Giemsa solution (Merck, Darmstadt, Germany) for 10 min. Slides were rinsed with aqua dest. and dried for 5 min. To determine cells differentially, the percentage of different cell types of on the slide specimen, were counted with a manual tally counter (Denominator, Connecticut, USA) using a light microscope with an objective lens of x100 under oil (ZEISS, Azioskope, Germany). To determine the absolute count, the percentage of each white blood cell was multiplied by the total white blood count.

2.4.5   Determination of protein with Bradford Assay

To measure the protein concentration in *B. malayi* extract, was performed Bradford protein assay as described by the manufacturer's protocol. In brief, serial dilutions of BSA (PAA) were used as standards and samples were diluted in RPMI1640 (PAA). Following this, 300µl per well of Coomassie blue G (Cytoskeleton, Denver, USA) reagent was distributed in duplicate in the wells of an ELISA plate and 3µl of standard and samples were added accordingly. The protein concentration was quantified at 590 nm using a plate reader SpectraMax 340 Pc (Molecular Devices). Data were analyzed with SOFTmax Pro 3.0 software.

2.4.6   Quantification of endotoxin levels in *B. malayi* extract

To test for endotoxin levels in the B.m. extract, the Pierce Limulus amoebocyte lysate (LAL) Chromogenic quantification kit (88282) (Thermo Fisher Scientific, Schwerte, Germany) was used according to the manufacturer's instruction. Here, 50µL of each standard and unknown sample were added to respective wells and incubated for 5 min at 37°C. After this, 50µL of LAL was added to each well; the plate was shaken for 10 seconds and incubated at 37°C for 10 min. Next, 100 µL of substrate solution (Chromogenic) was added and incubated for 6 min at 37°C. To stop the reaction, 50µL of 25% acetic acid was added to the plate and immediately measured at an absorbance of 405-410 nm on the SpectraMax 340 Pc (Molecular Devices, Sunnyvale, USA). The B. m. extract was used for further assays when endotoxin levels were below 0.1 EU/ml.

2.4.7   Quantifying filarial-specific immunoglobulins by ELISA in plasma

To assess filarial-specific immunoglobulin profile during filarial infection, plasma from all study participants in the LF cohort was screened for levels of filarial-specific IgA, IgE and IgG1-4. Polysorb plates (96-wells, Nunc, Roskilde, Denmark) were coated overnight at 4°C with 50 µl/well of 10 µg/ml *B. malayi* extract diluted in 1% BSA/PBS at pH 9.6. Plates were washed 3 times with washing buffer and once in PBS. Plates were blocked with 200 µl/well 1% BSA/PBS for one hour at RT. Following an additional washing step, 50µl/well of diluted plasma was added (1:500 for specific IgG1-4, IgA and 1:20 for specific IgE) and incubated overnight at 4°C. After the next washing step, 50 µl/well of the biotinylated secondary antibodies were added for two hours at RT (IgG1-4, Sigma-Aldrich, Germany, IgG1 1: 1,000, IgG2 1:15,000, IgG3, 1:4,000, IgG4 1:15,000; IgA 1:15,000; and IgE Southern Biotechnology, AL, USA 1:1,000). Following

another washing step, 50µl/well of Streptavidin-HRP (eBioscience, Frankfurt, Germany; 1:250) were incubated for 45 minutes at RT. After the last wash, 50µl/well of substrate solution containing TMB (Sigma-Aldrich GmbH, Germany) was added to the wells for 15 minutes and thereafter the reaction was stopped with 25µl/well of 2N H_2SO4 (Merck KGAA, Darmstadt, Germany). Pooled plasma samples from 10 infected patients were used for the generation of calibration curves and assigned in optical density (OD) for the specific anti-filarial antibodies. Data were analyzed with SOFTmax Pro 3.0 software.

2.4.8 Determination of charcot leyden crystal/galectin-10 (CLC/Gal-10) in plasma

Plasma from all study individuals was screened for the presence of CLC/Gal-10 using commercially available ELISA kits (CLC, Cloud-Clone Corp. Houston, USA). In short, 50µl/well of each dilution of standard, blank and samples (diluted 1:4) was pipetted into a pre-coated 96 well plate. Plates were covered and incubated for 2hrs at 37°C, after which the liquid in each well was carefully discarded. Without washing, 50µl/well of a biotinylated detection antibody specific for CLC was added to each well. The plates were then covered and incubated for 1hr at 37°C. Thereafter, plates were washed three times with wash buffer (350µl/well), following which 50µl/well of Horseradish Peroxidase conjugate was added to each well. The plates were then incubated for 30 min at 37°C after being covered with a plate sealer. The washing step was then repeated five times, after which 45µl/well of Substrate Solution (TMB) was added to each well and incubated in the dark for 15 min. Finally, 30µl/well of Stop Solution was added and plates were immediately read at 450nm using the SpectraMax Pc (Molecular devices) with wavelength correction (450 nm and 570 nm). Data were analyzed with SOFTmax Pro 3.0 software.

2.4.9 Cellular characterization of flow cytometry

To analyse the immune cell profile in PBMCs from *W. bancrofti*-infected individuals, flow cytometry was used. Flow cytometry has become a mainstay technique in life sciences used for analyzing multiple parameters of individual cells within heterogeneous populations. The technique performs analysis by passing thousands of cells per second through a laser beam and capturing the light that emerges from each cell as it passes through. In flow cytometry, a laser and a sample intersect and optics collects the resulting scatter and fluorescence. Data generated can be analyzed statistically on flow cytometer software to report cellular characteristics, such as size, granularity and phenotype.

2.4.9.1   Characterization of surface markers

All reagents were obtained from eBioscience, ImmunoTools and R&D systems. Staining was done as previously described [131]. To determine the frequency of different lymphocyte populations in *W. bancrofti*-infected individuals and EN volunteers, 1×10^5cells/100µl staining buffer were incubated in FACS buffer PBS/2% FCS for 30 min at 4°C with 1) CD4-PeCy7 (clone: RPA-T4) for CD4 T cells, PD-1-FITC (clone: MHA) for PD-1, CTLA-4-PE (clone: I4D3) for CTLA-4, CD107a-FITC (clone: eBioH4A3) for CD107a, CD244-APC (clone: eBioDM244) for CD244, and CD25-PE (clone:) for CD25 T cells; 2) CD8-APC (clone: SK1) for CD8$^+$ T cells and as well as all the markers mentioned for CD4 T cells staining. Cells were acquired on a FACSCanto (BD^{TM}, Heidelberg, Germany).

2.4.9.2   Characterization of intracellular markers

Following the surface staining, intracellular staining was performed on PBMCs from *W. bancrofti*-infected and endemic normals either directly or following activation with a Cells Stimulation Cocktail (eBioscience, Frankfurt, Germany) containing phorbol 12-myristate 13-acetate (PMA), Ionomycin, Brefeldin A, and Monensin for 6hrs. Thereafter, staining was performed using in 4 distinct panels; single stain panels Th1, Th2 and Th17 and CD25-PECy7 (clone: BC96) for regulatory T cell panels for both CD4$^+$ and CD8$^+$ T cells. After 30 min incubation at 4°C, cells were washed once in FACS buffer. After fixation and permeabilization in x1/4 Fix-Perm reagent (eBioscience), cells were incubated at 4°C for 30 min with either 1) anti-human T-bet-PE (clone: eBio4B10) and IFN-γ-FITC (clone: 4S.B3), for Th1 panel; 2) GATA3-PE (clone: TWAJ); IL-4-FITC (clone: B-S4) for Th2; 3) IL-17A-FITC (clone: eBio64DEC17); RORC2-PE (clone: AFKJS-9) or 4) Foxp3-FITC (clone: 236A/E7); IL-10-PE (clone: JES3-9D7) for regulatory T cells. Cells were again washed two times and thereafter re-suspended in fix-perm buffer (eBioscience). To avoid unspecific binding, 3µl of Human Fc block (eBioscience) was used and for spectral overlap correction, fluorescence compensation was done using UltraComp ebeads (eBioscience). Data were acquired and analyzed on a FACSCanto flow cytometer (BD™) using DIVA software.

2.4.9.3   Determination of intracellular proteins (granzymes and galectin-10)

Granzyme-expressing CD4$^+$ and CD8$^+$ T cells in the PBMCs from *W. bancrofti*-infected individuals and uninfected controls were assessed directly or after activation with a Cells

Stimulation Cocktail (eBioscience) containing PMA, Ionomycin, Brefeldin A, and Monensin for 6 hours. Thereafter, surface staining was performed using anti-human CD4-APC (clone: OKT4) for CD4 and CD8-PeCy7 (clone: RPA-T8) for CD8 for 2 distinct panels 1) GZMA-FITC (BD Pharmingin 558905) or GZMA-PeCy7 (clone: CB9) for granzyme A; and 2) GZMB-PE (clone: GB11) for granzyme B. Furthermore, CLC/galectin-10 expressing-CD4$^+$ and CD8$^+$ T cells were evaluated by staining cells with anti-human galectin-10 antibodies (clone: AF5447) and later with secondary anti-goat galectin-10 antibody-Fluorescein (clone: F0109). Data were acquired and analyzed on a FACSCanto flow cytometer (BD^{TM}).

2.4.10 *In vitro* cultures

2.4.10.1   Antigen-specific stimulation of PBMCs from the study subjects

Frozen PBMCs from the LF study cohorts were thawed and washed in complete RPMI 1640 medium with supplements (Appendix). PBMCs were cultured in 96-well plates (U-shaped, Greiner Bio-one, Frickenhausen, Germany) and left either unstimulated, for spontaneous cytokine secretion, or stimulated with either i) adult *Brugia malayi* extract (40µg/ml) or ii) αCD3/αCD28 (10000 beads/well, Invitrogen) or the combination of iii) BmAg and αCD3/αCD28 in duplicate for 7 days at 37°C under 5% CO_2.

2.4.11 Statistical analysis

Statistical analyses were performed using the software PRISM 5.02 (GraphPad Software, Inc., La Jolla, USA). Statistical differences were observed using a Kruskal-Wallis-test with Dunn's correction for multiple comparisons or ANOVA and where necessary a Mann-Whitney-U test for a further comparison of two groups. *P*-value of 0.05 or less were considered significant (*p<0.05, **p<0.01 and ***p<0.001.

3 RESULTS

3.1 *Wuchereria bancrofti* infection

3.1.1 Characterization of the study population

In total, 184 subjects were recruited for the *W. bancrofti* study and grouped into endemic normals (EN, n=57), patently infected (MF+, n=52) and latently infected (MF-, n= 75) individuals based on the presence of peripheral MF diagnosis. The study comprised of adult otherwise clinically healthy adults, of which 26.6% were female and 73.4% were male, with an age range from 18-55. Following the determination of adult worm burden, 127 (69 %) of the study subjects were positive for the CFA test, whereas 57 (31%) were negative. The geometric mean of MF in the patently infected individuals ranged from 1-3620 MF/ml (Table 3.1.1).

In total, 103 (55.9%) study participants had not participated in (MDA) programmes beforehand and in those that had received IVM treatment, 69 (37.5%) had had 1 round and 12 (6%) had had 2 rounds. The percentage of rounds of IVM intake for 0/1/2 round(s) for EN: 49.2%, 50.8% and 0%; MF+: = 67.3%, 30.7%, 2%; MF- : 53.3%, 32.0%, 14.7%, as shown in Table 3.1.1. Out of 184 subjects, 31 (16.8%) were co-infected with other known infections, such as helminth, protozoa and malaria. Of these, the number of co-infected individuals in EN, MF+ and MF- was 4 (7%), 7 (13.4%) and 19 (25.3%), respectively. Of note, co-infection with *Ascaris lumbricuides* was recorded in 11 individuals (6.0%), followed by *Plasmodium* spp. 9 (4.9%), *Giardia lamblia* 6 (3.2%), Hookworm 5 (2.7%) and *Trichuris trichiura* 4 (2.1%), whilst co-infection with *Schistosoma mansoni* 1 (0.5%) was the lowest.

Table 3.1.1: Characteristics of the study population: *W. bancrofti*-infection

	EN (n=57)	MF+ (n=52)	MF- (n=75)
Age (median)	32.0 (18-50)	28 (18-53)	30 (18-55)
Sex (F/M)	24/29	4/48	21/54
CFA	negative	positive	positive
GM MF (MF/ml)	-	382 (1-3,620)	
Rounds of IVM (0/1/2)	28/29/0	35/16/1	40/24/11
Co-infections	4	7	19

Age: median (range); sex: number of (female/male); IVM: rounds (1 or 2 X), GM (geometric mean); MF count: mean (range); CFA=Circulating Filarial Antigen; MF=microfilaria; EN=endemic normals

3.1.2 Transcriptome profile of *W. bancrofti*-infected individuals and endemic controls using ingenuity pathway analysis (IPA)

Genes are the molecular units in living organisms, which carry the important biological information to produce proteins. Interactions amongst genes are complicated, some of which may regulate the behavior of others. To explore the biological meaning of expressed genes during *W. bancrofti* and *O. volvulus* infections, normalized whole blood was drawn from infected or uninfected individuals and mRNA was isolated. Expression of genes was measured using Illumina Human HT-12 version 4 (San Diego, CA). Up- and down-regulated genes, which showed at least a 1.3 fold-expression difference, were uploaded on IPA (IngenuitySystem.com, Redwood City, USA) application. Analysis of canonical pathways and molecular networks was subsequently performed.

Canonical pathway analysis identifies molecular pathways from the IPA library of canonical pathways (part of the Ingenuity Pathway Knowledge Base, IPKB) that were most significant to the data set. Genes from the data set that were associated with a canonical pathway in the IPKB were considered for the analysis. The significance of the association between the genes from the dataset and the canonical pathway (in the IPKB) was measured in two ways as described in IPA documentation: 1) A ratio was calculated of the number of genes from the dataset in a given pathway divided by the total number of molecules that make up the canonical pathway; 2) Fisher's exact test was used to calculate a *p*-value determining the probability that there is an association between the genes in the dataset and the canonical pathway that cannot be explained by chance alone. A pathway was considered significant if the *p*-value was less than <0.05, as determined by Fisher exact test.

Different to canonical pathway analysis (in which a set of differentially expressed genes can only be associated to genes of known functions based on the literature), in network analysis, networks of genes are algorithmically generated based on their connectivity. In this study, network analysis, was undertaken to identify clusters of coordinately expressed genes, and subsequently mapped to functional groupings, including pathways. Particular emphasis was placed on exploring loci associated with immunological response as well as others that could plausibly contribute, directly or otherwise, to the host response to infection. Networks are formed de novo, i.e., depending on the gene/molecule interaction with other gene/molecules within the data set. The IPA generates networks and overlays these networks with a score. The score is derived from a *p*-value and indicates the probability of the focus genes in a network

being found together due to random chance. For instance, suppose that a network of 35 molecules has a Fisher Exact Test result of 1x10-6. The networks score = -log (Fisher's Exact test result) = 6. This can be interpreted as, "There is a 1 in a million chance of getting a network containing at least the same number of focus genes by chance when randomly picking 35 molecules that can be in networks from the Ingenuity Knowledge Base. Therefore, it stands to reason that the higher the score, the higher the confidence level of the network not being generated by random chance alone. In this study, each network was arbitrarily set to 35 focus genes with networks of direct relationship selected. Gene products were represented as nodes and the biological relationship between the nodes is shown as edges. The intensity of a node indicates the degree of up (red) or down (green) or non-regulated (gray). A functional analysis of the associated network was identified by the biological function and/or disease that were most significant to the genes in a network. Differentially expressed genes may not directly be translated to have biological relevance. To understand the underlying molecular mechanisms and signaling pathways involving host response to filarial infections, in-depth analyses were performed on the transcriptomics data on filarial infected subjects using IPA application. The study focused on regulated genes, canonical pathways and regulatory networks as well as predicted biological functions. Gene expression analyses showed that most genes were below the cut-off (Fold change (FC) ≥1. 3; adj. *p*-value <0.05) after multiple correction methods, as shown in Table 3.1.2.

Table 3.1.2: Proportion of differentially expressed genes identified across comparisons in *W. bancrofti*-infected compared to EN

	adj. *p*<0.05;FC≥ 1.3	FC≥ 1.3
Infected vs EN	12	23
MF+ vs MF-	0	5
MF+ vs EN	0	33
MF- vs EN	12	25

The table lists the number of genes whose expression, in the filarial infected groups, exceeded that of endemic normals 1.3 fold (FC ≥1.3) EN. Microarray data are denoted for those genes that demonstrated a False Discovery Rate (FDR) less than 0.05; associated with or without adjusted (adj) *p*-value. FC, Fold change.

In general, 12 genes were significantly regulated in *W. bancrofti*-infected compared to EN. Coincidentally, 12 genes were also significantly upregulated between MF- individuals and EN, while no differences were observed between MF+ and EN. Thus, the number of regulated

genes appeared to be less. To this end, a second analysis strategy was employed in which all genes expressed greater than or equal to 1.3 fold were considered without adjusted *p*-value as described elsewhere [129, 130, 132, 133]. The number of regulated genes is shown in Table 3.1.2. Without adjusted *p*-value, 23 genes were found to be regulated in the *W. bancrofti*-infected groups relative to EN, 5 genes were found in MF+ compared to MF-, 33 genes in MF+ relative to EN, and 25 genes were identified in MF- compared against EN (see Table 3.1.2).

3.1.3   Comparison of regulated genes, canonical pathways and networks of *W. bancrofti*-infected individuals vs EN

In order to elucidate the underlying mechanism induced during *W. bancrofti* infection, the whole blood transcriptome of filarial infected individuals was compared against EN. Here,12 genes were upregulated, of which the top ten most up-regulated genes at (FC ≥1.3 and adj. p**<** 0.05) include nuclear localized genes, such as zinc finger, AN1-type domain 5 (*ZFAND5*) and probable ATP-dependent RNA helicase (*DDX5*), cytoplasmic localized genes such as Gamma-adducin *(ADD3)*, calcium-binding protein 39 (*CAB39*), cathepsin Z (*CTSZ*), integrin-ß-1(*ITGB1*), transmembrane protein 66 (*TMEM66*) and O-linked N-acetylglucosamine transferase (*OGT*), whereas the location of ubiquitin-conjugating enzyme E2D 3 (*UBE2D3*), arginine and glutamate rich 1 (*ARGLU1*) is yet to be defined (Table 3.1.3). Most of these upregulated genes are associated with inflammatory responses as well as immune cell migration. There were no downregulated genes identified in this comparison at the set threshold. Analysis of regulated genes without adjusted *p*-value revealed 23 genes of which most were associated with the development and function of eosinophils (Table 3.1.3). Amongst the top 10 genes in the analysis without adjusted *p*-value, 6 genes matched those identified in the analysis with adjusted *p*-value, whilst the rest differed. Interestingly, it was also observed that analyses without adjusted *p*-value led to the identification of genes with higher intensity of expression, but were submerged by stringent statistics approach. These included genes, such as the Charcot-Leyden crystal protein *(CLC/Gal-10)*, being the most highly regulated followed by major histocompatibility complex class II (MHC II), DR beta 1 (*HLA-DBR1),* ribosomal protein S4, y-linked 1 (*RPS4Y1)* and ribonuclease, RNase A family, 2 (*RNASE2)* as shown in Table 3.1.3. Interestingly, pathway response analyses based on the regulated genes between *W. bancrofti*-infected and EN, revealed 14 significant canonical pathways (Fisher's exact test, *p*<0.05).

Among the top five were the Actin Nucleation by ARP-WASP Complex (p<7.55E-04), Cdc42 signaling (p<3.58E-03), Rac signaling (p<2.53E-03), RhoGD1 signaling (p<6.88E-03), which primarily associates with *ITGB1*, a gene that codes for integrin beta proteins; whilst the Ephrin receptor signaling (p<6.88E-03) is activated by *ARGLU1* as shown in Table 3.1.4. These canonical pathways relate to cell-cell communication, cell migration as well as immune cell trafficking (Figure 3.1).
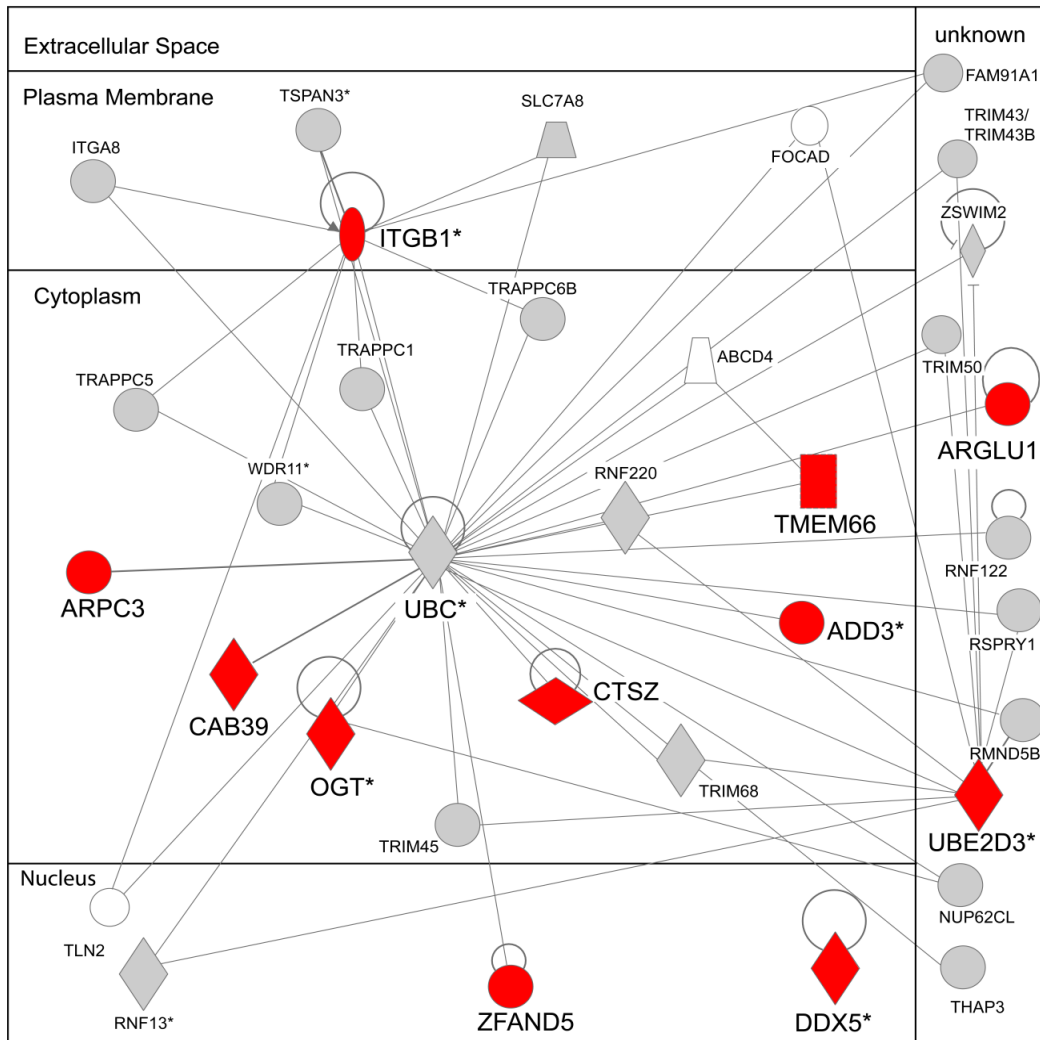
Figure 3.1: Cell-to-cell migration and signaling interaction network in infected relative to EN using ingenuity pathway analysis.
Genes were differentially expressed at FC≥1. 3, *p*< 0.05 adjusted for multiple comparisons using the Benjamini-Hochberg correction and False Discovery Rate (FDR<0.05). Lines represent direct relationships between molecules. Up-regulated genes highlighted in red, white/gray indicate genes not differentially expressed, but with defined relation to other genes in the network. (Key: circle=transcriptional regulator, upright diamond= enzyme, tranverse diamond=peptidase, rectangle=G protein coupled receptor, trapezoid= transporter, oval= transmembrane receptor).

In a further analysis without the adjusted p-value between *W. bancrofti*-infected and EN, 21 canonical pathways were identified. Among these were the CD28 signaling in T helper cells ($p<$ 6.67E-03) which is essential for T cell activation and is associated with *HLA-DRB1* and *ZFAND5*, whereas *DDX5* is involved in the Regulation of eIF4 and p70S6K signaling ($p<$1.13E-02), which modulates translation of mRNAs as well as cell proliferation.The regulated networks revealed the cell-to-cell migration and signaling interaction network with a score of 33 when analysed with adjusted p-value (Figure 3.1) and (Table 3.1.5), whilst the hematological disease and cell-to-cell signaling interaction as well as the post translational modification networks were identified following analysis without adjusted p-value (Table 3.1.5). These networks associate with bio-functions, such as inflammatory response, phagocytic activity; molecular and cellular functions, such as cell cycle cell death and survival, cell morphology and carbohydrate metabolism.

3.1.4   Comparison of regulated genes, canonical pathways and networks of patently (MF+) vs latently (MF-) infected individuals

Asymptomatic *W. bancrofti*-infected individuals can be subdivided into two groups. A patent infection represents an immune permissive state that favours the survival of adult worms to produce MF in an immunologically tolerant host [11]. The immune profile of this infection phenotype has been associated with a regulatory phenotype in order to facilitate survival within the host. In contrast, a latent infection is characterized by presence of adult worms but the absence of MF in the periphery. Since cellular immune responses of this group are characterised by enhanced adaptive immune response [13], it is postulated that these responses lead to MF clearance. Thus, identifying expressed genes that differ between the two infection phenotypes can be important for the search of new effective antifilarial drugs or vaccines. To this end, a comparison on regulated genes between the two asymptomatic groups was performed. None of the genes passed the analysis with adjusted p-value; however, without adjusted p-value, five genes were up-regulated, composed of the ribosomal protein s4, y-linked 1 (*RPS4Y1*)*,* whereas carbonic anhydrase 1 (*CA1*) and aminolevulinate, delta-, synthase 2 (*ALAS2*) and two unknown genes were down-regulated as shown in Table 3.1.3.

To explore the molecular interactions induced in the two infection phenotypes, pathway analysis was performed. The top 5 canonical pathways included the down-regulated tetrapyrrole biosynthesis II ($p<$1.03E-03) and heme biosynthesis II pathways ($p<$1.85E-03), which is

associated with *ALAS2*, whilst *RPS4Y1* is involved in the regulation of eIF4 and p70S6K ($p<2.89E-02$), eIF2 ($p<3.48E-02$) and mTOR signaling ($p<3.70E-02$) pathways (Table 3.1.4). In order to determine the unknown underlying molecular events that differ between patent and latent infection, network analysis was performed. Here, the cell morphology and development network was upregulated in the patently infected subjects relative to the latent group as shown in Table 3.1.5. This network associates with molecular and cellular functions, such as molecular transport, small molecular biochemistry, cell function and maintenance, cell development and gene expression.

3.1.5 Comparison of regulated genes, canonical pathways and networks of patently (MF+) infected individuals vs endemic normals (EN)

As opposed to infected individuals, EN include individuals living in the same endemic region and despite their persistent exposure to parasite transmission do not develop an infection. Therefore, comparing the transcriptome between patent and EN group is expected to unravel how filarial parasites modulate the apparent divergent immune responses in these groups. There were no significantly expressed genes between individuals with patent infection and EN after analysis with adjusted *p*-value. However, after analysis without adjusted *p*-value, 33 genes were found. The 10 most up-regulated transcripts included ribosomal protein S4, y-linked 1 (*RPS4Y1),* major histocompatibility complex class II, DR beta 1 (*HLA-DRB1),* arginine and glutamate-rich protein 1 (*ARGLU1),* neuroblastoma breakpoint family, member 15 (*NBPF15),* adducin gamma 3 (*ADD3),* zinc finger and AN1-type domain 5 (*ZFAND5),* integrin binding protein beta 1 (*ITGB1),* cathepsin Z *(CTSZ),* calcium binding protein 39 (*CAB39)* and signal transducer and activator of transcription 1 (*STAT1),* whereas the most down-regulated genes are aminolevulinate, delta-, synthase 2 (*ALAS2),* carbonic anhydrase 1 (*CA1),* selenium binding protein 1 *(SELENBP1),* biliverdin reductase B *(BLVRB),* erythrocyte membrane protein band 42 (*EPB42),* interferon, alpha-inducible protein 27 (*IFI27),* alpha hemoglobin stabilizing protein *(AHSP),* family with sequence similarity 46, member C *(FAM46C),* cell division cycle 34 (*CDC34),* and peptidase inhibitor 3 (*PI3)*, as shown in Table 3.1.3 as well as in Figure 3.2.

In pathway analysis between patently infected and EN, 8 canonical pathways were identified. Among the top five activated pathways found were the T helper cell differentiation ($p<3.89E-03$) which associates with *HLA-DRB1* and *STAT1*; hypoxia signaling ($p<4.01E-03$) associates with genes, such as *CDC34* and *UBE2D3*; heme degradation pathway ($p<6.02E-03$) and tetrapyrrole

biosynthesis (*p*<7.52E-03) II involves *BLVRB,* whereas the heme biosynthesis II pathways (*p*<1.35E-02) is regulated by *ALAS2* as shown Table 3.1.4.
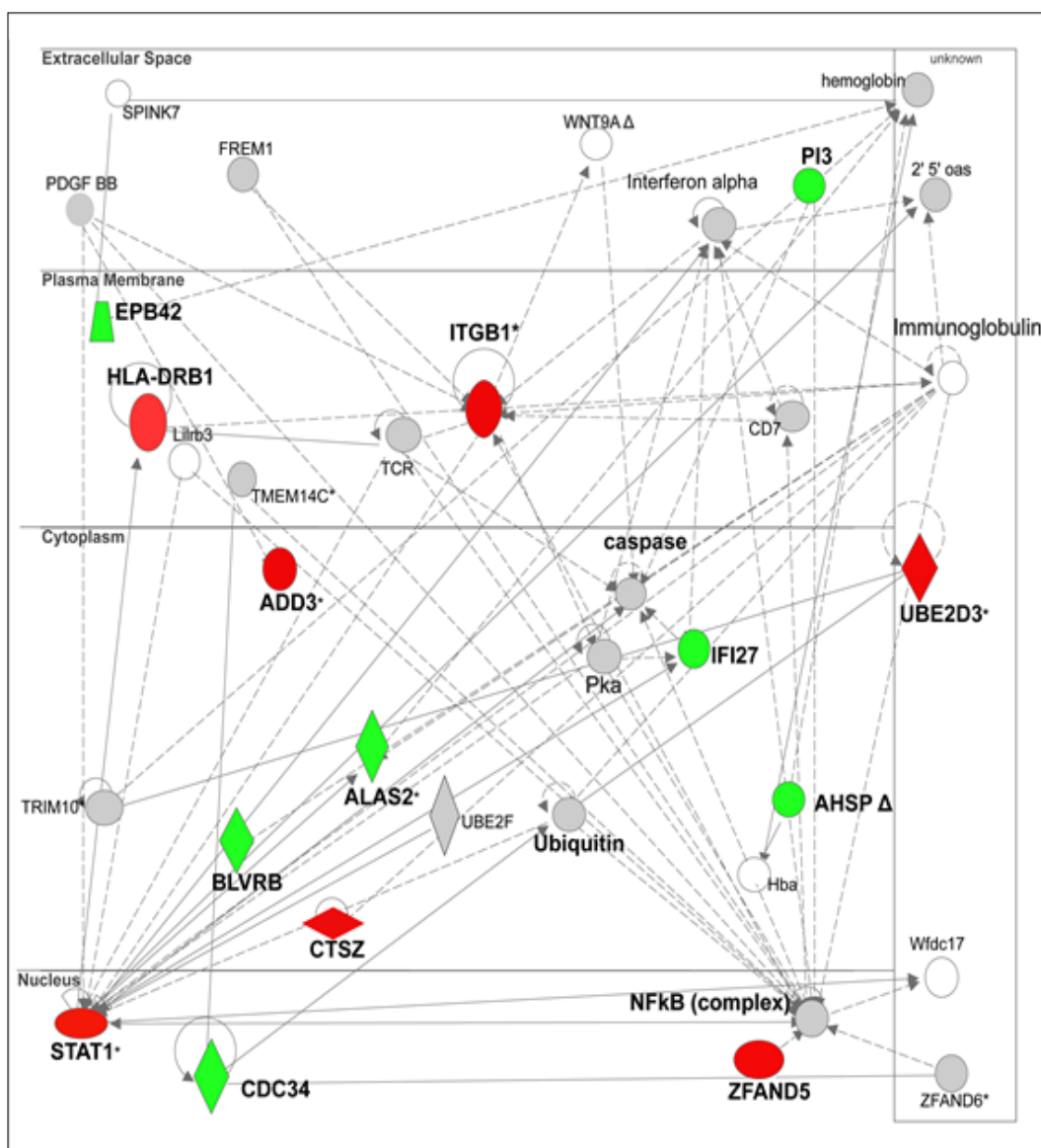
Figure 3.2: Hematological disease, development and function regulatory network in patent infected relative to EN.
Genes were differentially expressed at FC≥1. 3. Lines represent direct (solid lines) and indirect (dashed lines) relationships between molecules. Up-regulated genes are highlighted in red, down-regulated genes are shown in green; whereas gray indicates genes not differentially expressed but with defined relation to other genes in the network. (Key: circle=transcriptional regulator, upright diamond=enzyme, transverse diamond=peptidase, oval=transmembrane receptor, trapezoid= transporter, small circle=other).

Network analysis revealed the hematological disease, development and function (Figure 3.2), the tissue morphology and post translational modification and increased level of potassium regulatory network to be altered between the patently and EN group as shown in (Table 3.1.5).

Both regulatory networks associate with molecular functions, inflammation, cellular growth and proliferation of immune cells.

3.1.6 Comparison of regulated genes, canonical pathways and networks of latent vs EN

Having addressed the comparison between all infected individuals towards EN, patent vs latent, patent vs EN, gene expression profiles between latently infected individuals and EN were considered. The 10 most regulated genes in this comparison following analysis with adjusted p-value included adducin 3 (gamma) (*ADD3*), arginine and glutamate-rich protein 1(*ARGLU1*), calcium binding protein 39 (*CAB39*), zinc finger and AN1-Type domain 5 (*ZFAND5*), transmembrane protein 66 (*TMEM66*), actin related protein 2/3 complex (*ARPC3*), transmembrane protein 123 (*TMEM123*), ubiquitin-conjugating enzyme E2D 3 (*UBE2D3*), catalase (*CAT*) and cathepsin Z (*CTSZ*). After analysis without adjusted p-value, genes such as Charcot-Leyden crystal protein (*CLC*), ribonuclease, RNase A family, 2 (*RNASE2*), major histocompatibility complex, class II, DR beta 1 (*HLA-DBR1*), DEAD helicase 5 (*DDX5),* and o-linked Nacetylglucosamine (GlcNAc) transferase (*OGT*) were identified and differed from those found in the adjusted p-value category (Table 3.1.3)*.* The majority of these regulated genes associate with inflammation, cell migration, cell movement and most notably eosinophil development and activity. Among these were *CLC* and *RNASE2,* which are associated to the development and functionality of eosinophils [134], (Table 3.1.3). To determine the immune pathways, which differ between latent infection relative to EN, a comparative analysis revealed 20 canonical pathways. The top five of these canonical pathways were Actin Nucleation by ARP-WASP Complex (p<7.55E-04), Rac signaling (p<2.53E-03), Cdc42 signaling (p<3.58E-03), RhoGD1 signaling (p<6.88E-03) which are regulated by *ARGLU1* and *ARPC3*. Genes such as *ZFAND5, HLA-DRB1*, *TMEM66* and *TMEM123* are involved in CD28 signaling in T helper cells (p<6.67E-03) as described in Table 3.1.4. In comparative analysis on regulated genes without adjusted p-value, 22 canonical pathways were identified (Table 3.1.4).

The two regulatory networks identified include the cell death and survival with a score of 28 and cell-to-cell signaling interaction, post-translational and modification, cellular assembly and organization with network score of 2 (Table 3.1.5). In a further comparison without adjusted p-value, two different regulatory networks were identified. These are the cell-to-cell signaling interaction and immune trafficking with a score of 24, and the tissue morphology and post translational modification with a predicted score of 22. Thus, the activation of these immune

regulatory networks suggests that stronger immune activation is associated with the latent infection in which individuals do not have peripheral MF.

Table 3.1.3: Regulated genes in *W. bancrofti*-infected groups and EN

Inf. vs EN[1]	FC	Inf. vs EN[2]	FC	MF+ vs MF-[2]	FC	MF+ vs EN[2]	FC	MF-vs EN[1]	FC	MF-vs EN[2]	FC
UPREGULATED											
ADD3	1.39	CLC	1.46	RPS4Y1	1.35	RPS4Y1	1.73	ADD3	1.40	CLC	1.58
ARGLU1	1.38	HLA-DRB1	1.45			HLA-DRB1	1.49	ARGLU1	1.38	RNASE2	1.49
ZFAND5	1.36	RPS4Y1	1.44			ARGLU1	1.39	CAB39	1.37	HLA-DRB1	1.43
CAB39	1.35	RNASE2	1.44			NBPF10	1.39	ZFAND5	1.37	ADD3	1.40
ITGB1	1.32	ADD3	1.39			ADD3	1.38	TMEM66	1.34	ARGLU1	1.39
DDX5	1.32	ARGLU1	1.38			HLA-H	1.38	ARPC3	1.32	CAB39	1.37
CTSZ	1.32	ZFAND5	1.36			ITGB1	1.37	TMEM123	1.32	ZFAND5	1.37
TMEM66	1.32	CAB39	1.35			ZFAND5	1.37	UBE2D3	1.32	DDX5	1.36
OGT	1.31	DDX5	1.32			CTSZ	1.36	CAT	1.31	TMEM66	1.34
UBE2D3	1.31	CTSZ	1.32			CAB39	1.34	CTSZ	1.31	OGT	1.31
DOWNREGULATED											
				Unknown	-1.44	CA1	-1.45				
				CA1	-1.43	ALAS2	-1.48				
				Unknown	-1.38	Unknown	-1.61				
				ALAS2	-1.38						

The table lists genes whose expression, in the filarial infected patients, exceeded that of endemic normals 1.3 fold (FC ≥1.3). Inf: Infected, MF: microfilariae, EN: endemic normals, FC: fold change, [1] (FC≥1. 3, adj. p<0.05), [2] (FC ≥1. 3)

With regard to all regulated genes in the various comparisons, there were some similarities and differences in the pattern of gene expression after analysis with adjusted *p*-value as well as following analysis without adjusted *p*-value. For instance, among the 10 most regulated genes in the infected vs EN, 8 of these were also found in the comparison between MF- vs EN, however, there were no regulated genes in comparison between MF+ vs MF-. In the analysis without adjusted *p*-value in the infected vs EN, 6 genes were similarly expressed in MF+ vs EN, while 7 were also found to be similarly expressed in MF- vs EN. Interestingly, it was observed that in the analysis without adjusted *p*-value, genes such as *CLC/Gal-10* and *RNASE2* were highly upregulated in the infected individuals when compared to the EN group, as well as MF- vs EN as shown in Table 3.1.3.

Table 3.1.4: Predicted canonical pathways in *W. bancrofti*-infected groups and EN

Inf. vs EN[1]	Inf. vs EN[2]	MF+ vs MF-[2]	MF+ vs EN[2]	MF- vs EN[1]	MF- vs EN[2]
Actin Nucleation by ARP-WASP Complex	Cdc42 signaling	Tetrapyrrole Biosynthesis II	T helper cell differentiation	Actin Nucleation by ARP-WASP Complex	Cdc42 signaling
Cdc42 signaling	Actin Nucleation by ARP-WASP Complex	Heme Biosynthesis II	Hypoxia signaling	Rac signaling	Actin Nucleation by ARP-WASP Complex
Rac signaling	Rac signaling	Regulation of eIF4 and p70S6K signaling	Heme Degradation	Cdc42 signaling	Rac signaling
RhoGD1 signaling	CD28 signaling in T helper Cells	EIF2 signaling	Tetrapyrrole Biosynthesis II	RhoGD1 signaling	Superoxide Radicals Degradation
Ephrin receptor signaling	Regulation of eIF4 and p70S6K signaling		Heme Biosynthesis	CD28 signaling in T helper Cells	CD28 signaling in T helper Cells

Inf: Infected, MF: microfilariae, EN: endemic normals, [1] (FC≥1. 3, adj. $p<0.05$), [2] (FC ≥1. 3).

Similar to the regulated genes, there were some similarities and differences, with regard to pathway analysis in this study. Interestingly, out of the top 5 pathways, when comparing infected vs EN, 4 were also found in MF- vs EN, while none of these were identified in comparison between MF+ vs MF-. These regulated pathways in infected vs EN as well as in MF- vs EN indicate active immune response in these groups and reflect the increased transcripts, which associate with immune cell migration and cellular trafficking. In contrast, the pathways found in comparison between MF+ vs MF- were tetrapyrrole biosynthesis, heme biosynthesis and regulation of eIF4 and p70S6K signaling (Table 3.1.4). In network analysis, there were similarities in the networks identified in the infected vs EN as well as MF- vs EN and predominantly associate with cell to-cell signaling and interaction, whilst between MF+ vs MF- the cell morphology and development network was revealed.

Table 3.1.5: Regulated networks in *W. bancrofti*-infected groups and EN

Inf. vs EN[1]	SC	Inf. vs EN[2]	SC	MF+ vs MF-[2]	SC	MF+ vs EN[2]	SC	MF- vs EN[1]	SC	MF- vs EN[2]	SC
Cell-To-Cell migration and signaling interaction	33	Hematological diseases and cell to cell signaling interaction	28	Cell Morphology and Development	9	Hematological disease, development and function	35	Cell death and survival	28	Cell-To-Cell signaling interaction and immune trafficking	24
		Post-translational modification	14					Tissue morphology and post translational modification, increased level of potassium	24	Cell-To- Cell signaling and interaction post-translational and modification, Cellular assembly and organization	2	

Inf: Infected, MF: microfilariae, EN: endemic normals, SC: score, [1] (FC≥1. 3, adj. p<0.05), [2] (FC ≥1. 3).

3.1.7 Impact of confounding factors: Comparison of regulated genes, canonical pathways and networks of regional differences

Given that gene expression patterns may be significantly altered by a number of factors, the study further determined whether regional differences influenced the gene expression profile. The *W. bancrofti* study was conducted in the two regional areas, i.e. Ahanta West and Nzema East districts. Although, communities within the two regions are close to each other, the intensity and transmission of *W. bancrofti* infection, as well as rounds of ivermectin treatment (MDA programme) are expected to vary from one community/region to another. Further comparative analysis showed that the single factor that strongly influenced gene expression profiles in this study was whether the participants originated from Ahanta West or Nzema East. Remarkably, 197 genes were differentially regulated using the first analysis strategy, while 267 genes were found to be regulated using the second comparison approach as shown in Table 3.1.6.

Table 3.1.6: Number of differentially expressed genes identified in Ahanta West relative to Nzema East

W. bancrofti infection	adj. p<0.05;FC≥ 1.3	FC≥1.3
Ahanta West vs Nzema East	197	267

The table presents the number of regulated genes in the Ahanta West samples compared Nzema East.

Among the top 10 up-regulated genes (in Ahanta West samples relative to Nzema East samples) were the family with sequence similarity 73, member A (*FAM73A*), zinc finger protein 682 (*ZNF682*), solute carrier family 4, sodium bicarbonate co-transporter, member 5 (*SLC4A5*),

zinc finger protein 223 (*ZNF223*), dopey family member 2 (*DOPEY2*), family with sequence similarity 175, member A (*FAM175*), HAUS augmin-like complex, subunit 2 (*HAUS2*), small integral membrane protein 14 (*SMIM14)*, X-ray repair complementing defective repair in chinese hamster cells 2 (*XRCC2*) and protein tyrosine phosphatase-like A domain containing 2 (*PTPLAD2*). On the contrary, genes such as *RPS4Y1, ARGLU1*, *CAB39*, *OGT*, *ADD3*, *TMEM66*, *UBE2D3, ZFAND5*, ribosomal protein L17 (*RPL17)* as well as protein kinase, cAMP-dependent, regulatory type I alpha (*PRKAR1A*) were down-regulated in the Ahanta West samples compared to Nzema East (Table 3.1.7).

Table 3.1.7: Top 10 significantly regulated genes based on study regions

AW vs NZ[1]	FC	AW vs NZ[2]	FC
UP-REGULATED			
FAM73A	1.44	*SEMA3E*	1.46
ZNF682	1.41	*FAM73A*	1.44
SLC4A5	1.40	*SNAPC1*	1.42
ZNF223	1.40	*BLZF1*	1.41
DOPEY2	1.39	*CHRNA5*	1.41
FAM175A	1.39	*ZNF682*	1.41
HAUS2	1.39	*SLC4A5*	1.40
SMIM14	1.39	*ZNF223*	1.40
XRCC2	1.39	*BLOC1S6*	1.39
PTPLAD2	1.37	*C11orf63*	1.39
DOWN-REGULATED			
RPS4Y1	-1.53	*RPS4Y1*	-1.53
ARGLU1	-1.46	*ARGLU1*	-1.46
CAB39	-1.46	*CAB39*	-1.46
OGT	-1.41	*OGT*	-1.41
ADD3	-1,40	*ADD3*	-1,40
TMEM66	-1.39	*TMEM66*	-1.39
UBE2D3	-1.37	*UBE2D3*	-1.37
ZFAND5	-1.36	*ZFAND5*	-1.36
RPL17	-1.36	*RPL17*	-1.36
PRKARIA	-1.36	*PRKARIA*	-1.36

The table lists the genes whose expression fold change exceeded [1] (FC≥1. 3, adj. *p*<0.05) and (FC≥1. 3) in the Ahanta West (AW), compared to the, Nzema East (NE) samples. The gene expression data are denoted as the fold change for those genes that demonstrated an FDR of less than 0.05; associated with or without adjusted *p*-values as shown in parentheses. Fold change (FC).

Next, canonical pathway analysis was performed and surprisingly among the regulated pathways, the top five (5) were all down-regulated in Ahanta West compared to Nzema East. These included eIF2 signaling (*p*<8.7E-05) associated with genes, such as *EIFA42, PP1CC, RPL17, RPS3A* and *RPS4Y1*, the chondroitin sulfate degradation (*p*<4.52E-04) and dermatan

sulfate degradation (p<5.33E-04) involved with *CD44* and *MGEA5*, the regulation of eIF4 and p70S6K (p<5.43E-04) linked with *EIFA2, PAIP2, RPS3A* and *RPS4Y1,* whereas *CREB1, PPP1CC, PRKAR1A, YWHAQ* are associated with the ERK/MAPK signaling (p<1.43E-03) (Table 3.1.7).

Such strong differences in gene expression between the two study areas were highly unexpected. To determine whether such a similar scenario reflects the activity of regulatory networks between the two areas, a comparative analysis was performed. In all, the regulated networks included the cell and organ morphology, reproductive system development and function, the cellular assembly and organization, cellular function and maintenance, cell cycle and the protein synthesis, gene expression, cell death and survival (Table 3.1.8)**.** The predominant molecular and cellular functions associated with these networks included cell growth and proliferation, gene expression, protein synthesis, cell morphology and post-translational modification. In analysis without adjusted *p*-value, activated networks are listed in Table 3.1.8.

Table 3.1.8: Regulated networks in study regions

AW vs EN[1]	SC	AW vs EN[2]	SC
Cell Morphology and Organization Morphology	39	Amino Acid Metabolism, Small Molecule Biochemistry, DNA Replication, Recombination, and Repair	37
Cellular Assembly and Organization	31	Nutritional Disease, Psychological Disorders, Cellular Assembly and Organization	30
Protein synthesis and Gene Expression	30	Cellular Assembly and Organization, Cellular Function and Maintenance, Cell Cycle	30
		Cell Morphology, Organ Morphology, Reproductive System Development and Function	29
		Cellular Assembly and Organization, Cellular Function and Maintenance, Development and Function	27

The table presents lists of regulatory networks activated in the Ahanta West compared Nzema East. [1] (FC≥1. 3, adj. *p*<0.05) and [2] (FC≥1. 3).

3.1.8 Impact of confounding factors: after removal of individuals with IVM treatment and / or other parasite infections

Almost 57.6% of the study participants (EN, n =31, MF+, n =24, MF-, n =51) were co-infected with other known parasites such as helminths or protozoa and had had prior MDA treatment (Table 3.1.9). Thus, to explore whether gene expression profiles were significantly altered after the removal of individuals with other known infections and/or had IVM treatment, further group-wise analysis was performed. While there were no differences in the gene expression pattern at

adjusted *p*-value of 0.05 and FC ≥1.3; across group comparisons, some genes were detected at FC ≥1.3, without adjusted *p*-value in the various groups as shown in Table 3.1.10.

Table 3.1.9: Rounds of IVM intake and proportion of other known parasites across study groups

	Total (N=184)	EN (N=57)	MF+ (N=52)	MF- (75)
Without IVM	N=103	N=28	N=35	N=40
1 round of IVM treatment	N=69	N=29	N=16	N=24
2 rounds of IVM treatment	N=12	-	N=1	N=11
Plasmodium falciparum	N=5	N=2	-	N=3
P. falciparum + Giardia	N=2	-	-	N=2
P. falciparum + Ascaris	N=1	-	-	N=1
P. vivax	N=1	-	-	N=1
Giardia	N=4	-	N=1	N=3
Ascaris	N=8	N=2	N=2	N=4
Ascaris + Hookworm	N=2	-	-	N=2
Trichuris	N=4	-	N=1	N=3
Hookworm	N=3	-	N=3	-
Schistosoma	N=1	-	-	N=1
No other infection or round of IVM	N=78	N=26	N=28	N=24

The table describes rounds of ivermectin (IVM) intake and the number (N) other parasites across study groups.

Table 3.1.10: Regulated genes in *W. bancrofti*-infected groups and EN individuals without co-infection and/or IVM treatment

Groups	FC≥3;adj.*p*<0.05	FC≥3
Patent v latent	0	204
Patent v EN	0	94
Latent v EN	0	139

The table describes differentially expressed genes across study groups after removal of individuals who have other known infections (Helminth, Protozoa or Malaria) and had IVM treatment.

3.1.8.1 Comparison of regulated genes, canonical pathways and networks of patent and latent infection after removal of individuals with IVM treatment and/or had other parasite infections

The classification into patent and latent groups provides a framework for understanding the immune regulation in infected individuals. Since the primary aim of this study was to identify the factors that drive these two infection phenotypes, further analyses were performed to explore *W. bancrofti*-specific determinants between these groups. Here, the top 5 highly regulated genes are described. When compared to latent infected individuals, genes such as granzyme B (*GZMB*), granzyme A (*GZMA*), granzyme H (*GZMH*), granulysin (*GNLY*), myomesin 2

(*MYOM2*)*,* chemokine ligand 5 (*CCL5*) were upregulated in patently infected, whilst carbonic anhydrase 1 (*CA1*)*,* membrane protein palmitoylated 1 (*MPP1*)*,* aminolevulinate, delta-synthase 2 (*ALAS2*) and interferon, alpha-inducible protein 27 (*IF127*) were down regulated in the patently infected individuals as shown in Table 3.1.11.

Table 3.1.11: Number of statistically significant differentially expressed genes identified across comparisons in individuals without IVM treatment

MF+ vs MF-[2]	FC	MF+ *vs* EN[2]	FC	MF- vs EN[2]	FC
UP-REGULATED					
GZMB	1.84	*HLA-DRB1*	1.97	*HLA-DRB1*	1.91
GZMH	1.67	*RPS4Y1*	1.73	Unknown	1.52
GNLY	1.61	Unknown	1.61	*RPS4Y1*	1.51
MYOM2	1.61	*LOC644936*	1.46	*LYZ*	1.49
Unknown	1.53	*LOC100133678*	1.43	*LYZ*	1.47
FGFBP2	1.52	Unknown	1.42	*S100A8*	1.43
LOC100133678	1.51	*ZFAND5*	1.41	*C1orf128*	1.40
GZMA	1.49	*RPS29*	1.41	*CA1*	1.40
RASSF6	1.46	*CTSZ*	1.4	*MPP1*	1.39
CCL5	1.46	*ARGLU1*	1.4	*LOC644936*	1.39
DOWN-REGULATED					
Unknown	-2.00	Unknown	-1.97	*GZMH*	-1.78
CA1	-1.93	*SPRYD3*	-1.75	*GZMB*	-1.62
MPP1	-1.85	Unknown	-1.74	*GNLY*	-1.56
ALAS2	-1.80	*DPYSL5*	-1.71	*BLZF1*	-1.48
IFI27	-1.78	Unknown	-1.65	*TNFSF15*	-1.45
SNCA	-1.78	*MUC6*	-1.62	*ZNF577*	-1.44
SELENBP1	-1.77	*LOC100131391*	-1.60	*TRIM13*	-1.44
C1orf128	-1.66	*RN18S1*	-1.59	*SEMA3E*	-1.42
SLC4A1	-1.65	Unknown	-1.56	*LOC100128288*	-1.42
EPB42	-1.60	*IFI27*	-1.54	*GZMA*	-1.42

Table lists regulated genes in patent, latent infected and EN (after removal of individuals with other helminths and had IVM treatment) in which expression had exceeded 1.3 fold [2] (FC≥1. 3).

Canonical pathways predicted on IPA to be involved in the patently infected relative to latently infected were the chemokine signaling (*p*<1.40E-03), which associates with *CCL5*, granzyme B signaling (*p*<5.66E-03) which happens to be activated by *GZMB*. The granzyme A signaling (*p*<6.38E-03) pathway known to be regulated by G*ZMA*, while calcium signaling (*p*<7.38E-03) and NFAT signaling (*p*<8.31E-03) associate with *MYOM2* (Table 3.1.12).

Table 3.1.12: Regulated pathways in *W. bancrofti*-infected and EN individuals without co-infection and IVM treatment

MF+ vs MF-[2]	MF+ vs EN[2]	MF- vs EN[2]
Chemokine signaling	Regulation of eIF4 and p70S6K Signaling	Superoxide Radicals Degradation
Granzyme B signaling	EIF2 signaling	Ethanol Degradation IV
Granzyme A signaling	T helper Cell Differentiation	Semaphorin signaling in Neurons
Calcium signaling	B Cell Development	Amyotrophic Lateral Sclerosis signaling
NFAT signaling	Crosstalk between Dendritic Cells and Natural Killer Cells	Mitochondrial Dysfunction

The table describes the canonical pathways for genes whose fold change exceeded (FC ≥1.3) in the MF+, MF- and EN groups, [2] (FC≥1. 3).

Table 3.1.13: Regulated networks in *W. bancrofti*-infected and EN individuals without co-infection and/or IVM treatment

MF+ vs MF-[2]	SC	MF+ vs EN[2]	SC	MF- vs EN[2]	SC
Antimicrobial Response	46	Cell Death and Survival, Cellular Assembly and Organization, Cellular Compromise	39	Cellular Development, Organismal Survival, Nervous System Development and Function	20
Amino Acid Metabolism Small molecules	36	Cell Morphology, Cellular Function and Maintenance, DNA Replication, Recombination, and Repair	34		
Dermatological diseases	33	Nervous System Development and Function, Tissue Development, Tissue Morphology	30		
Metabolism Disease, Cellular Compromise	29	Carbohydrate Metabolism, Developmental Disorder, Gastrointestinal Disease	26		
Small Molecular , Nucleic acid Metabolism Cellular Movement	27	Cell Death and Survival, Cellular Assembly and Organization, Cellular Compromise	2		

The table lists networks activated in comparisons of these groups: MF+, MF+ and EN [2] (FC≥1. 3). SC: score.

Activation of these pathways suggests enhanced innate and adaptive immune responses in patently infected individuals with only *W. bancrofti* infection. On regulated networks, the antimicrobial response network was identified with a score of 46 (Figure 3.3) and (Table 3.1.13), while the amino acid metabolism small molecules network had the second highest score of 36. The third, fourth and fifth networks had scores of 33, 29 and 27, respectively as shown in Table 3.1.13. These networks correlate with antimicrobial activity, small molecules biochemistry, phagocytosis, nucleic acid metabolism, cell-to-cell signaling and interactions, cell death and survival.
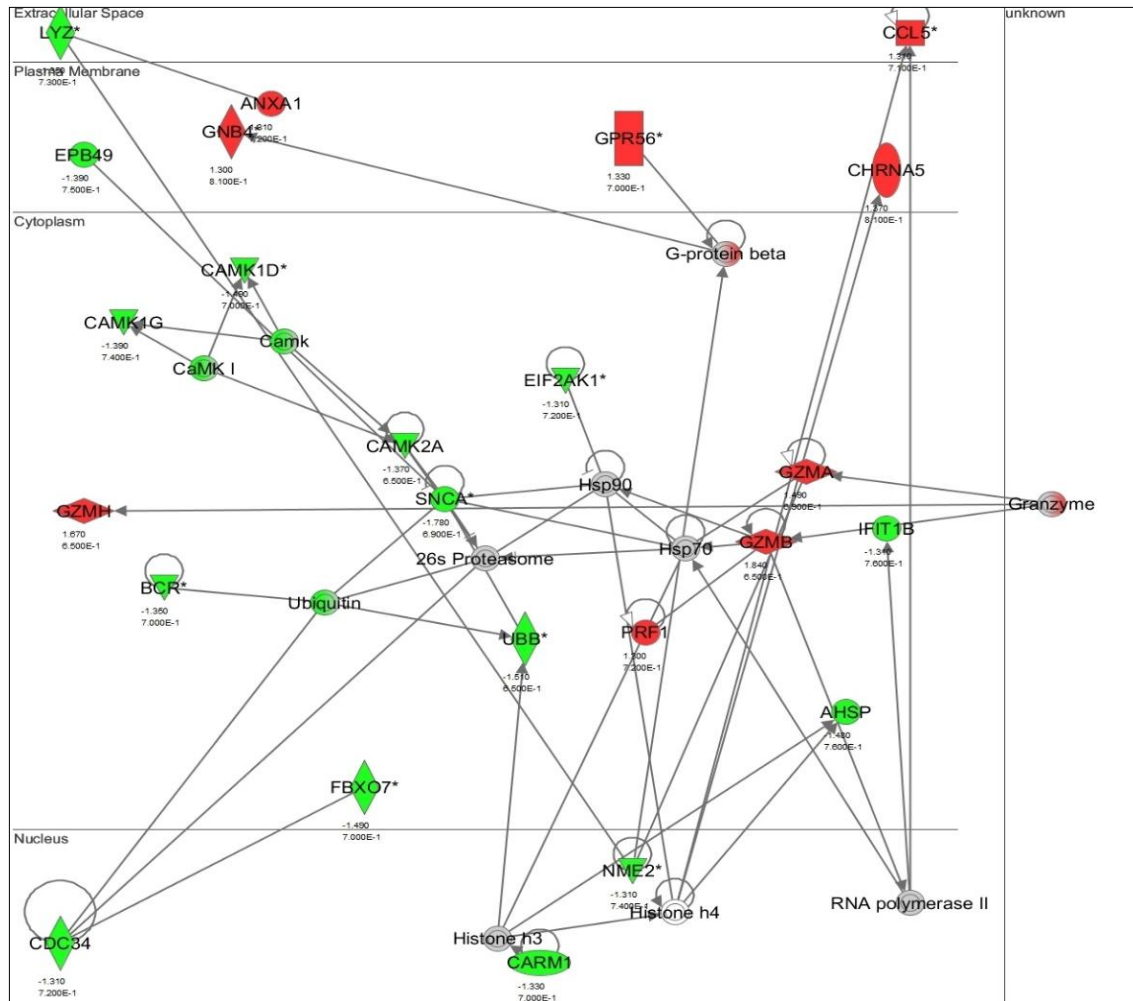
Figure 3.3: Antimicrobial response network in patent relative to latent infected individuals.

Genes were differentially expressed at FC≥1. 3. Lines represent direct relationships between molecules. Up-regulated genes are highlighted in red, down-regulated genes are shown in green; whereas gray indicates genes not differentially expressed but with defined relation to other genes in the network. (Key: circle=transcriptional regulator, upright diamond=enzyme, tranverse diamond=peptidase, rectangle=G protein coupled receptor, trapezoid= transporter, oval= transmembrane receptor, square=cytokine, triangle=phosphatase, small circle=other)

3.2 *Onchocerca volvulus* infection

3.2.1 Characteristics of study population: *Onchocera volvulus* infection

Similarly, 224 individuals were recruited for the *O. volvulus* study. Study subjects were categorized as EN (n =58), MF+ (n= 114) and a-MF (n=52), depending on skin MF and nodule. Of these, 102 (45.5%) were female and 122 (54.5%) were male. The median age for individuals in this study was similar as described for the *W. bancrofti* study. The proportion of MF/skin mg ranged from 0.1-86.10 MF/mg. The number of nodules was higher in MF+ compared to a-MF

individuals. In this study, percentage of rounds of IVM intake for 0/1 is for EN: 69% and 31%, MF+ = 60.5% and 39.5%, a-MF= 53.8% and 48.2%. The number of individuals with co-infection is also indicated in Table 3.2.1. For the *O. volvulus* infection study, microarray experiments were only performed between the EN and MF+ groups.

Table 3.2.1: Characteristics of the study population *O. volvulus* infection

	EN (n=58)	MF+ (n=114)	a-MF (n=52)
Age (median)	40 (18-55)	40 (19-55)	38.5 (19-55)
Sex (F/M)	37/21	42/72	23/29
MF load (mg/skin)	-	8.99 (0.1-86.10)	-
Number of nodules	-	1.97 (1-9)	1.16 (1-5)
Rounds of IVM (0/1)	40/18	69/45	28/24
Co-infections	11	20	9

Age: median (range); sex: number of (F/M=female/male); IVM: rounds (0, or 1); MF count: mean (range); EN: endemic normals; MF: microfilaria, amicrofilaridermia: a-MF.

3.2.2 Transcriptomics of *O. volvulus*-infected compared to EN using ingenuity pathway analysis (IPA)

Analysis of the transcriptome was performed on whole blood derived from *O. volvulus*-infected individuals. The methods are equal to those described for the *W. bancrofti* infection. In the first comparison, none of the genes exceeded the cut-off as described in section 3.1.2. Therefore, the second comparative analysis approach was applied, after which 10 genes were identified (Table 3.2.2).

Table 3.2.2: Differentially expressed genes identified across comparisons in *O. volvulus*-infected compared to EN.

O. volvulus infection	adj. *p*<0.05;FC≥ 1.3	FC≥1.3
Infected (MF+) vs EN	0	10

The table presents the number of genes whose expression in the *O.volvulus*-infected compared to EN exceeded 1.3 fold (FC ≥1.3). Microarray data are denoted for those genes that demonstrated an FDR less than 0.05; associated with or without adjusted *p*-values.

3.2.3 Comparison of regulated genes, canonical pathways and networks of *O. volvulus*-infected vs EN

A fascinating feature that characterizes onchocerciasis infection lies in the fact that the majority of infected individuals harbours relatively high parasite loads with an average of approximately 1-500 MF/mg skin [5]. This infection phenotype suggests a more compromised immune response hence promoting adult worm development. Transmission of infection is facilitated by

the large number of MF released by the worm over its average life expectancy of 10 years and the immunoregulatory mechanisms by the worm which facilitates MF survival. To delineate the underlying molecular mechanisms in this infection, the transcriptome data between the *O. volvulus*-infected was compared to endemic normals.   Ten (10) genes were found to be expressed exceeding a cut-off at 1.3 fold (FC≥1.3) (see Table 3.2.3). Most of these up-regulated genes have a strong association with effector functions of eosinophils and include: Charcot-Leyden crystal protein (*CLC*)*,* ribonuclease, RNase A family, 2 (*RNASE2*)*,* ribonuclease, RNase A family, 3 (*RNASE3*)*,* chemokine receptor 3 (*CCR3*) and CD24 molecule (*CD24*) and neutrophils which comprise of: catalase (*CAT*)*,* defensin, alpha 1 (*DEFA1*) and cathelicidin antimicrobial peptide (*CAMP*)*,* defensin, beta1 (*DEFB1*). Interestingly, it was observed that genes, such as *CLC, RNASE2 and RPS4Y1* were the most commonly up-regulated transcripts which popped-up across the comparisons in the *W. bancrofti* infection as described in Table 3.1.3.

Table 3.2.3: Differentially expressed genes in *O. volvulus*-infected relative to EN

(Infected vs EN)[2]	UP-REGULATED GENES	FC
	CLC	1.89
	RNASE2	1.68
	RPS4Y1	1.65
	DEFA1	1.55
	RNASE3	1.47
	CAT	1.40
	CCR3	1.37
	CD24	1.36
	CAMP	1.34
	DEFB1	1.33

This table shows genes whose expression in the *O. volvulus*-infected patients exceeded that of endemic normals 1.3 fold [2] (FC ≥1. 3), Endemic normals. Microarray data are denoted for those genes that demonstrated an FDR of less than 0.05; without adjusted *p-* values. FC, Fold change.

Within this comparison, 10 canonical pathways were predicted by IPA. Among the top 8 regulated canonical pathways identified in the *O. volvulus*-infected subjects included the chemokine signaling ($p<4.06E-02$) and CCR3 signaling in eosinophils ($p<6.60E-02$), which supports the involvement of eosinophils in *O. volvulus* infection. In addition, pathways such as superoxide radicals degradation ($p<3.64E-03$) [135], ethanol degradation IV ($p<1.03E-02$) associate with eosinophil metabolism as well as the protein synthesis regulatory signaling,

whereas VDR/RXR Activation ($p<4.58E-02$) promotes Th2 differentiation. Th2 responses and eosinophil function are important players in the defence against helminth parasites, such as filariae. Regulation of eIF4 and p70S6K signaling ($p<8.30E-02$) and EIF2 signaling ($p<9.92E-02$) involved in protein synthesis were also found to be up-regulated in the infected group compared to endemic normals Table 3.2.4.

Table 3.2.4: Regulated canonical pathways in *O. volvulus*-infected relative to EN

(Infected vs. EN) [2]	Superoxide Radicals Degradation
	Ethanol Degradation IV
	Chemokine signaling
	VDR/RXR Activation
	Amyotrophic Lateral Sclerosis signaling
	CCR3 signaling in Eosinophils
	Regulation of eIF4 and p70S6K signaling
	EIF2 signaling

The table describes the canonical pathways for genes whose folds change exceeded [2] (FC ≥1. 3) in *O. volvulus*-infected patients relative to endemic normals (EN). *P*-values were determined using the two-sided Fisher's exact test [137].

As described for *W. bancrofti* infection, the regulatory networks induced in *O. volvulus*-infected individuals compared to EN group were determined. Regulatory networks between the infected versus EN identified included the infectious diseases, respiratory diseases and cellular movement, hematological system development and function, hypersensitivity responses (Table 3.2.5).

Table 3.2.5: Regulated networks in *O. volvulus*-infected relative to EN

(Infected vs EN)[2]	Networks	SC
	Infectious Disease, Respiratory Disease, Cellular Movement	23
	Cellular Movement, Hematological System Development and Function, Hypersensitivity Response	2

The table shows regulatory networks activated in the *O.volvulus*-infected individuals against EN. [2] (FC≥1. 3). SC: score.

These networks associate with bio-functions, such as chemotaxis of eosinophils, neutrophils as well as cell movement of phagocytes. In the first regulatory network, although not being themselves activated, the main nuclear localized transcriptional factors were NF-kappa B complex and STAT3 seem to contribute essential to the function of this network (Figure 3.4) as they are known to involve in p38MAPK and ERK1/2 phosphorylation resulting in increased NF-

kappa B activity [136]. Interesting among the activated genes in this network was *CLC*. *CLC* regulate important cytokine signaling proteins, such as JAK1, JAK2 and STAT3 and were themselves regulated by the IL-6 signal transduction. These genes associate with the function and development of eosinophil and neutrophil activated, indicating the importance of these cells during *O. volvulus* infection.
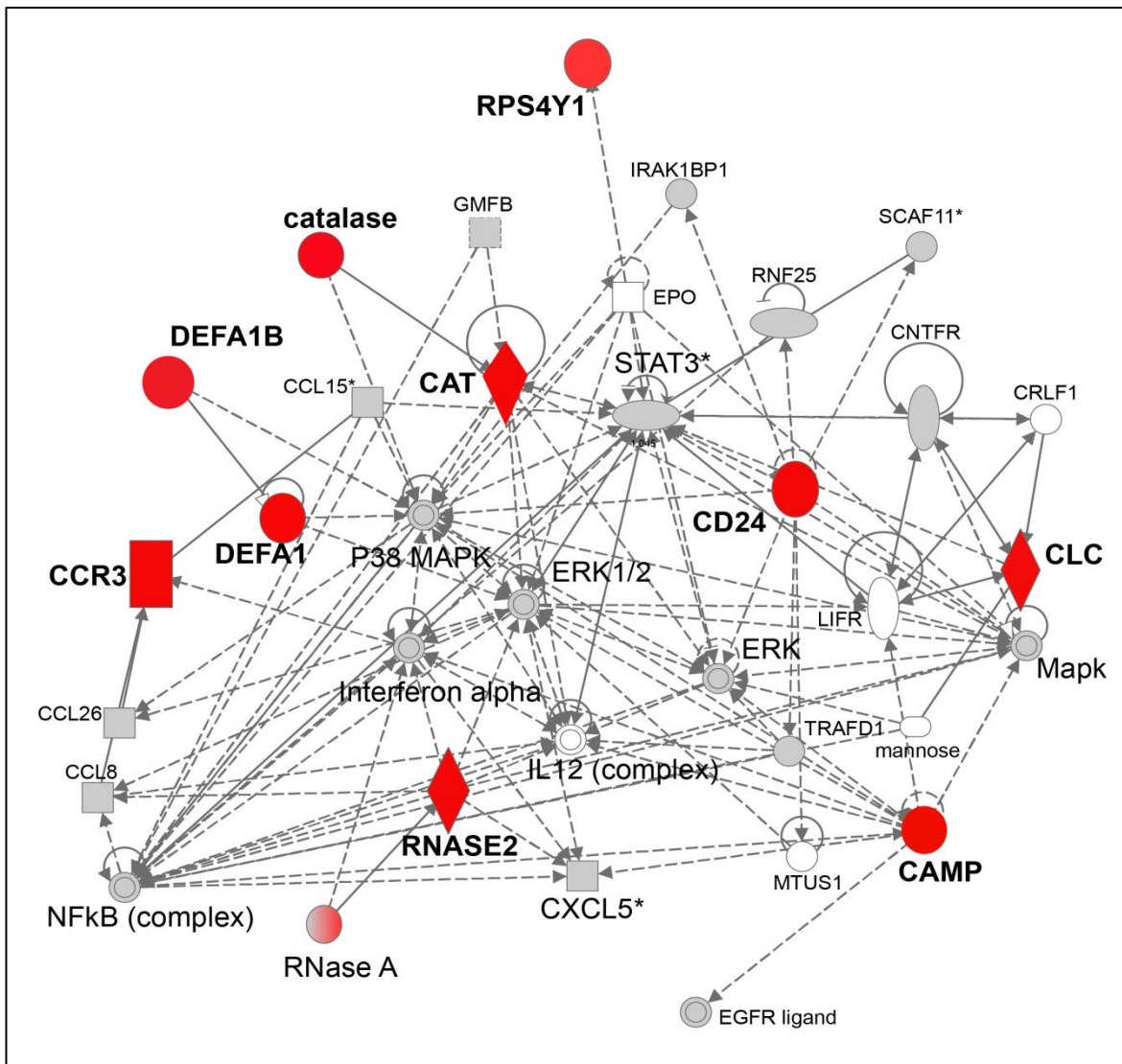
Figure 3.4: Infectious disease, respiratory diseases and cellular movement network in *O. volvulus*-infected patients relative to EN.
Genes were differentially expressed at FC≥1. 3. Lines represent direct (solid lines) and indirect (dashed lines) relationships between molecules. Up-regulated genes are highlighted in red, whereas gray indicates genes not differentially expressed but with defined relation to other genes in the network. (Key: circle=transcriptional regulator, upright diamond=enzyme, rectangle=G protein coupled receptor, oval=transmembrane receptor, square=cytokine, triangle=phosphatase, double circle=complex group, small=other)

3.2.4   Impact of confounding factors

Similarly, gene expression profiles from individuals with *O. volvulus* infection were performed to determine whether other confounding factors influenced our gene expression data. However, none of the factors analysed was found to influence the transcriptomic data in these cohorts.

3.2.5   Summary of the top ten differentially regulated genes in *W. bancrofti* and *O. volvulus*-infected subjects

Comparative transcriptome analysis across the various infection groups revealed that inasmuch as both filarial parasites induced several different sets of genes, three genes were similarly expressed. While more genes were regulated in *W. bancrofti*-infected individuals, the intensity of expression (fold change) was stronger in the *O. volvulus*-infected group. Such differential regulation suggests that different filarial parasites induce specific immune responses despite their evolutionary similarities. Genes induced by *W. bancrofti*-infected are shown in the left circle, whereas the right circle contains set of genes highly expressed in *O. volvulus*-infected subjects (Figure 3.5). Two of the three differentially expressed genes (*CLC* and *RNASE-2*) are known to enhance both the development and functions of eosinophils, while the third gene, *RPS4Y1* associates with gender clustering in the data set. Such regulations reliably confirm previous reports on the role eosinophils in filarial biology. The next section of the results will focus on selected genes regulated in the transcriptome data, such as *CLC/Gal-10*, *GZMB* and *GZMA* among others that were further characterized at the *in vitro* level in order to establish their role in filarial infections.
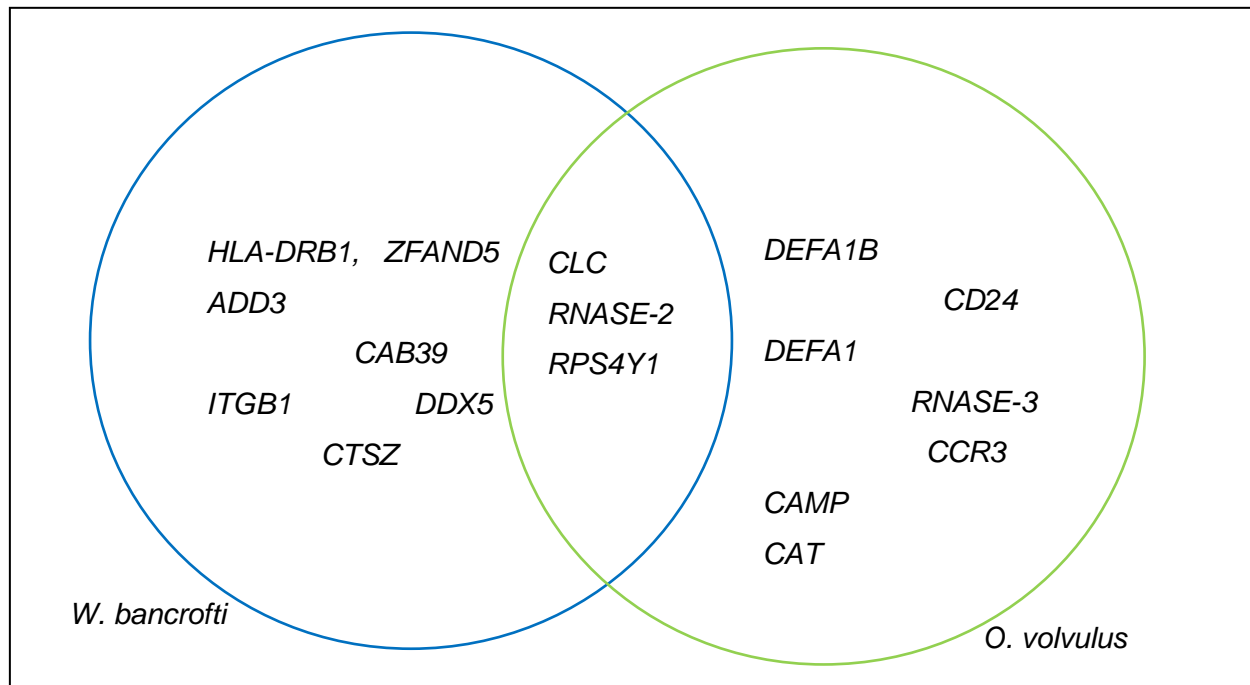
Figure 3.5: Ten most highly regulated genes in *W. bancrofti* and *O. volvulus*

3.3   Higher levels of CLC/Galectin-10 protein in plasma from MF+ infected individuals

To confirm the up-regulation of the *CLC/Gal-10* gene in the microarray data (*W. bancrofti* and *O. volvulus*), see Tables 3.1.3 and 3.2.3, *CLC/Gal-10* was further investigated at the protein level. To this, CLC/Gal-10 protein levels in plasma from the study participants (in both infection cohorts) whose blood was previously subjected to the transcriptome study were measured by ELISA. In keeping with the gene expression data, there were significantly higher levels of CLC/Gal-10 in the plasma of both *W. bancrofti* and *O. volvulus*-infected individuals when compared to levels in EN (Figures 3.6 A and B), respectively.
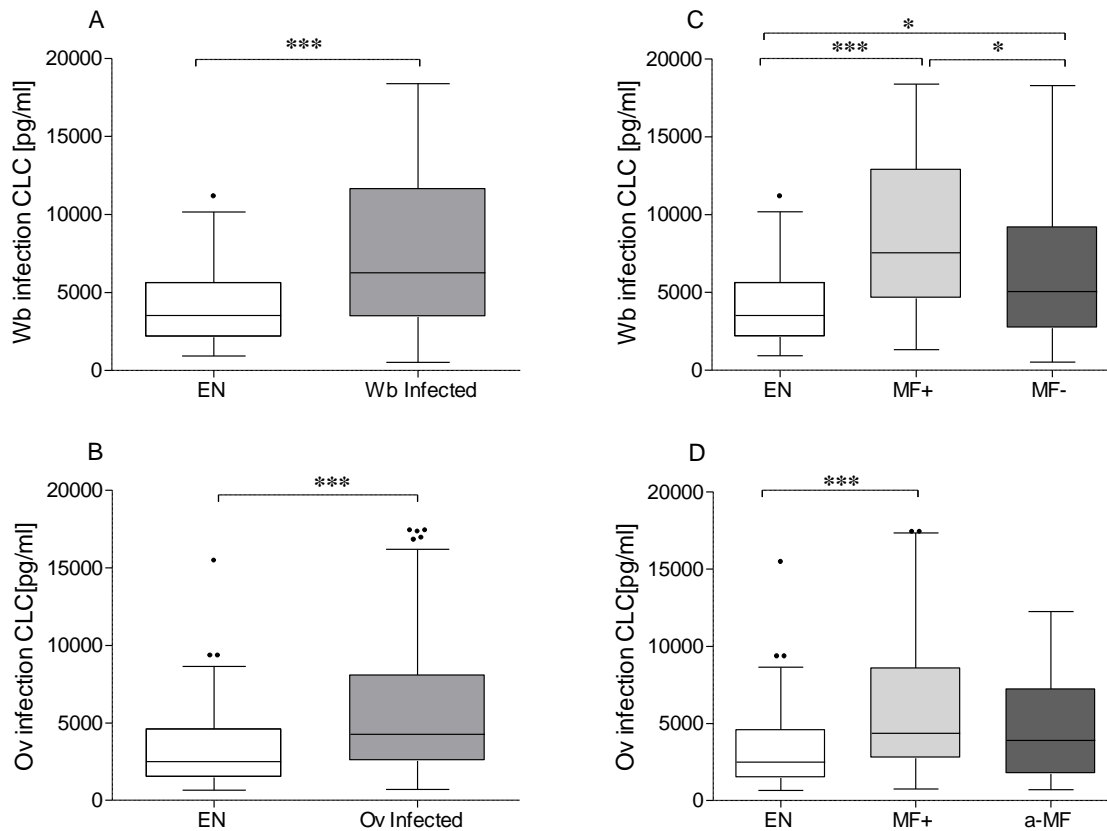
Figure 3.6: Plasma levels of CLC/Gal-10 protein in filarial-infected subjects compared to the EN group.
A and B represent the amount of plasma CLC/Gal-10 in individuals with *W. bancrofti* and *O. volvulus* infections compared to EN, respectively, whereas C and D depict levels CLC/Gal-10 in subjects with *W. bancrofti* (EN=47, MF+=48, MF+ n=70) and *O. volvulus* (EN n=58, MF+ n=114, MF- n=52) based on infection status. The levels of CLC/Gal-10 (pg/ml) were measured using ELISA. Graphs show box whiskers with outliers. Data of each group were compared using Kruskal-Wallis test and Mann-Whitney test and significant differences are given as *p< 0.05, **p< 0.01 and ***p<0.001.

A subsequent analysis within the groups based on MF status showed increased levels of plasma CLC/Gal-10 protein in infected individuals that were MF+ when compared to EN or those not presenting MF in both infections (Figures 3.6 C and D). The level of CLC/Gal-10 was also significantly higher in MF- or a-MF patients when compared to the EN group. In contrast to the protein expression data, the level of CLC/Gal-10 in the gene expression data was higher in MF- when compared to MF+ (Table 3.1.3).

3.3.1 Relationship between levels of CLC/Gal-10 protein in plasma and peripheral blood or skin MF

The role of CLC/Gal-10 protein continues to be debated. While it is believed to have protective immunity, recent studies have attributed it with regulatory functions [69]. In filariasis, individuals without MF have enhanced adaptive immune responses, while the presence of MF is associated with immunosuppression. Since the data described above showed that CLC/ Gal-10 levels are higher in infected individuals and more importantly in MF+ patients, further investigations were performed, namely a correlation between the CLC/Gal-10 level and the number of MF. Albeit being highly expressed in MF+ individuals, there was no correlation between MF levels and the plasma levels of CLC/Gal-10 (Figures 3.7 A and B) using the Spearman correlation test. This was consistent for both infections. It has to be noted that MF load of patients does not reflect the adult parasite load, as they do undergo reproductive cycles, leading to varying MF levels in the periphery.
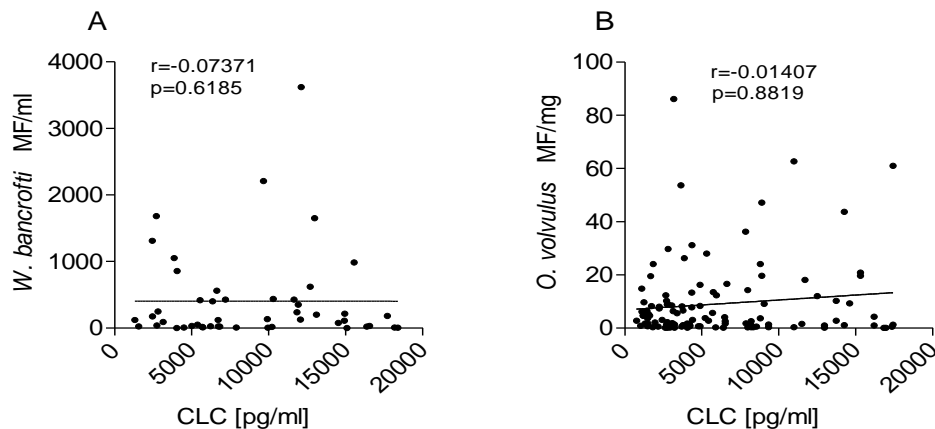
Figure 3.7: CLC/Gal-10 protein levels in plasma do not correlate with peripheral MF.
The levels of CLC/Gal-10 protein in plasma and peripheral blood or dermal MF counts were correlated for both sets of filarial-infected individuals as shown in (A) *W. bancrofti* (r=-0.07371; *p*=0. 6185), and (B) *O. volvulus* (r=-0.01407; *p*=0. 8819), respectively. As indicated, there was no correlation between CLC/Gal-10 protein and peripheral blood or skin MF in both infections using non-parametric Spearman test.

3.3.2 Increased frequency of peripheral eosinophil in absence of MF

Increased expression of eosinophil and neutrophil-associated transcripts were observed in the transcriptome data. Interestingly, the most commonly regulated transcript (CLC/Gal-10) in the transcriptome of both studies is primarily produced by eosinophils. Eosinophils promote protective immunity in filarial infections [137] and as such contribute significantly to filarial infection outcome. Eosinophils in addition to basophils and mast cells contain granules and are the cells, which attack extracellular large parasites. To investigate whether filarial nematodes

lead to alterations in blood cell types, blood smears of study subjects were assessed for the absolute cell counts of eosinophils and neutrophils using standard Grünwald-Giemsa staining procedure.
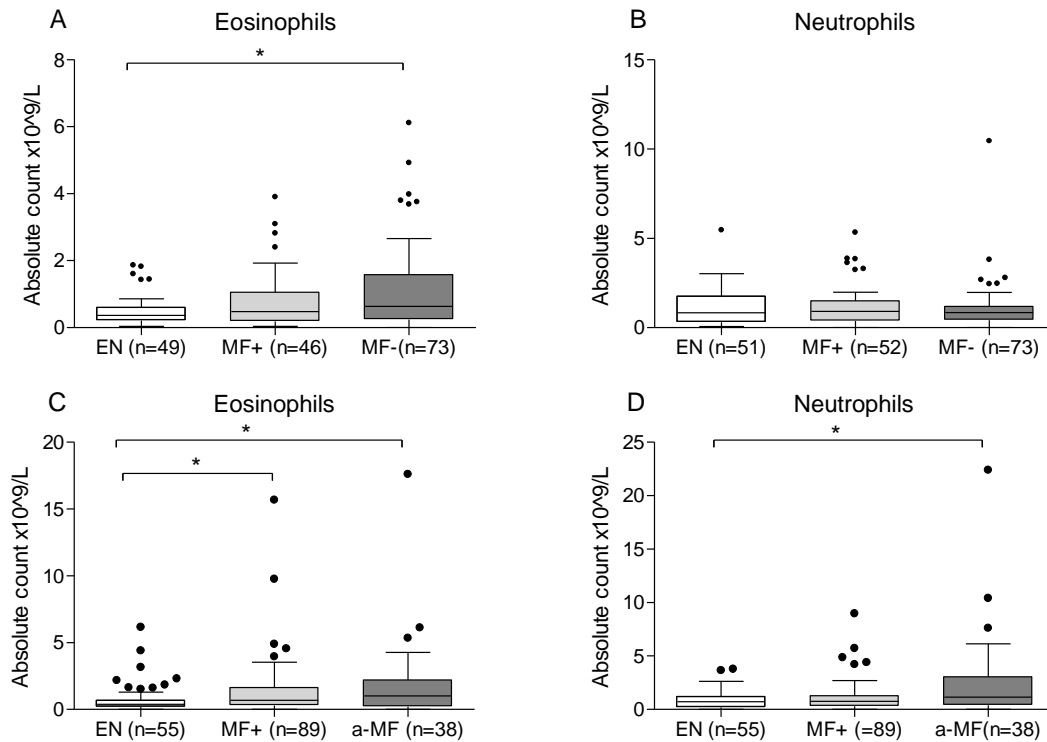
Figure 3.8: Frequencies of blood eosinophils and neutrophils in individuals with filarial infections.
Total white blood counts were determined with a haemocytometer. The absolute numbers of leukocytes were determined from differential counts in peripheral blood smears stained with a pre-diluted May-Grünwald solution (Carl Roth, Karlsruhe, Germany) and Giemsa solution (Merck, Darmstadt, Germany). The absolute number was calculated from the white blood cell count and differential count. Results show increased eosinophil and neutrophil numbers in the *W. bancrofti-*and *O. volvulus-*infected individuals compared to their endemic normals. Frequencies of eosinophils in *W. bancrofti* study (EN=49, MF+=46, MF-=73) (A) and neutrophils in *W. bancrofti* study (EN=51, MF+=52, MF-=73) (B) are described. Similarly, in *O. volvulus* infection, frequencies of eosinophils (EN=55, MF+=89, a-MF=38) (C) and neutrophil (EN=55, MF+=89, a-MF=38) (D) are shown. Graphs show box whiskers with outliers. Data of each group were compared using Kruskal-Wallis test and Mann-Whitney test and significant differences are given as *p< 0. 05.

In the *W. bancrofti*-infected subjects, there was a significant difference in eosinophil numbers between MF- and EN (Figure 3.8 A), but no differences in the neutrophil population were observed (Figure 3.8 B). In the onchocerciasis study, significant differences were observed in eosinophil and neutrophil numbers (Figures 3.8C and D) when the a-MF group was compared to EN. Again, the number of eosinophils was highly distinct in the MF+ individuals relative to EN. In this study, while the number of eosinophils and neutrophils was elevated in individuals without MF in both infections compared to EN, there was no significant difference in

lymphocytes, and monocytes populations among the study groups (data not shown). The higher levels of eosinophils and neutrophils in a-MF *O.volvulus*-infected patients may suggest protective function against MF themselves or MF production/embryogenesis. To establish whether the presence of eosinophils and neutrophils associates with MF load in both infections, the levels of these cells were assessed. While a moderate correlation between blood eosinophils and skin MF was found in the onchocerciasis study, no association was found in eosinophil and neutrophil numbers with MF counts in either infection cohort, (data not shown). The findings confirm that filarial infections actively induce peripheral eosinophils, albeit not very strongly.

3.4 Characterization of T lymphocytes in PBMCs from individuals with *W. bancrofti* infection: *Ex-vivo* (Base line) expression pattern

3.4.1 Increased frequencies of CD4$^+$ and CD8$^+$ T cells in individuals with *Wuchereria bancrofti* infection

Results in this study showed elevated numbers of peripheral eosinophils but not neutrophils in subjects with *W. bancrofti* infection, while in the onchocerciasis study both eosinophils and neutrophils were higher in infected individuals compared to EN individuals. Since eosinophils are the main source of CLC/Gal-10, it was of interest to further characterize the expression of this molecule in eosinophils under *in vitro* settings. However, this was not possible in this study because of the challenge associated with obtaining eosinophils from the study patients. Additionally, eosinophils are known to release many granules following activation, hence *in vitro* detection of eosinophil-producing molecules such as CLC/Gal-10 may be associated with the issue of non-specific binding. However, recent studies have shown that in addition to eosinophils, T cells are a potential source of CLC/Gal-10 in human PBMCs. In general, T cells are essential for host immunity and are primarily divided in two main subtypes: T helper (CD4) and cytotoxic (CD8) T cells. Therefore, the study used T cell lymphocytes as surrogate cells to investigate cytokines which support granulocyte recruitment during filarial infection. For *in vitro* assessment of T cell responses, 10 samples from each group were randomly selected from the *W. bancrofti* study. To investigate whether *W. bancrofti* infection alters the differentiation of T lymphocytes, the frequencies of CD4$^+$ and CD8$^+$ T cells in PBMCs from MF+, MF- and EN individuals were determined. In short, without prior stimulation, PBMCs were stained with anti-CD4 and anti-CD8 surface antibodies and analysed using flow cytometry.
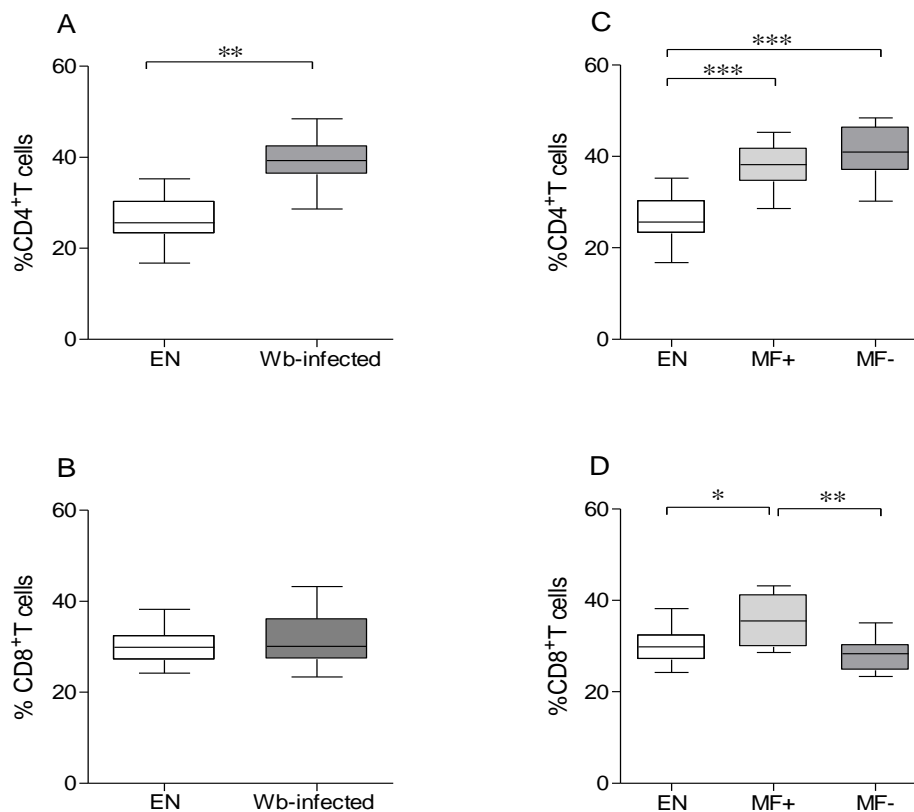
Figure 3.9: Increased frequencies of CD4$^+$ and CD8$^+$ T cells in *W. bancrofti*-infected individuals.
PBMCs from EN and MF+ and MF- subjects were stained for CD4$^+$ and CD8$^+$ T cells (A and B) EN verses Wb-infected individuals, respectively. Similarly, based on infection status, CD4$^+$ and CD8$^+$ T cells (C and D) are shown. Cell population frequencies were determined via flow cytometry. Graphs show percentages of box whiskers with outliers from (EN n=10, MF+ n=10 and MF- n=10). Data of each group were compared using ANOVA (Bonferroni's multiple comparison test and T test); significant differences are given as *p<0.05, **p<0.01 and ***p<0.001.

As shown in Figure 3.9A and B, when compared to EN, there were significantly higher frequencies of CD4$^+$ T cells but not CD8$^+$ T cells in *W. bancrofti*-infected individuals. Interestingly, upon further analysis and based on infection status, MF- and MF+ persons presented significantly higher frequencies of CD4$^+$ T cells compared to EN but frequencies in the infected groups were comparable (Figure 3.9C). With regard to CD8$^+$ T cells, MF+ individuals exhibited significantly higher frequencies of CD8$^+$ T cells when compared to EN and latently-infected individuals (Figure 3.9D). These results indicate that infections with *W. bancrofti* induce high proportions CD4$^+$ and CD8$^+$ T cells, which may influence outcome of infection.

3.4.2 Increased frequencies of T-bet⁺, GATA-3⁺ and RORC2⁺ in MF- subjects, whereas FOXP3⁺ is pronounced in the CD4 T cells in MF+ individuals

Having observed the cytokine profiles in all three study cohorts, we were interested in the patterns of T cell lineage transcriptional factors. To do this, the baseline expression profiles of Th1 (Tbet), Th2 (GATA-3), Th17 (RORC2) and Tregs (FOXP3) transcriptional factors were determined in all study groups. There were no significant differences in the expression levels of CD4$^+$Tbet$^+$ T cells in all study groups, however there was a tendency of increased expression in MF- subjects (Figure 3.10A).
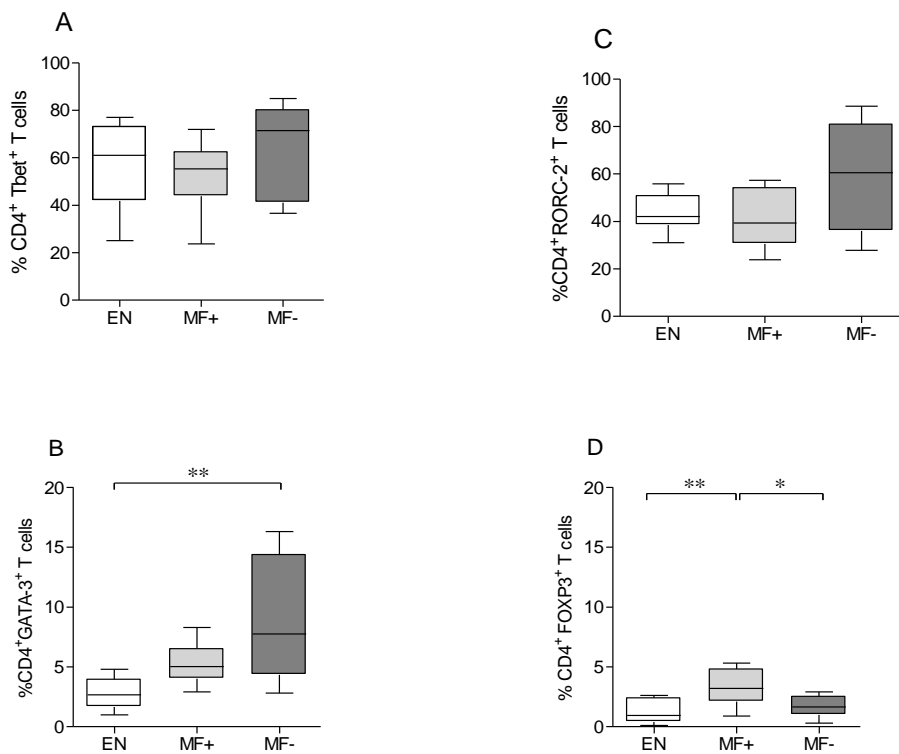
Figure 3.10: Elevated frequency of FOXP3 in CD4$^+$ T cells from MF+ infected subjects, while T-bet, GATA-3 and RORC-2 were enhanced in MF- individuals.
PBMCs were isolated from EN and MF+ and MF- subjects and stained for CD4 and transcriptional factors, T-bet (A), GATA-3 (B), RORC-2 (C) and FOXP3 (D) in each individuals (EN n=8, MF+ n=8 and MF- n=8). Cell population frequencies were determined with flow cytometry. Graphs show percentages of box whiskers plot with outliers. Data of each group were compared using ANOVA (Bonferroni's multiple comparison test); and significant differences are given as *p<0.05 and **p<0.01.

It was observed however that the CD4$^+$GATA-3$^+$ T cells were significantly higher in MF- individuals compared to EN, while there were no differences between the MF+ persons (Figure 3.10B). Additionally, there were no distinct differences in the expression levels of the Th17 transcriptional factor, RORC2 in all study groups, but again, there was an increased tendency in the MF- individuals (Figure 3.10C). When compared to the EN, the expression frequency of

CD4$^+$FOXP3$^+$ T cells was significantly distinct in MF+ (Figure 3.10D). Thus, the results shown demonstrate that MF- individuals have a strongly increased Th2 profile with elevated Th1 and Th17 lineages too whereas MF+ individuals had a strong FOXP3 expression. These findings are consistent with the cytokine data which showed elevated IL-17 and slight increase in IL-4 although not significant in MF- individuals; while IL-10 was predominant in the MF+ persons (section 3.5.1).

3.4.3 Elevated frequencies of CLC/Gal-10 expressing CD4$^+$ and CD8$^+$ T cells in patently-infected *W. bancrofti* individuals

Although, CLC/Gal-10 is primarily produced by eosinophils, T cells have also been shown to secrete this molecule [69]. Thus, following the up-regulation of the *CLC/Gal-10* gene in our microarray data (*W. bancrofti* and *O. volvulus,* see sections 3.1.4 and 3.2.3), the intracellular expression CLC/Gal-10 in CD4$^+$ and CD8$^+$ T cells in PBMCs from *W. bancrofti*-infected and EN individuals was determined using flow cytometry. When compared to levels in EN, CLC/Gal-10-expressing CD4$^+$ T cells were higher in individuals with *W. bancrofti* infection (Figure 3.11A).
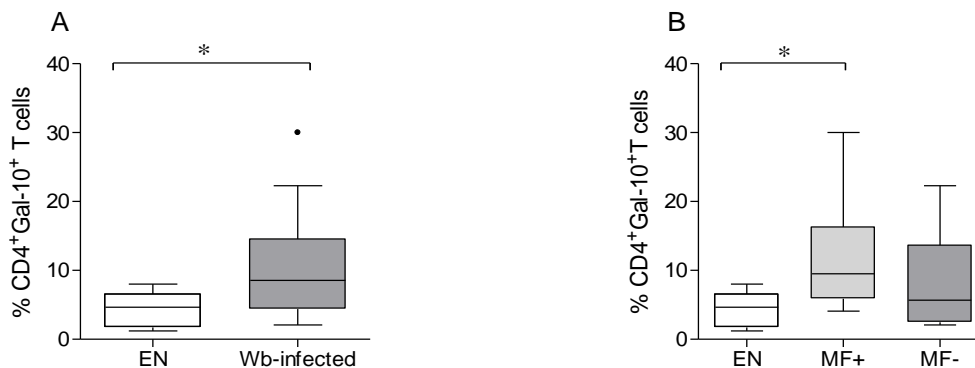
Figure 3.11: Increased frequencies of CLC/Gal-10-expressing CD4$^+$ T cells in individuals with *W. bancrofti* infection.
PBMCs were isolated from EN and MF+ and MF- subjects and stained with antibodies to determine the frequencies of CD4$^+$ and CD8$^+$ expressing CLC/Gal-10 T cells by flow cytometry. (A) presents frequencies of CD4$^+$ T expressing CLC/Gal-10 T cells, comparing EN and *W. bancrofti*-infected group, whilst (B) shows frequencies of CD4$^+$ T expressing CLC/Gal-10 based on infection status. Graphs show percentages of box whiskers plots with outliers from EN n=10, MF+ n=10 and MF- n=10. Data of each group were compared using ANOVA (Bonferroni's multiple comparison test) and significant differences are given as *$p < 0.05$.

Further investigation revealed that the frequency CLC/Gal-10 expressing CD4$^+$ T cells was more predominant in the MF+ individuals when compared to EN individuals (Figure 3.11B). The frequency of CLC/Gal-10-expressing CD8$^+$ T cells was comparable to CD4 T cells (data not shown). These results demonstrate that not only is *CLC/Gal-10* detectable at the mRNA level, but at the peripheral protein level and most importantly, it associates with patent infections.

3.4.4   Baseline frequencies of GZMA and GZMB in individuals with *W. bancrofti* infection

The transcriptome data described in (section 3.1.8.1) showed increased granzyme expression in the patently infected subjects compared to latently infected after removal of individuals with other known infections, such as helminth and protozoa and/or had IVM treatment of the gene expression data (Tables 3.1.12). Granzyme A and B have been shown to play crucial role in *L. sigmodontis* infection outcome [96], however, their importance in *W. bancrofti* infection remains to be fully characterized. To determine the frequencies of human granzyme A and B in *W. bancrofti*-infected individuals and EN, FACS staining was performed on PBMCs from study groups and measured with flow cytometer. As shown in Figure 3.12, the frequencies of CD4$^+$ and CD8$^+$ T cells expressing GZMB were significantly higher in *W. bancrofti*-infected subjects when compared to EN (Figures 3.12 A and B).

To further establish whether CD4$^+$ and CD8$^+$ T cells expressing GZMB were dependent on the infection status, group-wise comparisons were performed. Interestingly, significantly increased frequencies of CD4$^+$GZMB$^+$ and CD8$^+$GZMB$^+$ expressing T cells were observed in the MF+ population when compared to EN (Figures 3.12 C and D). In contrast, there were no significant differences in the frequencies of CD4$^+$ or CD8$^+$ T cells expressing GZMA when comparing EN and *W. bancrofti*-infected persons (Figures 3.12 E and F). However, upon further analysis, GZMA$^+$-producing CD4$^+$ T cells were significantly increased in MF- individuals when compared to both EN and MF$^+$ individuals (Figure 3.12 G). CD8$^+$GZMA$^+$ T cells were also significantly elevated in latently-infected participants when compared to MF+ individuals (Figure 3.12 H). In general the proportion of CD8$^+$GZMA$^+$ expressing T cells was almost 2 fold higher than that of CD4$^+$GZMA$^+$-expressing T cells. The results demonstrate that individuals with patent infection present increased frequencies of GZMB-producing CD4$^+$ and CD8$^+$ T cells, whereas MF-individuals present upregulated levels of GZMA.
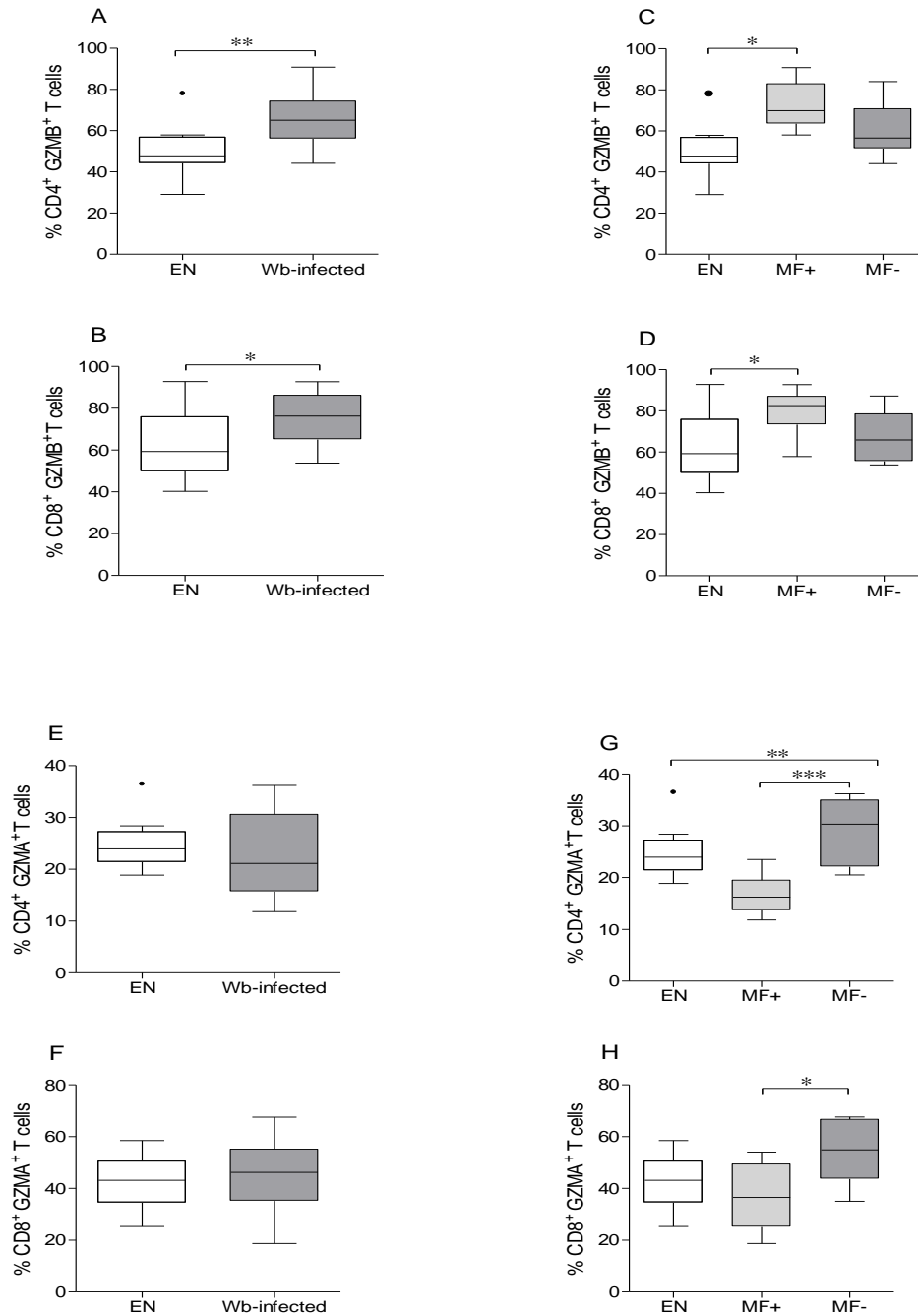
Figure 3.12: Increased frequencies of CD4+ and CD8+ T cells expressing GZMB is associated with MF status, while GZMA is enhanced in individuals with latent infection.

PBMCs from study subjects were stained with antibodies against surface markers, and then fixed, permeabilized, and stained with anti-human granzyme specific antibodies at *ex vivo*. Frequencies of CD4+ and CD8+ T cells expressing GZMB and GZMA were determined. Here, A and B show CD4+ and CD8+ T cells expressing GZMB, whereas C and D present frequencies of CD4+ and CD8+ T expressing GZMB based on the various infection phenotypes. Similarly, E and F present the frequencies of CD4+ and CD8+ T cells expressing GZMA in EN verses Wb-infected groups, whilst the frequencies of CD4+ and CD8+ T cells-expressing GZMA are shown in G and H. Cell population frequencies were determined via flow cytometry. Graphs show percentages of box whiskers plots with outliers from, EN n=10, MF+ n=10 and MF- n=10. Data of each group were compared using ANOVA (Bonferroni's multiple comparison test and T test); significant differences are given as *$p<0.05$, **$p<0.01$ and ***$p<0.001$.

3.4.5   Increased frequencies of PD-1$^+$CD4$^+$ and CTLA-4$^+$CD4$^+$T cells in microfilaremic individuals

In addition to producing GZMB and GZMA, recent genomic studies in T cells have shown increased frequency of exhaustion markers, such as program death-1 (PD-1) and CTLA-4 in T cells after persistent exposure to viral infection [101] as well as cancer related infections [139]. Exhausted T cells are less effective in fighting against chronic infections. Since filarial nematodes cause chronic infections, it was of interest to investigate whether *W. bancrofti* infection alters CD4$^+$ and CD8$^+$ T cells activity via the expression of these inhibitory markers. Hence, the frequency of programmed death-1 (PD-1) and CTLA-4 on CD4$^+$ and CD8$^+$ T cells from PBMCs of EN, MF+ and MF- was determined *ex vivo* using flow cytometry. As shown in (Figure 3.13 A), *W. bancrofti*-infected individuals exhibited significantly higher frequencies of CD4$^+$-expressing PD-1 T cells compared to EN.
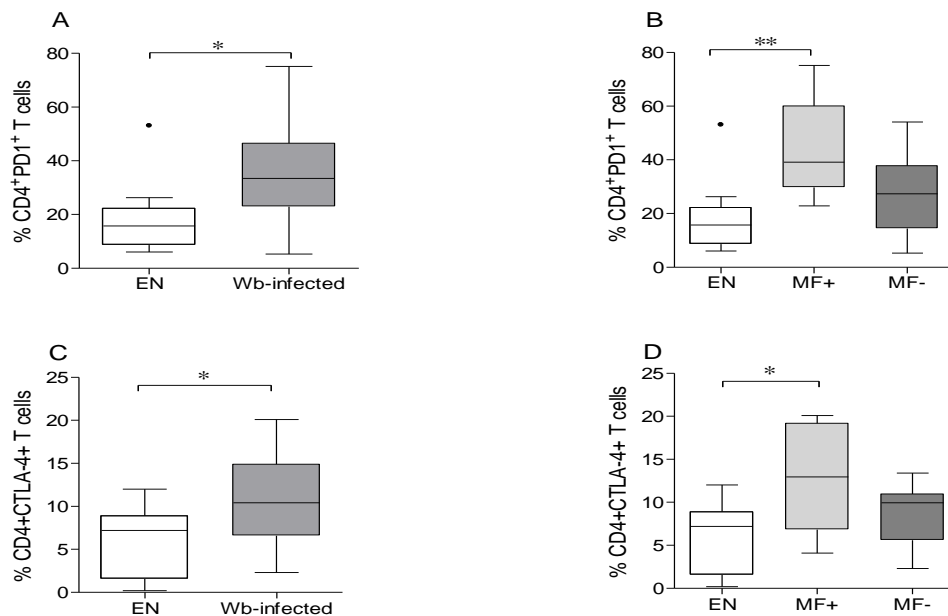
Figure 3.13: Patent filarial infections are associated with increased frequencies of PD-1-and CTLA-4-expressing CD4$^+$ and CD8$^+$ T cells.
PBMCs from EN, MF+ and MF- subjects were stained with antibodies to determine the frequencies of PD-1-expressing CD4$^+$ T cells. (A) presents the frequencies of CD4$^+$ T expressing PD-1, whilst (B) shows frequencies of CD4$^+$ T expressing PD-1 based on infection status. Frequency of CD4$^+$ T-expressing CTLA-4 (EN verses Wb-Infected) is shown in (C), whilst (D) shows CD4$^+$ T-expressing CTLA-4 based on infection status. Graphs depict box whiskers with outliers from (EN n=10, MF+ n=10 and MF- n=10). Data of each group were compared using ANOVA (Bonferroni's multiple comparison test) and significant differences are given as *p<0.05 and **p<0.01.

Following a further group-wise comparison, percentages of CD4$^+$ T cells expressing PD-1 were found to be significantly higher in MF+ persons compared to EN as shown in (Figure 3.13 B). More interestingly, frequencies of CD8$^+$ T cells expressing PD-1$^+$ in the infection groups were

similar to the pattern observed in CD4$^+$ T cells (data not shown). Furthermore, *W. bancrofti*-infected individuals exhibited significantly higher frequencies of CD4$^+$CTLA-4$^+$-expressing T cells when compared to EN, as shown in (Figure 3.13 C). To explore whether CTLA-4 associates with infection status, a group-wise comparison was performed. Consistent with the percentage of PD-1, CTLA-4-expressing CD4$^+$ T cells were significantly higher in patently infected compared to MF- and EN as shown in (Figure 3.13 D). Furthermore, percentage of CTLA-4 expressing CD8$^+$ T cells in the study groups patterned after CTLA-4-expressing CD4$^+$ T cells. Taken together, these results show a higher frequency of PD-1 and CTLA-4 T cells in MF+ persons compared to MF- and EN groups, suggesting that these inhibitory markers may be altered in the presence of MF.

3.5   Intracellular staining after 6hrs of PMA/Ionomycin stimulation

3.5.1 Microfilaraemic individuals show predominant IL-10$^+$producing T cells, whereas MF- subjects exhibit increased frequencies of IFN-γ$^+$, IL-4 and IL-17A CD4$^+$ T cells

To study T cell responses, stimulated PBMCs were investigated for IFN-γ, IL-4, IL-17A and IL-10 production given that susceptibility or resistance to infection is characterized by these cytokines. As shown in A and B, PMA/Ionomycin treatment resulted in a significantly higher frequency of CD4$^+$ IFN-γ$^+$producing T cells in EN and MF- individuals than in MF+ subjects (Figure 3.14 A). With regard to CD4$^+$ T cells producing IL-4, there were no differences in frequencies in all study groups; however, there was a tendency of high occurrence in MF- subjects (Figure 3.14 B). A further analysis in the IL-17A-producing CD4$^+$ T cells showed increased frequencies in MF-individuals compared to EN and MF+ groups (Figure 3.14C), which is consistent with a recent finding in *O. volvulus* infection, where increased IL-17A-producing CD4$^+$ T cells characterised individuals without MF and pathology [17]. Interestingly and consistent with previous studies, elevated frequencies of CD4$^+$IL-10$^+$ T cells associated with MF+ individuals compared to EN and MF- groups (Figure 3.14 D). This trend was mirrored by the CD4$^+$ T cells in all study groups. Interestingly, IFN-γ, IL-4, IL-17A and IL-10 frequencies in CD8$^+$ T cells were comparable to CD4$^+$ T cells (data not shown). These results demonstrate that, while patent infection is characterized by pronounced IL-10$^+$-producing CD4$^+$ and CD8$^+$ T cells, latently infected individuals exhibit increased frequency of IFN-γ, IL-4 and IL-17A.

Figure 3.14: Increased frequencies of IFN-γ characterises EN groups
IL-10 is pronounced in MF+ subjects while in the absence MF- individuals present mixed responses characterised by higher IFN-γ, IL-4 and IL-17A CD4$^+$ T cells. Isolated PBMCs from EN and MF+ and MF- subjects were treated with PMA, Ionomycin, Brefeldin A and Monensin for 6hrs. Thereafter, cells stained for CD4$^+$ T cells producing IFN-γ (A), IL-4 (B), IL-17A (C) and IL-10 (D) in each individual (EN n=8, MF+ n=8 and MF- n=8). Graphs show percentages of box whiskers with outliers. Data of each group were compared using ANOVA (Bonferroni's multiple comparison test and T test); significant differences are given as**p<0.01 and ***p<0.001.

3.5.2 *W. bancrofti* infection is associated with elevated CD4$^+$Gal-10$^+$IL-10$^+$ producing T cells

In section 3.4.3, it was observed that CD4$^+$ and CD8$^+$ T cells from MF+ individuals expressed higher frequencies of CLC/Gal-10 after baseline expression analysis. To determine the phenotype of CLC/Gal-10 in filarial infections, PBMCs from EN, MF+ and MF- were treated with PMA/Ionomycin and subsequently assessed whether T cells co-express Gal-10 and IL-10. Consistent with the mRNA and peripheral protein levels, the frequency of CD4$^+$Gal-10$^+$IL-10$^+$ producing T cells was significantly higher in *W. bancrofti*-infected compared to EN individuals, (Figure 3.15A). Based on infection status, it was observed that CD4$^+$Gal-10$^+$/IL-10$^+$ double positive T cells were significantly higher in MF+ compared to EN, whereas no significant differences were revealed when comparing to MF-groups (Figure 3.15B). In a similar way, CD8$^+$Gal-10$^+$IL-10$^+$ producing T cells mirrored that of CD4 T cells (data not shown). The findings suggest that *W. bancrofti* infection has a tendency to induce CD4$^+$ and CD8$^+$ T cells co-

expressing Gal-10$^+$ and IL-10$^+$. Thus, these two molecules expressed by both, CD4$^+$ and CD8$^+$ T cells at the same time and both of them being involved in immune suppression pathways, adds another potential molecular mechanism to the pathways induced by parasites in order to survive within their hosts.
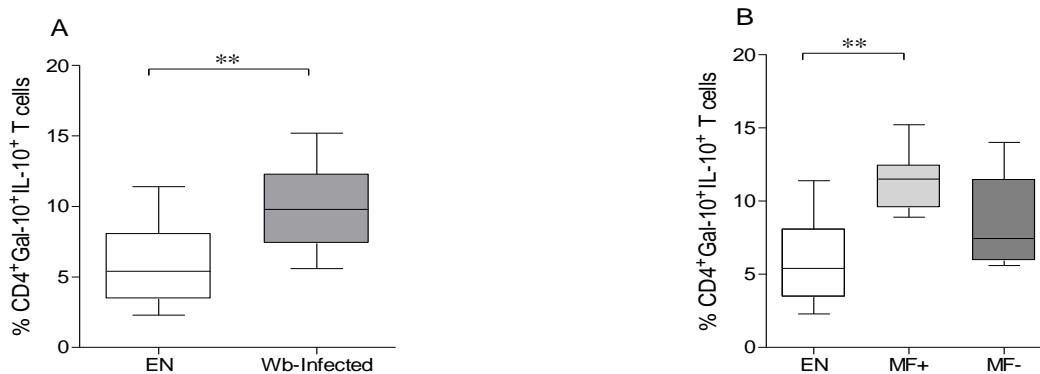
Figure 3.15: Increased proportions of Gal-10$^+$IL-10$^+$ expressing CD4$^+$ T cells in individuals with *W. bancrofti* infection.
PBMCs were isolated from EN and MF+ and MF- subjects and stained with antibodies to determine the frequencies of CD4$^+$Gal-10$^+$IL-10$^+$ T cells. Frequencies of CD4$^+$Gal-10$^+$IL-10$^+$ T cells in EN and *W. bancrofti* infected individuals (A), and based on infection status (B). Cell population frequencies were analysed with flow cytometry. Graphs show percentages of box whiskers with outliers (EN n=8, MF+ n=8 and MF- n=8). Data of each group were compared using ANOVA (Bonferroni's multiple comparison test and T test); and significant differences are given as *p<0.05 and **p<0.01.
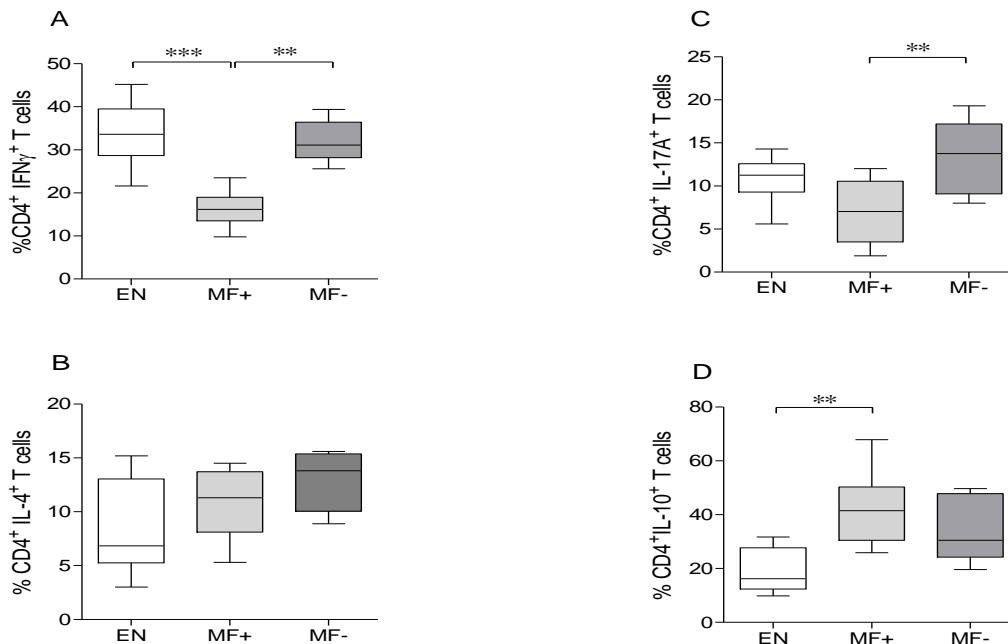
3.5.3 Increased frequencies of CD4$^+$ and CD8$^+$ T cells co-expressing GZMB and IL-10 in microfilaremic individuals

As shown in the previous section, the frequency of GZMB was significantly higher in both CD4$^+$ and CD8$^+$ T cells in patently infected individuals compared to EN. To further characterize these T cells, the frequencies of CD4$^+$ and CD8$^+$ T cells co-expressing GZMB and IL-10 were determined after stimulating PBMCs from EN, MF+ and MF- with PMA, Ionomycin, Brefeldin A and Monensin. As shown in (Figures 3.16 A and B), the frequencies of CD4$^+$GZMB$^+$IL-10$^+$ and CD8$^+$GZMB$^+$IL-10$^+$ T cells were significantly higher in *W. bancrofti*-infected when compared to in the EN group. More interestingly, based on infection phenotype, CD4$^+$ and CD8$^+$ T cells in MF+ persons presented significantly high proportions of GZMB$^+$IL-10$^+$ compared to EN. No significant differences were observed in both cell types when compared to MF- subjects as described in (Figures 3.16 C and D). These results support our transcriptome data and demonstrate that *W. bancrofti* infection induces high frequencies of CD4$^+$ and CD8$^+$ producing GZMB and IL-10 T cells, which are apparently associated with patency.
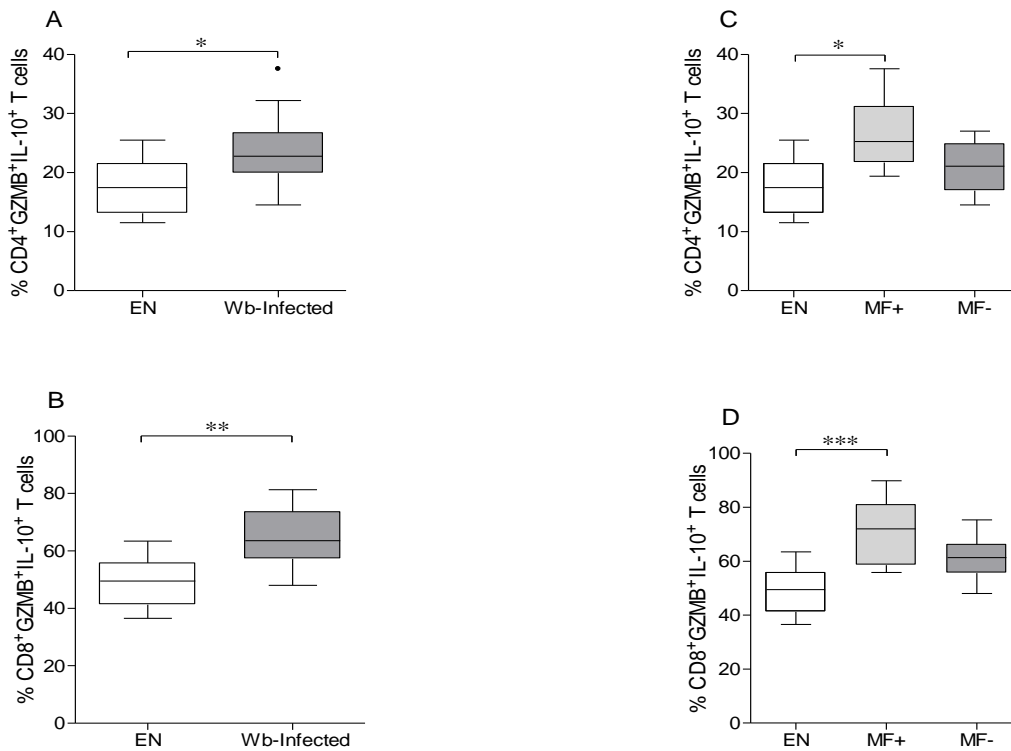
Figure 3.16: Patent infections are associated with increased frequencies of CD4$^+$ and CD8$^+$ T cell producing GZMB and IL-10.
PBMCs from study subjects were stained with antibodies against surface markers, and then fixed, permeabilized, and stained with anti-human granzyme specific and anti-human IL-10 antibodies following Cell Stimulation Cocktail (PMA, Ionomycin, Brefeldin A and Monensin) treatment for 6hrs. The frequencies of CD4$^+$ and CD8$^+$ T cells co-expressing GZMB and IL-10 were determined intracellularly through flow cytometry. A and B present the frequencies of CD4$^+$ and CD8$^+$T cells co-expressing GZMB and IL-10 in EN verses infected, C and D depict CD4$^+$ and CD8$^+$ T cells co-expressing GZMB and IL-10 in EN vs MF+ vs MF-. Graphs show percentages of box whiskers with outliers from (EN n=8, MF+ n=8 and MF- n=8). Data of each group were compared using ANOVA (Bonferroni's multiple comparison test and T test; significant differences are given as *$p<0.05$, **$p<0.01$ and ***$p<0.001$.

3.5.4 Elevated frequencies of PD-1$^+$IL-10$^+$ expressing CD4$^+$ and CD8$^+$ T cells in patently infected

Since the above section noted a higher frequency of PD1$^+$CD4$^+$ and CD8$^+$ T cells in MF+ individuals, and to further characterize the phenotype of these cells, PBMCs from EN, MF+ and MF- were assessed for CD4$^+$ and CD8$^+$ T cells co-expressing PD-1 and IL-10. PD-1$^+$IL-10$^+$-expressing CD4$^+$ and CD8$^+$ T cells were analyzed in study groups. In line with baseline expression, higher frequencies of CD4$^+$ PD-1$^+$IL-10$^+$ (Figure 3.17 A) and CD8$^+$ PD-1$^+$IL-10$^+$ expressing T cells (Figure 3.17 B) were found in *W. bancrofti*-infected individuals compared to EN after stimulation. Further analysis showed that MF+ persons exhibited higher frequencies of

CD4^{+}PD-1^{+}IL-10^{+} and CD8^{+}PD-1^{+}IL-10^{+} expressing T cells compared to EN. IL-10 is an essential immunoregulatory molecule, which has been found to be spontaneously released by MF+ individuals [77]. While these results may not be entirely conclusive in establishing the underlying mechanism, they point to the fact that T cell exhaustion during *W. bancrofti* infection maybe MF-mediated via up-regulating PD-1 and IL-10 pathways.
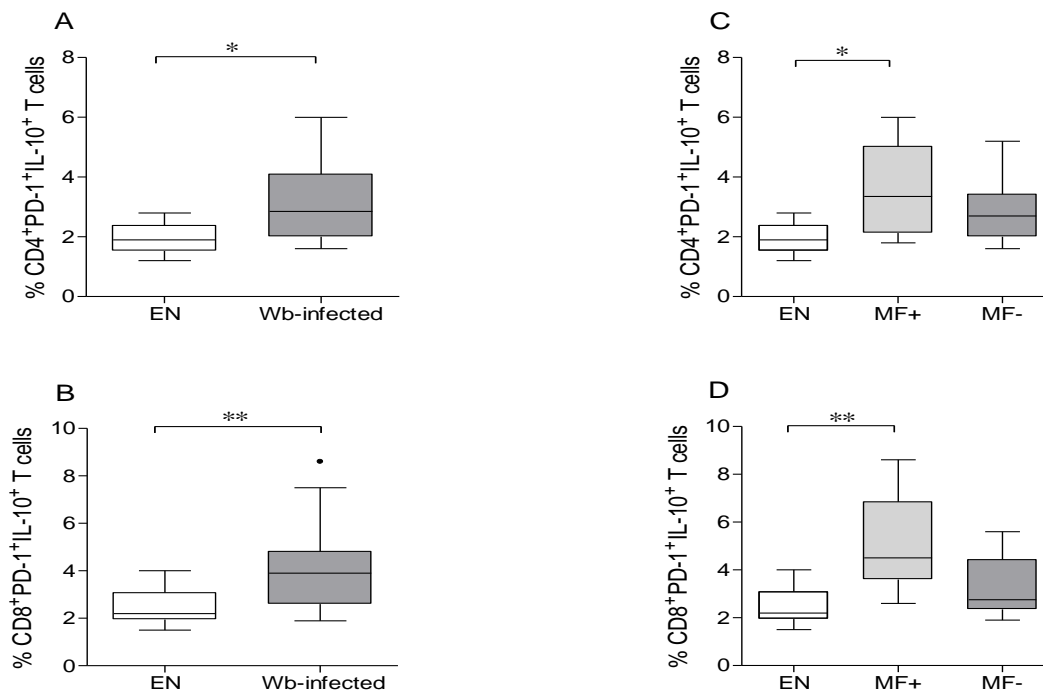
Figure 3.17: Markers of T cell exhaustion are up-regulated in CD4^{+} and CD8^{+} T cells in MF+ individuals.
PBMCs from study subjects were stained with antibodies against surface markers, and then fixed, permeabilized, and stained with anti-human PD-1 and anti-human IL-10 antibodies following Cell Stimulation Cocktail (PMA, Ionomycin, Brefeldin A and Monensin) treatment for 6hrs. The frequencies of CD4^{+} and CD8^{+} T cells co-expressing PD-1 and IL-10 were determined through intracellular flow cytometry. A and B present the frequencies of CD4^{+} and CD8^{+} T cells co-expressing PD-1 and IL-10 in EN vs. infected individuals. C and D depict the frequencies when separated into their respective infections status. Graphs show percentages of box whiskers with outliers from EN n=8, MF+ n=8 and MF- n=8. Data of each group were compared using ANOVA (Bonferroni's multiple comparison test and T test) ; significant differences are given as *p<0.05 and **p<0.01.

3.5.5   Filarial infections are associated with increased frequency of CD244 and CD107a expressing T cells

Since the frequencies of CD4^{+} and CD8^{+} T cells expressing PD-1 were higher in MF+ compared to MF- as described in the previous sections, the potential involvement of CD244 (2B4) in cytolysis was assessed in the study subjects by measuring levels of the degranulation marker,

CD107a (LAMP-1) in CD4$^+$ and CD8$^+$ T cells from PBMCs from study groups after PMA/Ionomycin stimulation. For instance, CD107a is a protein detectable by flow cytometry surface staining after transient lysosomal fusion to the cellular membrane and release of granule proteins during T cell activation. Surface expression of CD107a is also associated with granule release by human CD4$^+$ and CD8$^+$ T cells, and correlates with CTL effector function [140]. High expression of these markers associates with exhausted T cells and impair responses needed to combat viral infections [100, 101]. However, their frequencies remain to be defined in filarial infections. Therefore, to determine whether the functional activity of CD4$^+$ and CD8$^+$ T cells are altered in *W. bancrofti* infection on, the frequencies of CD244 and CD107a were assessed in PBMC from study subjects after PMA/Ionomycin treatment.
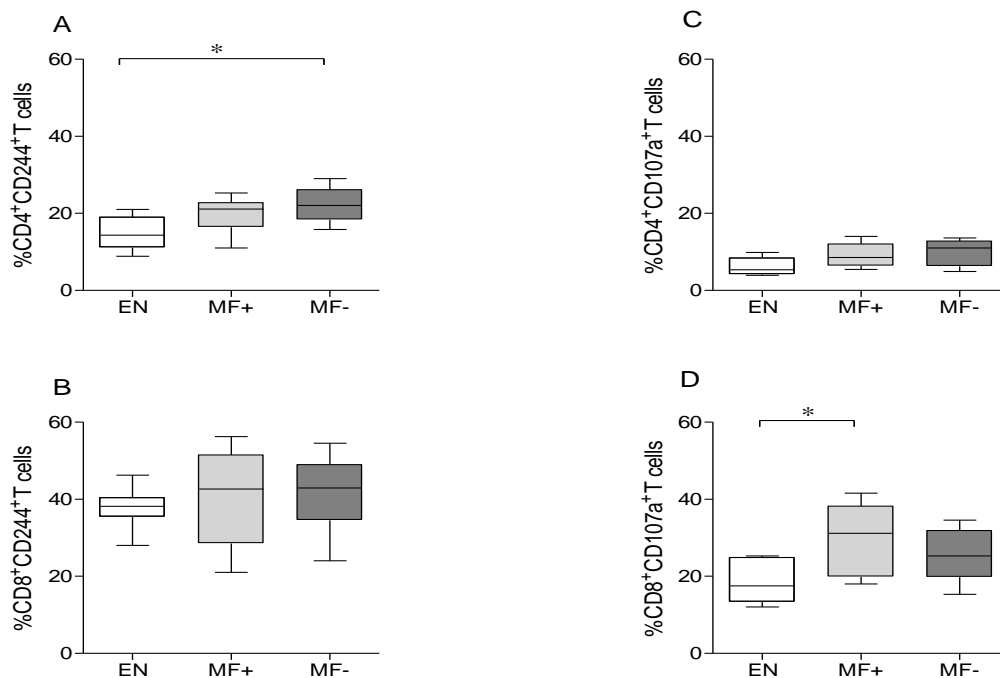
Figure 3.18: Patent infected individuals present higher frequencies of CD107a$^+$
Patent infected individuals present higher frequencies of CD107a$^+$ expressing CD4$^+$ and CD8$^+$ T cells in *W. bancrofti*-infected, while CD244 is highly expressed in latent infection. PBMCs from study subjects were stimulated with Cell Stimulation Cocktail (PMA, Ionomycin, Brefeldin A and Monensin) for 6hrs. Cells were stained for CD4 expressing CD244 (A), CD8 expressing CD244 (B). Similarly, CD4 expressing CD107a (C) and CD8 expressing CD107a (D) were also stained in each individuals (EN n=8, MF+ n=8 and MF- n=8). Cell population frequencies were determined via flow cytometry. Graphs show percentages of box whiskers with outliers. Data of each group were compared using ANOVA (Bonferroni's multiple comparison test and T test); significant differences are given as *p< 0. 05.

In this study, it was observed that the percentage of CD4$^+$ T cells expressing CD244 was highly significant in MF- subjects compared to MF+ and EN (Figure 3.18 A), while there were no distinct differences in the CD244-expressing CD8$^+$ T cells (Figure 3.18 B). There were no

significant differences observed in the percentage CD107a on CD4^{+} T cells (Figure 3.18C). In contrast, the frequency of CD8^{+} T cell-expressing CD107a was distinctly higher in MF+ compared to MF- (Figure 3.18 D). These results demonstrate that CD244-expressing CD4^{+} and CD8^{+} T cells are enhanced during filarial infection as well as support the hypothesis that *W. bancrofti* infection induces degranulation of both CD4^{+} and CD8^{+} T cells as evidenced by the increased degranulation as evidence by higher proportions of CD107a in MF+ subjects compared to EN.

3.6 Cell culture

3.6.1 Filarial antigen suppresses TCR-specific activation

In the previous sections, the frequencies of CLC/Ga-10, GZMB/GZMA, PD-1 as well as T helper related cytokines were shown to higher in the PBMCs of *W. bancrofti*-infected groups compared to EN after PMA/Ionomycin treatment. One of the hallmarks of filarial infection is the modulation of host immune responses in the presence of active infection.
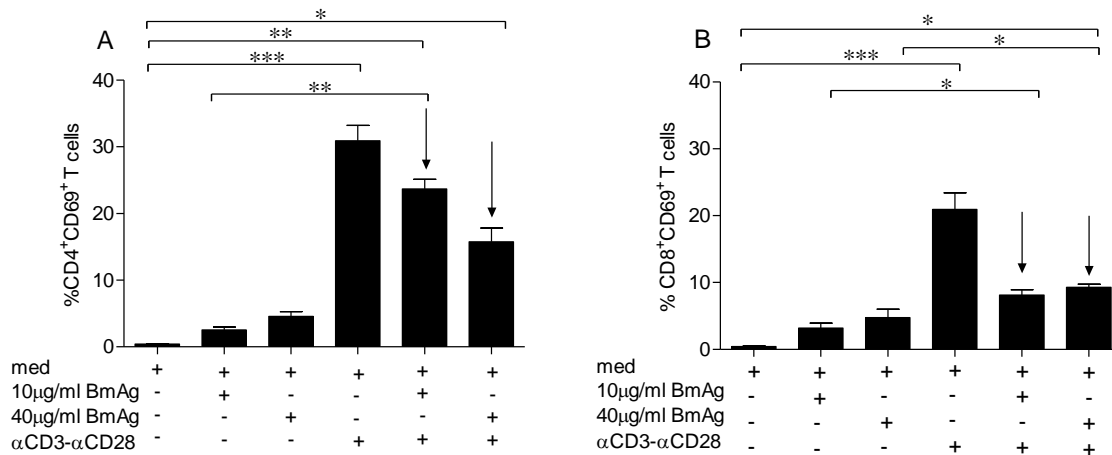
Figure 3.19: Activation of CD4^{+} T and CD8^{+} T cells after filarial and/or TCR-antigen specific stimulation. PBMCs from EN (n=6) were left unstimulated (med) or stimulated with *B. malayi* extract (BmAg at 10µg/ml, 40µg/ml), (αCD3/αCD28, 10000 beads/well) or combinations of TCR activation and BmAg. After 24 hours, levels of CD69 were measured on CD4^{+} and CD8^{+} T cells by FACS. A and B present percentages of CD4^{+}CD69^{+} T and CD8^{+}CD69^{+} T cells were assessed. Each bar represents mean percentage ± SEM of CD69 expression on CD4^{+} T and CD8^{+} T cells. Data were compared using Kruskal-Wallis test and Mann-Whitney test and significant differences are given as *$p<0.05$, **$p<0.01$ and ***$p<0.001$.

To further investigate the immunomodulatory capacity of filarial antigens and to obtain a better understanding of the physiological nature of the host-parasite interaction that occurs *in vivo,*

PBMCs from patients were studied for filarial-specific responses. To do this, it was necessary to establish assays with the right concentrations of filarial antigen by determining the optimum concentration of *B. malayi* extract needed for in *vitro* experiments. Here, 10µg/ml and 40µg/ml of BmAg were used to stimulate the cells. The activation of BmAg, αCD3/αCD28 or combinations of BmAg and αCD3/αCD28 was determined. It was noted that stimulation of PBMCs from EN with αCD3/αCD28 led to an increased in the frequency of activate CD69$^+$CD4$^+$ T and CD69$^+$CD8$^+$ T cells using FACS (bars 4 in Figures 3.19A and B), respectively. In the presence of 10µg and 40µg of *B. malayi*-antigen, TCR-specific activation was reduced in both T cell populations (Figures 3.19 A and B bars 2, 3). Interestingly, cultures of TCR-activated cells and BmAg results in suppressed activation of both T cell subsets (indicated by arrows on graph). Moreover, whereas increasing the dose of BmAg down-regulated CD4$^+$ T cell activation, both concentrations equally suppressed CD8$^+$ T cell activation. Based on these results, 40µg of BmAg was chosen for *in vitro* co-culture assays.

3.6.2   CLC/Gal-10$^+$IL-10$^+$-producing CD4$^+$ and CD8$^+$ T cell responses from infected individuals are increased upon filarial-specific stimulation in MF+ individuals

To investigate whether the induction of CLC/Gal-10 proteins is associated with filarial-specific immune responses with possible immunoregulatory functions (i.e. IL-10 secretion), cultures of PBMCs from MF+, MF- and EN were either left alone or activated with either BmAg, αCD3/αCD28 or combinations of αCD3/αCD28 and BmAg. After 7 days, cells were harvested and analyzed by FACS. When compared to medium control, the stimulation of PBMC with BmAg resulted in significantly higher proportions of CD4$^+$ T cells producing CLC/Gal-10$^+$IL-10$^+$ in MF+ and MF-, but not EN individuals (Figure 3.20 A). There was no significant difference in the frequencies of CD4$^+$ T cells expressing Gal-10 and IL-10 after TCR stimulation in study groups (Figure 3.20 A), but with regards to CD8$^+$ T cells, significant differences were observed compared to control (Figure 3.20 B). In the presence of BmAg and αCD3/αCD28, the percentage of CD4$^+$CLC/Gal-10$^+$IL-10$^+$T cells was slightly reduced compared to TCR stimulation alone, albeit non-significant. More interestingly, the pattern of CD8$^+$CLC/Gal-10$^+$IL-10$^+$ producing T cells (Figure 3.20 B) was comparable to that of CD4 T cells. This observation is consistent with previous protein expression data and demonstrates that CD4$^+$ and CD8$^+$ co-expressing CLC/Gal-10$^+$IL-10$^+$-producing T cells may be considered as key immunomodulatory participants in filarial-host interactions.
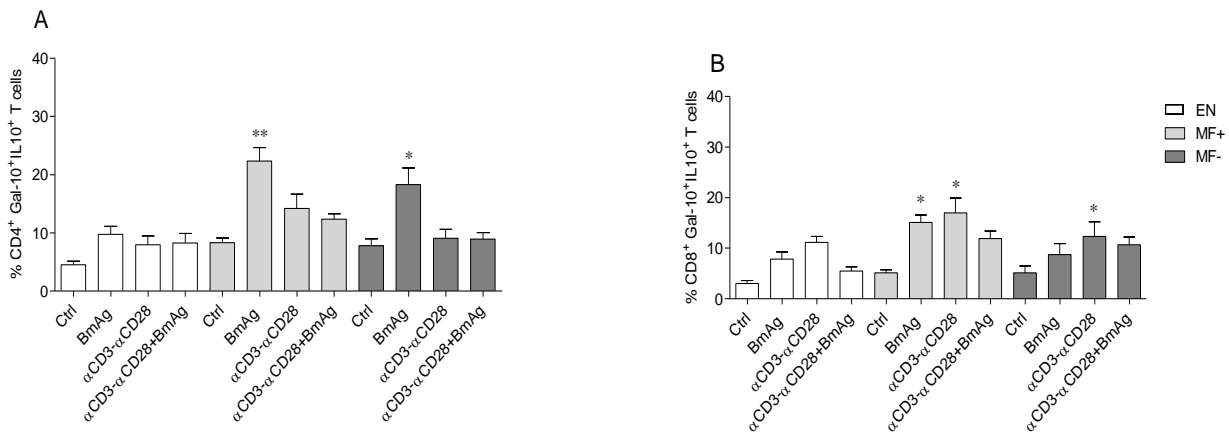
Figure 3.20: Re-stimulation of PBMCs from infected individuals with filarial antigen increases the frequencies of IL-10$^+$CLC/Gal-10$^+$ producing CD4$^+$ and CD8$^+$ T cells *in vitro.*
PBMCs from study subjects were left unstimulated (Ctrl) or activated with either *Brugia malayi* extract (BmAg, 40µg/ml), (αCD3/αCD28, 10000 beads/well) or a combination of BmAg and αCD3/αCD28 for 7 days. Thereafter cells were stimulated with PMA, Ionomycin, Brefeldin A and Monensin for 6hrs and stained for CD4$^+$Gal-10$^+$IL-10$^+$ T (A) and CD8$^+$Gal-10$^+$IL-10$^+$ T cells (B) in each individual (EN n=8, MF+ n=8 and MF- n=8). Cell population frequencies were determined via flow cytometry. Bars represent mean percentage ± SEM of CD4$^+$Gal-10$^+$IL-10$^+$ and CD8$^+$Gal-10$^+$IL-10$^+$T cells. Data of each group were compared using Mann-Whitney test (stimulus vs internal control) and significant differences are given as *p< 0. 05 and **p< 0. 01.

3.6.3 Increased frequencies of filarial-specific Th1 responses associate with EN; higher regulatory T phenotype accompanied with diminished Th1 and Th17 responses characterised MF+ persons, while a mixed Th1, Th2, Th17 and Treg responses were enhanced in latently infected individuals

Given that T cells play a critical role in regulating the immune response to nematode parasites, understanding of specificity of the T cell responses is essential for the elucidation of the mechanisms that underlie susceptibility and resistance to infection. Results from mitogen stimulation, i.e. PMA/Ionomycin of PBMCs from study subjects showed increased frequencies of IFN-γ in EN individuals; IL-10 was highly detected in MF+ individuals, whilst IL-4 and IL-17A frequencies were higher in MF- subjects. To define whether this observation was filarial-specific, PBMCs from MF+, MF- and EN were either left alone or activated with αCD3/αCD28 or BmAg or in combinations of αCD3/αCD28 and BmAg. When compared to control, the frequency of IFN-γ was higher in EN and MF- groups, but not in MF+ persons following BmAg, αCD3/αCD28 as well as in the presence of αCD3/αCD28 and BmAg compared to control (Figure 3.21 A). After TCR stimulation via αCD3/αCD28, and in the presence of both αCD3/αCD28 and BmAg, percentages of CD4$^+$IFN-γ$^+$ T cells were highly significant in all study groups. With regards to IL-

4, no distinct differences were observed in the frequency of CD4⁺IL-4⁺ T cells in EN groups under all conditions. While the percentage of CD4⁺IL-4⁺ T cells was significant in infected subjects, it was remarkably higher in MF- after BmAg, αCD3/αCD28 and in the presence of αCD3/αCD28 and BmAg after stimulation compared to control (Figure 3.21 B). Again, compared to control, filarial-specific frequencies of IL-17A-secreting CD4⁺ T cells were higher in the MF- compared to MF+ and EN following BmAg stimulation. After αCD3/αCD28 activation and in the presence of αCD3/αCD28 and BmAg, there was an increase in the frequency of CD4⁺IL-17A-secreting T cells in all study groups. Of note, this was more pronounced in the MF- individuals (Figure 3.21 C).
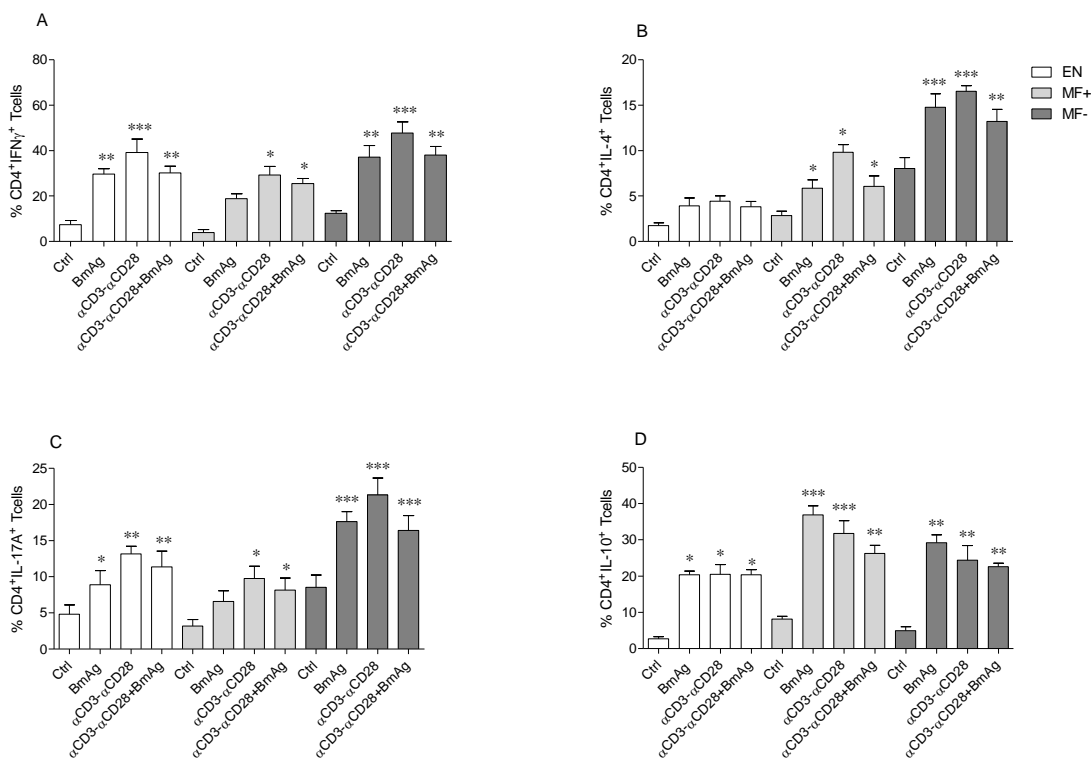
Figure 3.21: MF+ individuals present elevated frequencies of filarial-specific CD4⁺IL-10⁺ T cells, while MF-subjects exhibit pronounced frequencies of CD4⁺IFN-γ⁺, CD4⁺IL-4⁺, CD4⁺IL-17⁺ T cell phenotypes.
Isolated PBMCs (1 x10⁵ cells/100µl) from study subjects were left unstimulated (Ctrl) or activated with either *B. malayi* extract (BmAg, 40µg/ml), αCD3/αCD28 (10000 beads/well) or combinations of both and cultured for 7 days. Cells were stained for CD4 T cell signature cytokines, IFN-γ (A), IL-4 (B), IL-17A (C) and IL-10 T cells (D) in each subject (EN n=8, MF+ n=8 and MF- n=8). Cell populations were determined with flow cytometry. Each bar represents the mean percentage ± SEM of IFN-γ, IL-4, IL-17A and IL-10. Data of each group were compared using Mann-Whitney test (stimulus vs internal control) and significant differences are given as *$p< 0.05$, **$p<0.01$ and ***$p<0.001$.

In this study, a spontaneous secretion of IL-10 was observed in all study groups following BmAg, αCD3/αCD28 as well as in the presence of αCD3/αCD28 and BmAg compared to medium control. Interestingly, the percentage of CD4⁺IL-10⁺ T cells was higher in MF+ persons

(Figure 3.21 D). To determine whether T cell cytokine responses are modulated by filarial worms, the frequency of these cytokines in the presence of αCD3/αCD28 and BmAg was assessed. BmAg additional to αCD3/αCD28 stimulation resulted in slightly reduced frequencies of cytokines in all cohorts. These results show that higher IL-10 production is associated with MF+ individuals, whilst IFN-γ, IL-4 and IL-17-producing CD4$^+$ T cells characterize individuals with latent infection and further support the hypothesis that differential cellular immune responses in asymptomatic individuals are filarial antigen-specific.

3.6.4 Frequency of FOXP3 is enhanced in patently infected, whilst T-bet, GATA-3 and RORC2 were highly exhibited in individuals with latent infection after BmAg stimulation

Having investigated the T cell responses in cell culture of the study subjects, it was of interest to assess the effect of filarial-specific stimulation on the T cell lineage transcriptional factors, which regulates these cytokines described in section 3.6.3. To do this, PBMCs from EN, MF+, and MF- were cultured and left alone or activated with either αCD3/αCD28 or BmAg and in the presence of αCD3/αCD28 and BmAg. After 7 days, cells were harvested and analyzed by FACS. The percentage of CD4$^+$T-bet$^+$ T cells was significantly distinct in all groups after activation with BmAg, αCD3/αCD28 as well as in the presence of both αCD3/αCD28 and BmAg compared to medium control (Figure 3.22 A). Clearly, the frequency of T-bet was pronounced in EN and MF- groups than in MF+ subjects and patterned after the *ex-vivo* expression data. With regard to CD4$^+$GATA-3$^+$ T cells, there were significant differences found in the frequencies in MF- subjects after BmAg activation compared to the medium control, while no differences were observed in both EN and MF+ subjects. However, after TCR specific stimulation and in the presence of both αCD3/αCD28 and BmAg, the percentage of GATA-3$^+$-expressing CD4$^+$ T cells was highly significant in all study groups when compared to medium control (Figure 3.22 B). Analysis on CD4$^+$RORC2$^+$ T cells showed increased frequency in MF- individuals after BmAg activation, but this was not the case for both EN and MF+ since no differences were observed. Following activation of PBMCs with αCD3/αCD28 as well as in the presence of BmAg in addition to αCD3/αCD28, the percentage of CD4$^+$ T cells-expressing RORC2 was significantly elevated in all study groups, but higher frequencies were detected in MF- subjects (Figure 3.22 C). Since filarial nematodes are hallmarked for immune suppression, the impact of filarial-specific activation on FOXP3 frequency, the master regulator of regulatory T cells was assessed. Interestingly and consistent with the baseline data, the percentage of

CD4$^+$CD25^{hi}FOXP3$^+$ was higher in MF+ subjects following BmAg compared to medium control. While, there were no distinct differences in the percentages of CD4$^+$CD25^{hi}FOXP3$^+$ T cells in both EN and MF- subjects after BmAg stimulation, this T cell phenotype was slightly higher in MF- than EN. After TCR specific stimulation, percentage of CD4$^+$CD25^{hi}FOXP3$^+$ T cells were significantly recorded in MF+ and MF- groups, compared to medium control, whereas no differences were found in the EN group (Figure 3.22 D). Moreover, it was observed that BmAg in addition to αCD3/αCD28 activation caused a moderate reduction in the frequencies of these transcriptional factors, particularly in the *W. bancrofti*-infected individuals.
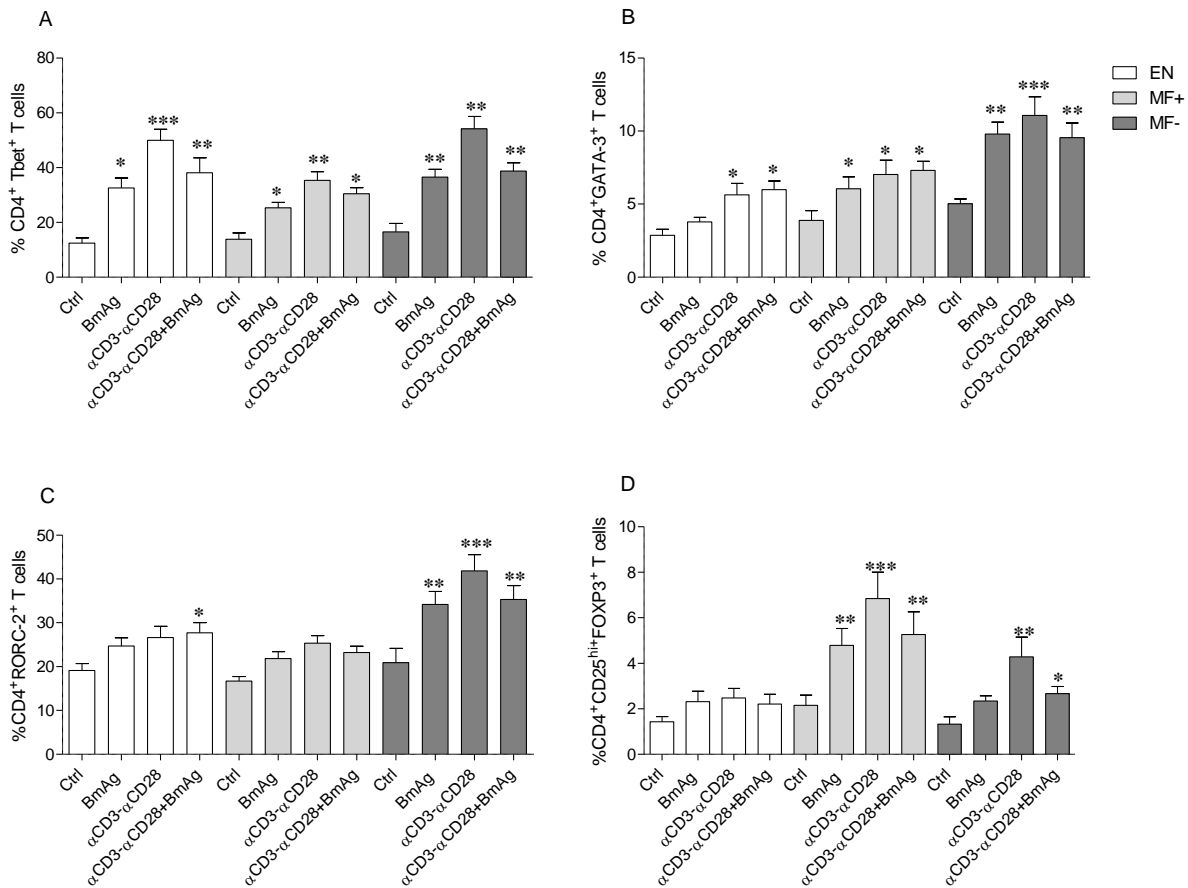
Figure 3.22: Microfilaraemics present higher frequencies of filarial antigen-specific CD4$^+$CD25^{hi}FOXP3$^+$ T cells, while MF- individuals exhibit increased frequencies of CD4$^+$T-bet$^+$, CD4$^+$GATA-3$^+$, CD4$^+$RORC2$^+$ T cell phenotypes.
Isolated PBMCs (1x10^5 cells/100µl) from study subjects were left alone (Ctrl), stimulated with either BmAg (40µg/ml), αCD3/αCD28 (10000 beads/well) or combinations of αCD3/αCD28 and BmAg for 7 days. Thereafter cells stimulated with PMA, Ionomycin, Brefeldin A and Monensin for 6hrs and stained for CD4 and the transcriptional factors, T-bet (A), GATA-3 (B), RORC2 (C) and CD4$^+$CD25^{hi}FOXP3 (D) in each individual (EN n=8, MF+ n=8 and MF- n=8). Cell population frequencies were analysed with Diva software. Bars represent the mean percentage ± SEM of each transcriptional factor expression. Data of each group were compared using Mann-Whitney test (stimulus vs internal control) and significant differences are given as *p<0.05, **p<0.01 and ***p<0.001.

3.6.5   Predominant release of GZMB by CD8^{+} T and CD4^{+} T cells in MF+ individuals upon BmAg re-stimulation

Since FACS analysis following direct *ex vivo* (Figure 3.12) revealed increased frequencies of GZMA-producing CD4^{+} and CD8^{+} T cells in individuals with latent infection, further investigations were performed to establish whether GZMA producing T cells could be triggered by activation with filarial antigens. Hence, PBMCs from MF+, MF- and EN were left alone or activated with either αCD3/αCD28 or BmAg or a combination of αCD3/αCD28 plus BmAg.
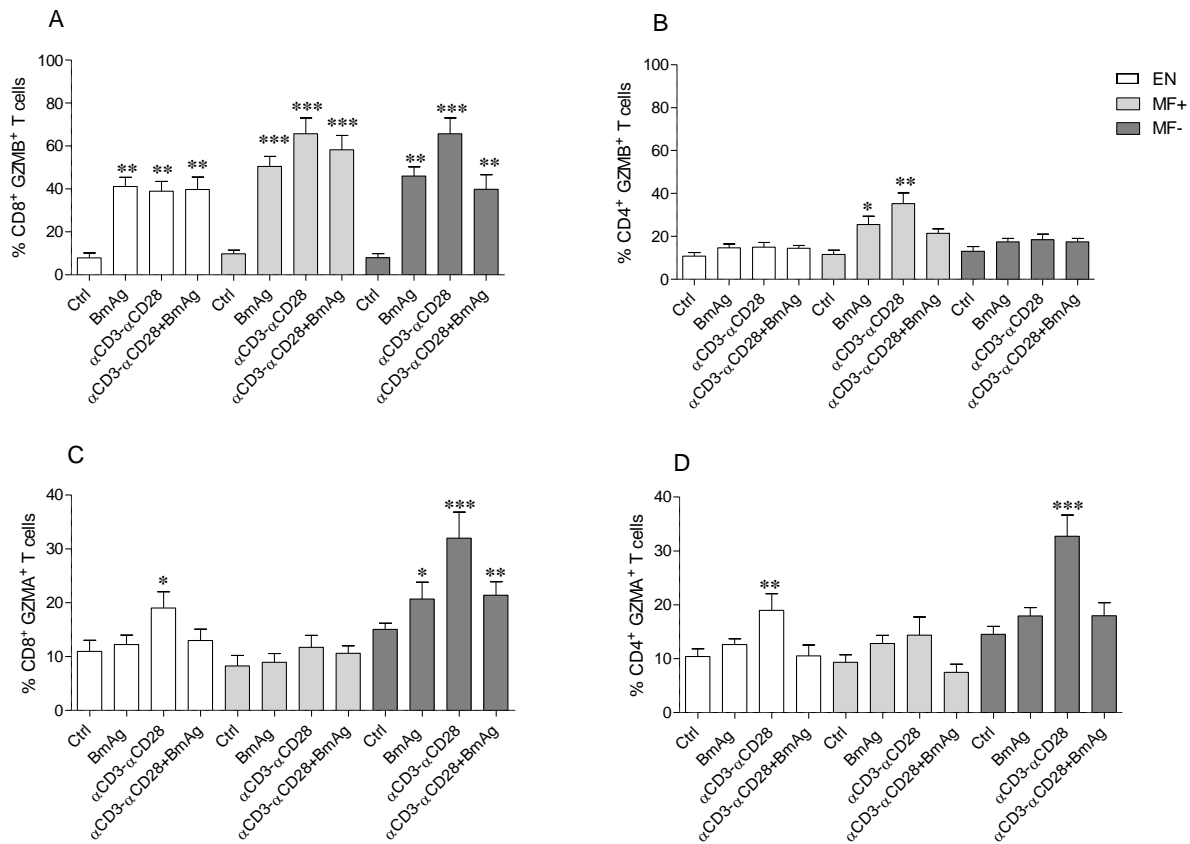
Figure 3.23: BmAg increases the frequency of GZMB expressing T cells *in vitro*

Isolated PBMCs (1 x10^{5} cells/100µl) from study subjects were left unstimulated (Ctrl) or activated with either *Brugia malayi* extract (BmAg, 40µg/ml), αCD3/αCD28 (10000 beads/well) or combinations of both and cultured for 7 days. Thereafter cells stained for CD8^{+}GZMB^{+} T cells (A) and CD4^{+}GZMB^{+} T cells (B). Similarly, cells were stained for CD8^{+}GZMA^{+} T cells (C) and CD4^{+}GZMA^{+} T cells (D) in each individual (EN n=8, MF+ n=8 and MF- n=8). Cell population frequencies were determined with flow cytometry. Each bar shows the mean percentage ± SEM of CD8^{+}GZMB^{+} and CD4^{+}GZMB^{+} T cells. Data of each group were compared using Mann-Whitney test (stimulus vs internal control) and significant differences are given as *p<0.05, **p<0.01 and ***p<0.001.

After 7 days, cells were harvested and analyzed by FACS. BmAg triggered the up-regulation of GZMB in CD8^{+} T cells in all group in a comparable manner (Figure 3.23A). Frequencies of CD8^{+}

producing GZMB T cells in infected groups were significantly elevated upon αCD3/αCD28 stimulation alone and the addition of BmAg did not dramatically alter these levels (Figure 3.23A). When compared to medium controls, the stimulation of PBMC with BmAg induced significantly elevated levels of CD4$^+$GZMB$^+$ producing T cells in MF+ individuals and levels were also significant (Figure 3.23B). Activation of T cells with αCD3/αCD28 elicited stronger and significantly higher levels of GZMB$^+$CD4$^+$ T cells in MF+ individuals which were lower in the presence of both αCD3/αCD28 and BmAg (Figure 3.23B). When compared to medium control, BmAg activation resulted in significant differences in the percentage of GZMA-producing CD8$^+$ T cells in MF- persons but not in EN and MF+ groups (Figure 3.23 C). After TCR-specific activation, the proportion of GZMA-producing CD8$^+$ T cells in MF- and EN was significantly highly, but not in MF+ subjects. Addition of BmAg to αCD3/αCD28 stimulation resulted in significant differences in GZMA-producing CD8$^+$ T cells compared to controls in MF- individuals, but did not dramatically alter these levels in EN and MF+ groups. With regard to the frequency of GZMA$^+$-producing CD4$^+$ T cells, there was no significant difference after BmAg stimulation in all the groups, however, following activation of T cells with αCD3/αCD28, significantly higher levels were found in EN and MF-, but not in the MF+ individuals (Figure 3.23 D). The results demonstrate that GZMB associates with individuals with patent infection, whereas GZMA characterizes with subjects without MF.

3.6.6   Increased *B. malayi* specific PD-1$^+$IL-10$^+$ expressing CD4$^+$ and CD8$^+$ T cells in co-cultures of PBMCs from *W. bancrofti* infected individuals

To investigate the effect of filarial-specific regulation on PD-1 producing T cells during filarial infection, PBMCs from *W. bancrofti*-infected individuals and EN were stimulated with *B. malayi* antigen and cultured for 7 days. When compared to medium control, BmAg activation induced increased frequency of CD4$^+$ and CD8$^+$ PD-1$^+$IL-10$^+$ producing T cells which was highly significant in all the groups (Figures 3.24 A and B). TCR specific activation with αCD3/αCD28 resulted in a moderate upregulation of CD4$^+$ or CD8$^+$ T cells expressing PD-1$^+$ and IL-10$^+$ in all groups and this was not altered upon the addition of BmAg. The increased expression of PD1 and IL-10 producing CD4$^+$ and CD8$^+$ T cells upon BmAg stimulation *in vitro* suggests that PD-1 and IL-10 signaling pathways are mediated by filarial nematodes in order to modulate host immune response.
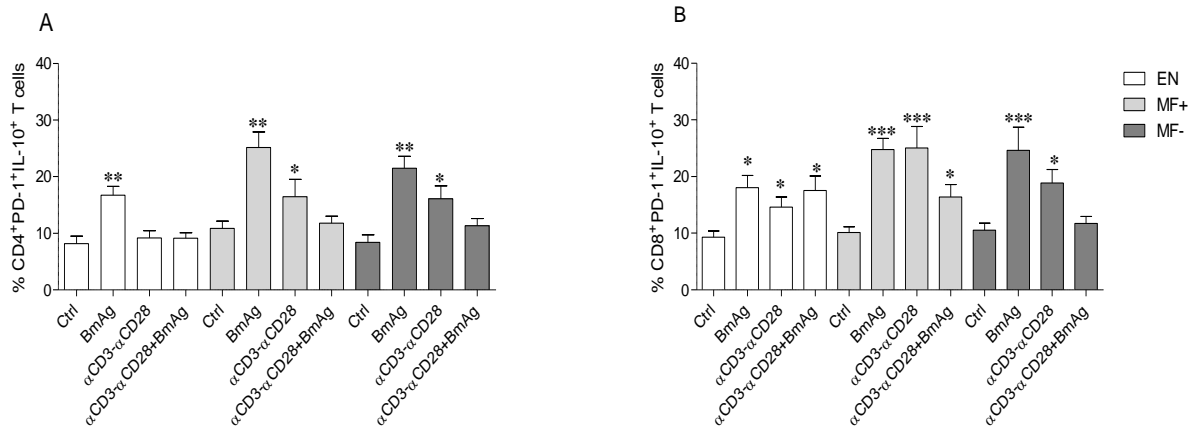
Figure 3.24: Filarial-specific induction of PD1$^+$IL-10$^+$-secreting CD4$^+$ and CD8$^+$ T cells in *Wb*-infected individuals.

Isolated PBMCs (1x10^5 cells/100µl) from study subjects were left unstimulated (Ctrl) or activated with either *Brugia malayi* extract (BmAg, 40µg/ml), αCD3/αCD28 (10000 beads/well) or combinations of both and cultured for 7 days. Thereafter cells were stained for CD4$^+$PD-1$^+$IL-10$^+$ (A) or CD8$^+$PD-1$^+$IL-10$^+$ (B) in each individual (EN n=8, MF+ n=8 and MF- n=8). Cell populations were analysed via flow cytometry. Bars present the mean percentage ± SEM of CD4$^+$PD-1$^+$IL-10$^+$ and CD8$^+$PD-1$^+$IL-10$^+$ T cells. Data of each group were compared using Mann-Whitney test and significant differences are given as *$p<0.05$,**$p<0.01$ and ***$p<0.001$.

3.7   Determination of total immunoglobulin levels in *W. bancrofti*-infected individuals

As mentioned in the previous introductory section (sections 1.4 and 1.6) *W. bancrofti* infections can give rise to an asymptomatic state or develop into lymphedema, hydrocele or urinary infections. Asymptomatic individuals usually present a regulated phenotype including high levels of IgG4 whereas those with pathology have higher levels of IgE. Thus, given the diverse role of antibodies during infection, plasma from EN, MF+ and MF- individuals were screened for levels of IgA, IgG1, IgG2, IgG3, IgG4, IgM and IgE using a human multiplex immunoglobulin kits. While significantly elevated levels of total IgA (Figure 3.25 A), IgG1 (Figure 3.25 B) and IgG3 (Figure 3.25 D) were observed in EN, there was no significant difference in the amount of IgG2 (Figure 3.25 C) or IgM (data not shown). Interestingly, the total antibody level of IgG4 was more pronounced in the patently infected individuals (Figure 3.25 E). Furthermore, significantly elevated amounts of total IgE was observed in MF- and MF+ groups when compared to EN subjects as shown in (Figure 3.25 F).
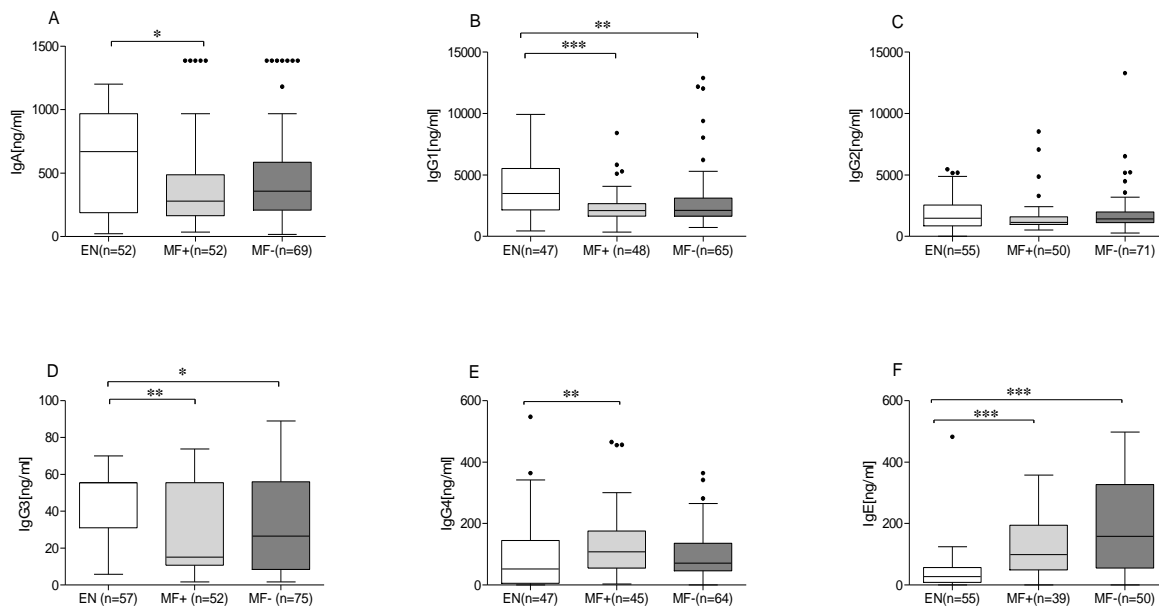
Figure 3.25: Immunoglobulin levels in individuals with filarial infection

Total antibodies were determined in plasma from *W. bancrofti* individuals via ELISA. The level of IgA (A), IgG1 (B), IgG2 (C), IgG3 (D), IgG4 and IgE (F) in EN, MF+ and MF- is shown. Graphs show box whiskers with outliers. Data of each group were compared using Kruskal-Wallis and Mann-Whitney test and significant differences are given as *p<0, 05, **p<0, 01 and ***p<0,001.

3.8   Filarial-specific IgG4, IgA and IgE in plasma can be associated with patent infections, no infection and latent infection respectively.

To investigate filarial-specific antibody levels induced during asymptomatic *W. bancrofti* infection, plasma from EN, MF+ and MF- individuals were screened using specific-Ig ELISA. The results showed no significant differences between the groups in terms of IgG1 levels (Figure 3.26 A). However, the levels of IgG2 were significantly increased in MF+ and MF- groups when compared to EN (Figure 3.26 B), while no significant differences were observed in the study groups regarding IgG3 (Figure 3.26 C) levels. More interestingly, and in keeping with previous studies [13] significant levels of IgG4 (Figure 3.26 D) were found in MF+ subjects when compared to either MF- or EN group. Furthermore, consistent with the total antibody data shown in section 3.7, increased amount of filarial-specific IgA in was measured in EN compared to individuals with asymptomatic filarial infection (Figure 3.26 E). Finally, latently infected individuals showed significantly higher levels of filarial-specific IgE when compared to both EN and MF+ groups (Figure 3.26 F). The results indicate that while IgG4 characterises with MF+ individuals, IgA associates primarily with subjects without *W. bancrofti* infection.
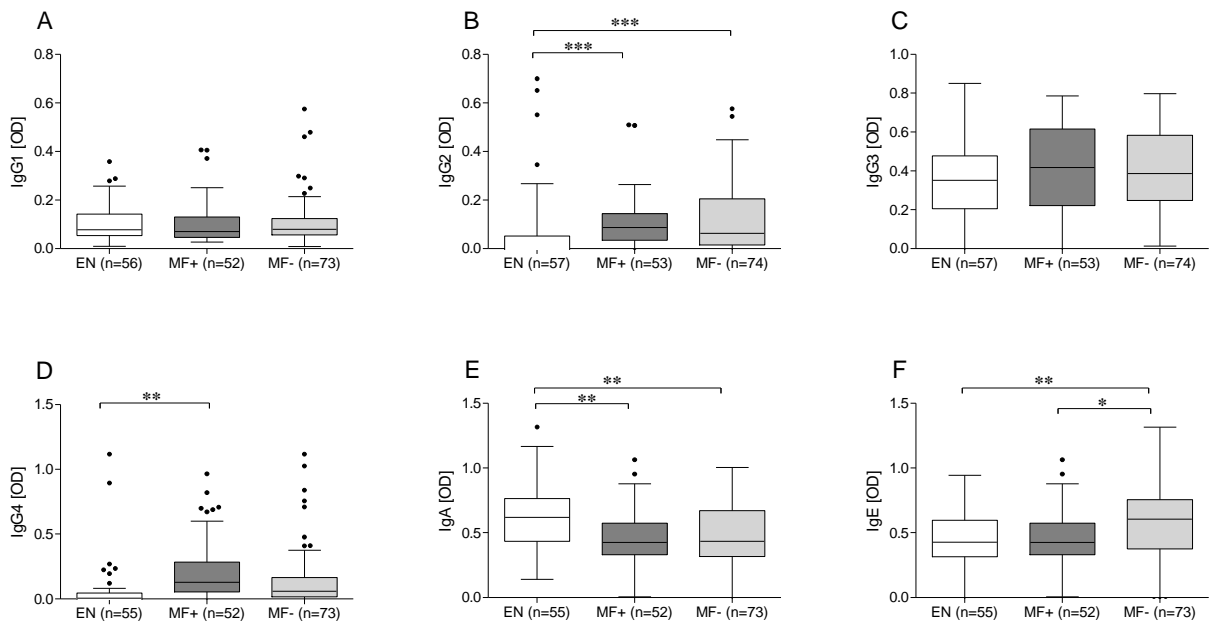
Figure 3.26: Increased filarial-specific IgG4 and IgG2 expression in microfilaraemic individuals; whilst endemic normals exhibit higher levels of filarial-specific IgA.

Plasma was obtained from EN, MF+ and MF- filarial-specific antibodies were determined through ELISA using BmAg. Figures A-F represent IgG1, IgG2, IgG3, IgG4, IgA and IgE, respectively. Graphs show box whiskers with outliers and asterisks show statistical differences (Kruskal-Wallis and Mann Whitney test) between the groups indicated by the brackets (*p<0.05, **p<0.01, ***p<0.001).

4 DISCUSSION

4.1 Transcriptomics in lymphatic filariasis and onchocerciasis

Filarial infections affect almost 200 million individuals and pose a major public health challenge in several endemic regions. Suboptimal responses to antifilarial drugs, such as ivermectin, has been documented in field studies [52, 59] coupled with the modelling data showing that ivermectin is to be given for a much longer time in other to achieve elimination goals by 2020/2025 in LF and onchocerciasis, respectively [141]. Current treatment options all have their obstacles and either do not kill adult worms, or as in the case for doxycycline, a macrofilaricidal treatment, require a longer treatment regimen and are not appropriate for pregnant women or children under 9 years. All these hurdles suggest the need to develop improved interventions. Therefore, one of the central goals in the fight against human filarial infections is the development of strategies that lead to the inhibition of MF transmission. Keeping MF within endemic populations under a certain threshold will stop transmission and eliminate the infection. Amongst the different approaches being discussed is the development of an effective vaccine. Anti-filarial vaccines would significantly reduce a major health burden in the tropics and could also become a promising tool for the elimination of filarial infections. Indeed effective vaccines have been hypothesized to improve economic development in endemic regions and thus, have a positive impact on health [142]. In various animal models and in life stock, vaccines against nematodes have been successfully tested [143]. Indeed, the use of two excretory-secretory antigens from *Heamonchus contortus* in sheep resulted in a significant decrease in faecal egg counts compared to an un-vaccinated control group [144]. Recently, the human hookworm vaccine initiative carried out a Phase 1 trial [145]. In the pursuit of developing a filarial vaccine, studying naturally occurring protective host immune responses against these nematodes may be highly informative. Towards this goal, the primary objective was to compare the immune responses in different phenotypes of *W. bancrofti* infection as well as *O. volvulus* infection. One phenotype is characterized by the absence of MF from peripheral blood or skin suggesting presence of immune responses that permit the circulation of MF. To identify factors of the immune response, the microarray technique has been used to elucidate gene regulation in the particular disease phenotypes. Recently, human microarray studies in *L. loa* infection have shown that CD4^{+} and CD8^{+} T cell associated networks and molecules are highly regulated in chronic infected individuals compared to subjects without chronic infection [124]. Yet, this technology has not been fully explored in human filarial infections. Therefore, in this study, transcriptome analyses using whole blood from *O. volvulus* and asymptomatic *W. bancrofti-*

infected individuals and endemic normals was performed and confirmation on the cellular level was performed.

The current study comprised of healthy adult individuals with either asymptomatic *W. bancrofti* or *O. volvulus* infection recruited from endemic regions of Ghana. For purposes of comparison, individuals who lived in the same communities but without infection were also recruited. In the LF study, patients were grouped on the basis of the presence of MF, absence of MF but positive for circulating filarial antigen (CFA) or MF- and CFA-. Most study participants belonged to either the Nzema or Ahanta ethnic groups. The Nzema East district has a population of about 60,000 with economic activities including fishing, farming, trading and small-scale mining. It is mainly made up rural communities with third class roads, which makes travelling difficult especially in wet seasons. On the other hand, the Ahanta West district has a population of 106,000 with similar economic activities as mentioned for Nzema East district. However, communities in the Ahanta West district are larger and closer to each other making travelling relatively easier. The median age of the study participants did not vary across the groups. The number of males infected was higher than the females, particularly in the patently infected group. Most of the males were involved in fishing, small-scale mining and thus happen to stay late in the night, which coincides with the biting time of the transmission vector, whereas the females were predominantly fish mongers, traders and farmers. In the *O. volvulus* study, participants were either positive for adult worm (nodules) in addition to MF, or positive of adult worm (nodules) but no MF as well as individuals without infection. Participants were involved in economic activities such as farming, trading and small-scale mining. There was a fair distribution in the median age of the study participants and almost half had participated (1x) in MDA programmes. Similar to the LF study, more males were found to be infected compared to females. The impact of host immune responses on confounding factors such as co-infections and IVM intake will be discussed in the later sections.

4.2   Genes and pathways regulation in filarial infections

In the present study, two consecutive strategies were employed to performed gene expression analysis. This is because following analysis with the fist strategy: FC and statistics (FC ≥1. 3, adj. p<0.05) few transcripts were found to be regulated. This led to the use of a second strategy which considered genes regulated with an change in expression exceeding 1.3 fold (without adjusted p-value) as described elsewhere [146]. Both approaches provided new insights that are likely of biological relevance. For instance, out of the 46,862 genes for LF, and 46,698

genes for onchocerciasis, 42 and 10 genes were regulated in LF and onchocerciasis, respectively, when compared to EN. The number of regulated genes across group comparison was found to be increased in both infections when a second analysis strategy, i.e. without adjusted *p*-value was applied as shown in Table 3.1.3. Interestingly, after analysis without adjusted *p*-value, genes such as *CLC*, *RNASE2*, *RNASE3* and *HLA-DBR1* were regulated in infected vs EN as well as MF- vs EN.

In the *O. volvulus* infection, no gene popped up when stringent analysis was applied in a comparison between infected (MF+) and EN. However, following gene expression analysis without adjusted *p*-value genes, such as *CLC, RNASE2, RNASE3* among others, were upregulated. CLC are proteins released predominantly by activated eosinophils, basophils and regulated T cells. In this study we found increased mRNA *CLC* levels in individuals with filarial infection compared to EN (discussed below). Pathways such as Actin Nucleation by ARP-WASP Complex, Cdc42 signaling, Rac signaling, CD28 signaling in helper T cells, heme biosynthesis and tetrapyrrole biosynthesis were found relevant in immune cell activation, recruitment and heme metabolism in individuals with LF. In comparison superoxide radical degradation, chemokine signaling, CCR3 signaling in eosinophils, regulation of eIF4 and p70S6K signaling and EIF2 signaling associated with eosinophil recruitment and metabolism, cellular movement, and protein synthesis were activated in persons with onchocerciasis when compared to EN. These pathways were previously unknown to be involved in filarial infections.

Although there was an overall low gene expression, this is thought to be a technical issue due to the presence of globin mRNA in total RNA, which interferes with the amount of gene transcripts [147, 148]. In order to reduce this potential skewing, blood samples from study subjects were collected using PAXgene tubes, because this approach has been shown to efficiently preserve cellular RNA species at the state of blood sampling which maintains the transcriptome profile [149]. Therefore, it is not clear what accounted for the low transcriptome pattern observed in this study. In another infection scenario, gene expression in *Loa loa*-infected individuals revealed a higher number of regulated genes; however, in that study, the expression profile was performed in CD4^{+} and CD8 [+] T cells from PBMCs [124] and not directly on whole blood.

4.3   Latently infected individuals show a stronger transcriptome regulation in *W. bancrofti* infection

In the LF study, 12 genes were significantly regulated in *W. bancrofti*-infected compared to EN. Coincidentally, 12 genes were also up-regulated in the latently infected when compared to EN, whereas no gene was down-regulated and therefore suggesting an elevated host gene response in this group. Subdividing the infected individuals by their MF status revealed that the number of genes upregulated was higher in the MF- persons versus EN compared to MF+ versus EN with most of the regulated genes in MF- comprising the regulated genes in the infected vs EN comparison. This suggests that the absence of MF in latent infected individuals may be due to immune responses, acting specifically against this life-cycle stage. Indeed, most of these regulated genes are associated with inflammatory responses as well as immune cell migration. For instance, amongst the highly up-regulated genes in the MF- group relative to EN was the transcription factor *ZFAND5*. ZFAND5 protein enhances the stability of TNF-α mRNA by suppressing deadenylation [150]. Suggesting that the increased expression of this gene and apparently the protein form could contribute to the stability of proinflammatory cytokines such as TNF-α, since ZFAND5 proteins bind to ARE$^{TNF-\alpha}$ mRNA and competes with the mRNA destabilising protein tristetraprolin. Vice versa, such observations suggest that the presence of MF is associated with a weaker transcriptional regulation/host response, supporting previous studies, in which immunoepidemiology profiling of MF+ and MF- individuals revealed that MF-persons had elevated immune response [13]. This phenomenon could also be modelled in animal experiments, in which the susceptibility of the rodent is associated with regulatory responses accompanied by IL-10 and FOXP3 whereas resistance is observed in Th1/Th2 settings [151, 152]. Thus, in humans susceptibility might be part of an immunosuppressive effect triggered by the patent infection or, alternatively, the weaker response to infection in these individuals allows the development of MF.

The present transcriptomics data emphasizes that *W. bancrofti* infection induces increased upregulation of cell migration and trafficking genes and pathways in the latent infected group compared to the patently infected individuals. Heightened expression of cell migration related genes might reflect recruitment of functional leukocytes to the site of infection. This observation may represent an active immunity in the latent infected persons compared to the microfilaremic counterparts. Immune cell migration is generally associated with inflammation as part of an immune response [153, 154] and ongoing infection [155].

In addition, Cdc42 signaling was highly activated in the MF- group compared to those with MF+ infection. Cdc42 protein modulates actin polymerization through its direct binding to Wiskott-Aldrich syndrome protein (WASP), which in turn activates the Arp2/3 complex through an associated-controlled mechanism [156]. Cdc42 promotes host defense against upper respiratory infections [157] and its loss leads to impaired migration in fibroblast and astrocytes [158]. Further, the activation of CD28 signaling in T helper cells in the latent compared against EN, suggests that latent infections fundamentally impacts the host adaptive immune response at the gene transcription level, whereas MF have been shown to block leukocyte migration [159]. Together, the robust genomic regulation in the latently infected individuals shows that cell migration is predominantly a feature of the on-going immune response directed against adult worms as described in previous studies [13].

In contrast, the MF+ cohort was the only group where 4 genes (2 annotated and 2 unknown) were downregulated when compared to MF- and EN groups indicating overall low host responses. These genes include the delta-Aminolevulinate synthase 2 (*ALAS2*) and carbonic anhydrase 1 (*CA1),* Table 3.1.4. Of ALAS two isoforms exist, which catalyze the conversion of glycine and succinyl-coenzyme A to 5-aminolevulinic acid (ALA) as the first and rate-limiting enzyme in the mammalian heme biosynthesis pathway [160, 161]. ALAS1 is found in all body cells, whereas ALAS2 produces heme precursors for the production of hemoglobin [161]. Further, *CA1* encodes cytosolic enzyme carbonic anhydrase (CA1), which catalyzes the reversible hydration of carbon (IV) dioxide to bicarbonate. Due to its potential harmful effects, the synthesis and catabolism of free heme is highly regulated. This is because free heme has been shown to promote inflammatory reactions associated with vascular injuries [162]. Reasons for downregulating the heme and tetrapyrrole biosynthesis pathways in the MF+ subjects are currently not clear, but may reflect a host/parasite compromised response that could leads to the inhibition of pathology development.

Interestingly, filarial worms need heme as a cofactor for the production of ecdysteroid-like hormone that regulate filarial moulting and embryogenesis [163]. As they are not able to produce heme, filarial nematodes obtain this molecule from their endosymbionts. However, the *Wolbachia* endosymbionts have retained this ability and might supply its host with tetrapyrroles [163-165]. Interestingly, the *Wolbachia* heme synthesis pathway has recently been exploited for the development of novel anti-filarial drug candidates [164, 165]. Yet, the *Wolbachia*-free filariae *L. loa* is incapable of *de novo* heme biosynthesis and apparently depends on the uptake of heme or precursors from the host, a scenario that may also apply for *Wolbachia*-harbouring

filarial nematodes [166]. The use of heme biosynthesis inhibitors, succinyl acetone, and N-methyl mesoporphyrin, which target aminolevulinic acid dehydratase (ALAD) and *Wolbachia*-ALAD inhibitors have been shown to affect both endosymbionts and adult worm viability leading to death [165]. However, heme biosynthesis may not be unique to filarial parasites, since it is present in certain parasites, such as *Plasmodium* infections and has been regarded as a potential drug target [167]. The findings therefore suggest targeting of the *Wolbachia* heme biosynthetic pathway as a suitable therapeutic intervention in the fight against filarial infections.

As already mentioned, *CA1* was markedly downregulated in MF+ compared to MF- infected persons. CA1 regulates several physiological processes, including the transport of CO_2 and bicarbonate between metabolizing tissues and lungs among others [168]. The regulation of CO_2 and bicarbonate concentration could influence periodicity of MF, a phenomenon which characterises *W. bancrofti* infection. Periodicity of MF in the blood have been associated with the different levels of oxygen pressure in the lungs [169]. Hence, suppressing *CA1* in MF+ could be a strategy that permits MF in peripheral blood at night; yet further transcriptomics investigation may be required in order to elucidate the mechanism underlying nocturnal periodicity in lymphatic filariasis.

4.4   Impact of confounding factors on host immune responses

Given that the study was conducted in communities not only endemic for filarial, but also protozoan and other helminth infections, further analyses were performed to establish whether confounding factors such as study regions, co-infection and/or IVM intake impacted gene expression profile in the study. Following the removal of individuals that had co-infection and/or had participated in IVM intake, it remained with a population who were only infected with *W. bancrofti*. In this population, gene expression analysis showed that lymphoid associated markers such as *GZMA* and *GZMB* were strongly up-regulated in patently infected individuals and were contrastingly strongly down-regulated in subjects with latent infection. Granzymes are serine proteases which are secreted by many cell types such as CD8, NK and regulatory T cells and are discussed below.   Additionally, with regards to impact as a result of study region, increased gene expression was associated with subjects from Nzema East district compared to those from Ahanta West district. A closer look at the transcriptomics data showed that most of the up-regulated genes in the Nzema East samples were similar to those identified in latently infected subjects. Reasons for this finding could be many. More potent immune response in these individuals are possible, but also altered infection intensity or transmission in the Nzema

East communities. It was also observed that the majority of the individuals in the Nzema East district had at least one or two round(s) of ivermectin when compared to those in the Ahanta West district. What accounts for differences in the rounds of ivermectin intake between the two districts is unclear since the LF elimination programme apparently began in the year 2001 in the Ahanta West district and subsequently in the Nzema East district in 2002. The LF elimination programme in these districts is managed on sub-district level by community health officers supported by village workers. Low remuneration for village workers or increased commuting of individuals in the Ahanta Districts may account for different MDA distribution. In addition, the Ahanta District is has a huge population size, and difficulties in achieving necessary coverages of IVM distribution could explain the dependency. Thus, different environmental pressure may affect parasite and host population, resulting in altered immune responses. Indeed, infection intensity has been observed to vary from one community to another [170, 171]. Furthermore, this study population has not been characterized with regard to the family history and therefore we cannot fully exclude the possibility of genetic divergence within the two ethnic groups in response to *W. bancrofti* infection. On the other hand, we also observed increased regulation of genes in the MF- individuals who had coinfections and/or had participated in IVM treatment more than their MF+ counterparts. Genes such as basic helix-loop-helix family, member e40 (*BHLHE40*), natural killer-tumor recognition sequence (*NKTR*), ELOVL family member 5, elongation of long chain fatty acids (*ELOVL5*) were highly expressed in MF- group. These genes were associated with pathways such as spliceosome, protein processing in endoplasmic reticulum, ubiquitin mediated proteolysis and circadian rhythm. Obviously, in this context, caution is required when handling human gene expression data since several factors such as ethnic background [172-174], previous treatment history and infection intensities among others could potentially impact expression pattern. In the *O. volvulus* infection there were no genes detected following analyses with respect to coinfection or IVM intake.

4.5 Evidence of increased numbers of peripheral eosinophils and neutrophils in latently infected individuals

To investigate differences between the study groups on the cellular level, we analysed blood smears for granulocytes, cells that are strongly involved in the defence mechanisms against parasitic nematodes. In the *W. bancrofti* study, an increase in eosinophil counts was observed in the MF- individuals but not in EN and MF groups, whilst neutrophil counts were not distinct between the study groups. In the *O. volvulus* study, there were significant differences in

eosinophils between MF+ subjects and EN as well as a-MF individuals and EN, whilst neutrophil counts were higher in a-MF individuals when compared to EN groups, but not in MF+ individuals. Furthermore, there was no association between MF counts and eosinophil and neutrophil numbers in the bancroftian infection, whilst MF counts significantly correlated with peripheral eosinophils but not neutrophils in *O. volvulus* study. In contrast, an association between blood eosinophil count and MF+ subjects but not in their MF- counterparts in an *O. volvulus*-infected population has been observed [18]. The peripheral leucocyte counts in both infections compared to EN are consisted with the transcriptome data presented in this study, i.e. upregulation of the eosinophil-associated CCR3-signaling pathway was observed in filarial infected individuals when compared to EN. In a mouse model, CCR3 promoted L3 larvae killing in *O. volvulus* infection [138], whereas CCR3 knockout mice sustained elevated muscle larvae burden in *Tricuris spiralis* infection [175]. However, the expression of CCR3 is not restricted to eosinophils alone, but also in cells, such as neutrophils [176] and basophils [177]. The activation of this signaling pathway indicates migration of eosinophils to site of infection.

Equally important, the transcriptome data give credence to a recent observation by Gentil *et al,* where in a mouse model of filarial infection, Eotaxin-1 (chemokine, which binds to CCR3) was found to modulate activation of inflammatory cells leading to helminth clearance [178], thus further confirming the protective functions of eosinophils during filarial infection. However, eosinophil activity in another study demonstrated their contribution to *L. sigmodontis* development [66], a scenario which needs to be carefully considered in human vaccine programmes to control helminth infections. Together, the current study shows direct evidence that the activation and recruitment of eosinophils and neutrophils and their secreted proteins could be linked with protection since eosinophils in (LF) and eosinophils and neutrophils in onchocerciasis infections were significantly expressed in subjects without MF; hence suggesting their important in determining filarial infection outcome.

4.6   Profiling immune response in individuals with *W. bancrofti* infection

Generally, filarial nematodes dampen the host's immune response in order to coexist for several years. However, in endemic regions, a few infected individuals develop severe clinical manifestations. This study focused on deciphering the underlying molecular mechanisms, which drive the two asymptomatic infection phenotypes, i.e. MF+ and MF-. To do this, the adaptive immunological profiles of MF+, MF- and EN (in the case of *W. bancrofti* infection) were performed *in vitro* by characterizing CD4$^+$ and CD8$^+$ T cells within PBMCs from study subjects.

4.7   Human filarial infection is associated with increased CLC/Gal-10 levels

CLC/Gal-10 was highly expressed on the mRNA level in both *W. bancrofti* and *O. volvulus* infections compared to endemic normals; therefore, we further investigated peripheral protein levels in study subjects. When compared to EN, CLC/Gal-10 expression was found to be enhanced in filariae-infected individuals on protein levels in CD4$^+$ and CD8$^+$ T cells. CLC/Gal-10 is produced by regulatory T cells and is released following activation [69]. Furthermore, following intracellular staining by flow cytometry, *W. bancrofti*-infected individuals exhibited an increased frequency of CLC/Gal-10-producing CD4$^+$ and CD8$^+$ T cells when compared to levels in T cells from EN. Additionally, filarial-specific stimulation of PBMC resulted in an increased secretion of CLC/Gal-10$^+$IL-10 by CD4$^+$ T cells in MF+ persons when compared with EN and MF- individuals. The expression pattern of CLC/Gal-10$^+$IL-10$^+$-producing CD8$^+$ T cell was comparable to CD4$^+$ T cells. In addition, eosinophils could be a potential source of CLC/Gal-10, as it constitutes approximately 10% of the total cellular protein in human eosinophils [179], whilst its percentage in Tregs remains to be characterised. Based on the literature, CLC/Gal-10 appears to have a dual role with both protective and immunosuppressive effects. CLC/Gal-10 has been reported to possess IgE binding activities [180] and although there is currently no available data, this may contribute to filarial clearance upon IgE binding. This hypothesis is supported by studies on other cytotoxic factors, such as eosinophil peroxidase (EPO) and major basic protein 1 (MBP) whose importance was reported using filarial murine model by Specht *et al.,* [65]. On the other hand, CLC/Gal-10 protein appears to also have immunosuppressive functions, since it enhanced the suppressive capacity of regulatory T cells [69]. The current data bring us one step closer to deciphering the role of CLC/Gal-10 in filarial infection since in both infections MF+ individuals had higher levels, therefore such observation could be a secondary reaction to the higher MF loads, or immunosuppression, but it is not associated with protection. Elsewhere, increased IL-10 and TGF-β are believed to be highly produced in patently infected individuals [77, 181]. It may be speculated that post-translational modifications may influence the conversion of *CLC/Gal-10* mRNA into proteins (splice variants) in the presence of MF during *W. bancrofti* and *O. volvulus* infection as demonstrated by a recent proteomics study where 3 variants of CLC/Gal-10 protein were identified [69]. The existence and functions of possible isoforms of CLC/Gal-10 proteins during filarial infection are not known and further investigation of this molecule may be important. Furthermore, galectin-9 from *Toxacaris leonina* shares 35% homology with human galectin-9 and recombinant forms lead to diminished intestinal

inflammation in mice via increased IL-10 and TGFβ [182]. Interestingly, the presence of galectin-1 and 9 supported the differentiation of CD4$^+$CD25$^+$ T reg cells *in vitro* [183, 184], while treatment of galectin 1 resulted in the expansion of IL-10 producing T cells and effectively suppressed autoimmune inflammation [185]. In this study, we observed higher amounts of CLC/Gal-10 MF+ infected individuals compared to EN group. Collectively, these data give rise to evidence that the galectin family of proteins may have intrinsic functions associated with immunomodulation of host responses and this should be exploited in filarial infection to fully characterize the underlying mechanisms.

4.8 Differential regulation of granzyme A and B expression during *W. bancrofti* infection

When further dissecting the study group by removal of patients with coinfections and those who had taken IVM as mentioned in section 4.5., the gene expression data showed increased expression of GZMA and GZMB in patently infected individuals compared to control. Granzymes are primarily produced by CD8$^+$ T, NK cells and Tregs [186]. GZMA belongs to the tryptase-like serine proteases and cleaves after the basic amino acids Arginine and Lysine, whilst GZMB has aspase activity and cleaves substrates at key aspartic acid residues. In the current study, the increased frequencies of CD4$^+$ and CD8$^+$ T-secreting GZMA were associated with MF- individuals, whereas the higher amounts of GZMB producing T cells were observed in MF+ subjects. Again, the pattern of GZMB but not GZMA in T cells in the MF+ individuals was in line with the transcriptome data following the removal of subjects with co-infection and/or with IVM intake. Additionally, we observed significantly increased frequencies of GZMB$^+$IL10$^+$-producing CD4$^+$ and CD8$^+$ T cells in MF+ subjects when compared to MF- individuals. These CD4$^+$ and CD8$^+$ T cells-producing GZMB$^+$IL-10$^+$-phenotype may have immunoregulatory properties in MF+ individuals but further studies are required to address this. Previous studies in onchocerciasis showed that FOXP3$^+$T cells interact with both GZMA/B following doxycycline treatment [104]. The authors found that an increased frequency of FOXP3$^+$T cells expressing GZMA and GZMB, which in turn inhibited the activity of effector cells. In the same study, GZMB expression was found to be distinct when study subjects were compared on a regional basis. However, this was not the case in the present study. Whether such differential expression of granzymes, has a genetic basis is currently unclear, and requires further investigation. Interestingly, studies in mice with different genetic background have shown that GZMB is enhanced in Tregs following activation with inhibitory activity, while GZMB-deficient mice failed

to induce suppression [187]. Interestingly, in individuals with tumor, GZMB-producing Tregs have been shown to suppress NK and CD8^{+} T cells activities [94, 188], as well as attenuate host immune responses. Such immune regulation via the release of GZMB could be a further immune evasion mechanism induced by filariae parasites, given their inherent ability to dampen host immune responses through increased regulatory T cells. Furthermore, antigen-specific CD8^{+} T cells expansion was regulated by GZMB-producing Tregs in a Senai viral (SeV) infection model of acute respiratory disease [95], which compromised the ability of CD8^{+} T cells to clear the virus.

More interestingly, the observations made within this work confirm that of Hartmann and colleagues, where they demonstrated that GZMA promotes protective immunity in rodent filarial infection with *L. sigmodontis*, whereas GZMB enhanced susceptibility to infection by suppressing Th2-related cytokines [96]. Contrarily, both granzymes have been shown to support proinflammatory conditions, i.e. GZMA catalyzes the conversion of IL-1β [189], leading to inflammation, while GZMB induces VEGFs from an extracellular cell matrix under inflammatory conditions [190, 191]. The increased expression of GZMB in T cells from MF+ individuals in this study may suggest its immunoregulatory function as described previously [96, 104], given that GZMB was co-expressed with IL-10 following filarial-specific stimulation. Along these lines, GZMB-producing IL-10 CD4^{+} and CD8^{+} T cells could promote re-infection via immune suppression, i.e. complicating current efforts to human eliminate filarial infections.

4.9   T cell responses in individuals with *W. bancrofti*-infection

In further characterising the host immune response in individuals with *W. bancrofti* infection, we found that MF+ subjects presented increased regulatory responses (IL-10), whilst MF- persons presented Th1, Th2 and Th17 responses accompanied with IFN-γ, IL-4 and IL-17A, respectively in CD4^{+} T cells. One interesting finding was the increased CD8^{+} T cells producing IFN-γ in the PBMCs from EN and MF- groups when compared to MF+ individuals. This observation corroborates previous findings, which showed that IFN-γ is upregulated in EN, while IL-4 and IL-10 producing cells in PBMC from filarial-infected were significantly higher in MF- and MF+ groups. Again, MF+ individuals have been shown to exhibit diminished Th1 and Th2 phenotype, but increased regulatory phenotype reflected in IL-10 and TGF-β and FOXP3 [77]. IL-10 has suppressive activity on cell types, thus attenuating the nature of the immune response. Consistent with previous studies, MF- individuals exhibited enhanced pro-inflammatory

conditions, which apparently promote protection against MF, but regulated, since individuals in this groups have the tendency to produce IL-10 following antigen specific stimulation [13]. One remarkable finding in this study is the characterisation of IL-17A producing T cells in asymptomatic filarial-infected individuals. The frequencies of CD4$^+$ T cells expressing IL-17A were increased in MF- persons compared to MF+ and EN groups, suggesting a protective role of this cell type and correlated with the expression level of the Th17 signature cytokines IL-17A. In contrast to this finding, Anuradha *et al*, observed no differences in CD8$^+$ T cells-expressing IL-17A in response to PMA and Ionomycin treatment in individuals with *Brugia malayi* infection [191]. This could be explained by several factors such as experimental setup, sample size as well as differences in concentration of antigen used in both studies. Recently, IL-17A has been implicated in several infections as well as filarial pathology, such as hyperreactive onchocerciasis [17] and lymphedema [82]. However, in response to filarial specific or anti-CD3/anti-CD28 activation, T-bet, GATA-3 and RORC2 were highly expressed in MF-individuals, whereas FOXP3 was again elevated in T cells from MF+ subjects. Furthermore, the frequency of CD8$^+$ T cells was significantly higher in MF+ persons compared to MF- individuals. This corroborates studies in animal models of human filariasis since MF have been reported to associate with activated CD8$^+$ T cells [192]. More intriguingly, soluble CD8 in plasma of individuals with patent infection was higher when compared to levels in healthy donors, i.e. non endemic normals (data not shown), and thus indicates a potential immunomodulation steered by MF. It is unclear how CD8$^+$ T cells are activated following *W. bancrofti* infection, although cross-presentation of extracellular antigens in the MHC-1 pathway is now a well-documented phenomenon [193, 194]. The findings within this study provide evidence that the frequencies and cytokine production by CD8$^+$ T cells are altered during *W. bancrofti* infection. Together, it was observed that while absence of MF associated with active immune response, patently infected individuals were characterised by regulatory response. Additionally, this study shows that besides CD4$^+$ T cells, CD8$^+$ T cells are implicated in filarial infections; and have a potential regulatory function in the establishment of patent infection a condition, which may implicate future vaccine program.

Furthermore, the study demonstrates that to a large extent filarial antigens dampen the activity of TCR activation. In the presence of both BmAg and anti-CD3/anti-CD28 compared to anti-CD3/anti-CD28 alone, the frequency of most expressed markers was slightly diminished in all study groups. The findings emphasize the modulatory potential of filarial antigen in the presence of TCR stimulation. The suppression was not IL-10 dependent, which indicates that to survive in

their host, filarial parasites release products, which suppress the activity of effector cells. This scenario may represent competition for binding sites. While the findings in these experiments by no means constitute a final analysis of TCR-specific suppression by filarial antigens, they suggest a potential immunomodulatory mechanism, which warrants further investigation. Elsewhere, the capacity of helminth-derived antigens to modulate innate immunity has been demonstrated [195]. The current study demonstrates that filarial antigens moderately modulate TCR specific activation, albeit not significantly, an area, which warrants further investigation. Such phenomenon suggests that outcome of filarial infection and consequently any resulting pathology may be influenced by confounding factors, such as co-infection.

4.10 T cell exhaustion is associated with microfilaremic infection

T cell exhaustion during chronic infection may impact protective immunity and some of the underlying mechanisms are beginning to be revealed. In this study, it was observed that CD4$^+$ and CD8$^+$ T cells in MF+ individuals showed elevated levels of PD-1 and CTLA-4 than individuals without MF as well as EN. It was also demonstrated that MF+ persons present increased frequencies of PD-1$^+$IL10$^+$-expressing CD4$^+$ and CD8$^+$ T cells compared to the MF- and EN groups following PMA/Ionomycin treatment as well as filarial-specific stimulation. Persistent antigen stimulation has been shown to result in the co-expression of inhibitory markers that lead to exhaustion. In fact, *Trichinella spiralis*-infected mice treated with anti-CTLA-4 resulted in an increased Th2 response during infection [197]. The results in this study are consistent with a previous study, which demonstrated that MF+ subjects display increased levels of CTLA-4 in PBMCs [198], while IL-5 levels were enhanced after anti-CTLA-4 antibody treatment. Intrinsic defects in T cell responses in human filarial infections are linked with expression of the T cell-inhibiting receptor, CTLA-4 [198], and neutralisation of CTLA-4 in mice results in enhanced *L. sigmodontis* killing [199]. In addition to this intrinsic T cell hypo-responsiveness, T cell responses in humans can be dampened by suppressive antigen-presenting cells [75]. Both mechanisms are operative in the *L. sigmodontis* model where macrophages that block proliferation of T cells are present at the site of infection prior to patency but become apparent in the draining lymph nodes only following patency [199]. Studies in susceptible BALB/c mice have demonstrated that *L sigmodontis* survival is dependent on the induction of a regulatory T cell populations that induces hypo-responsiveness [200]. This corroborates the data from human field studies demonstrating that T regulatory (Treg) cells can be isolated from onchocerciasis patients [201], and generalised onchocerciasis is associated

with antigen-specific Treg cells that can be found in nodules [202]. Additionally, CTLA-4, together with PD-1 have been reported by Babu *et al* to suppress Th1 and Th17 responses during co-infection with tuberculosis and LF [203]. Interestingly, the expression of the inhibitory receptor PD-1 in exhausted CD8^{+} T cells has been associated with the progression of viral infection [204]. In another infection scenario, PD-1 has been shown to suppress protective immunity to *Streptococcus pneumoniae* through a B-cell-mediated manner [205]. However, a recent study has shown that in addition to the negative regulatory role attributed to PD-1, a phenotype of tumour reactive cells exists which can be used to predict tumour regression following the infiltration of lymphocytes [206]. Further elucidation about the role of PD-1 in filarial pathologies may reveal a distinct T cell phenotype and function that may underlie developing pathologies. Further profiling of the T cells in this study exposed other exhausted markers too, namely CD244 and CD107. The frequencies of these markers were upregulated in the filarial-infected individuals compared to uninfected controls a phenomena that has been previously described in chronic viral infection [207]. Thus, the increased frequency markers related to T cell exhaustion in the MF+ subjects may indicate an impaired immune response, which supports MF survival. This scenario reflects hypo-responsiveness driven by MF in order to escape the protective host responses, and thus suggests developing antifilarial drugs, which inhibit PD-1 and CTLA-4 regulatory pathways in MF+ persons, may lead to immune responses, which control MF.

4.11 Profiling filarial-specific immunoglobulins

Individuals with filarial infection develop extraordinary diverse antigen immunoglobulin responses. In this study, *W. bancrofti* MF+ subjects produced spontaneous IL-10 and exhibited both increased total and filarial-specific IgG4, which also correlated with MF load. The current data are consistent with that of Kwan-Lim *et al*, where they documented that plasma IgG4 levels are associated with active infection [208]. A decade ago, elevated IgG4 levels in plasma from MF+ individuals was demonstrated in B cell class switching *in vitro* to be facilitated by IL-10 [87], TGF-β and GITR ligation but not CTLA-4 [88]. In this study, increased antigen specific IgG2 levels were associated with MF+ and MF- subjects when compared to EN group. This was in contrast to an earlier report where IgG2 levels were elevated in infection free individuals, suggesting protective immunity [209]. Such differences observations call for further work on the role of IgG2 in filarial infections. On the other hand, the current data showed that MF- persons produced increased IgG3 and IgE. These filarial specific antibody responses may contribute to

protective immunity and thus clearance of MF. In onchocercal infections, levels of IgE, IgG1, IgG2, IgG3 has been documented to be higher in sera from sowda individuals [210]. Interestingly, Peterson *et al* documented that individuals with *W. bancrofti*, co-infected with HIV showed significantly higher levels of filarial-specific IgG3 before DEC treatment but reduced levels of IgG4 following treatment indicating that therapy had a stronger antifilarial effect in these subjects [211]. But, since each infection has its own peculiarities, it stands to reason that coinfections will have both direct and indirect influences on immunological and pathological responses. Remarkably, the lack of pathology normally associated with the MF+ group is because IgG4 is monomeric in structure and blocks IgE mediated responses [105]. IgE is known to play an important role in the clearance of helminth infections. In the present study, both total and antigen-specific IgE levels were elevated in MF- individuals, suggesting its relevance in controlling MF. But IgE, has been shown to be more specific but less sensitive than IgG4 for instance in the diagnosis of toxocariasis. This is because in a follow-up study after chemotherapy, specific serum IgE levels were significantly decreased 1 year after treatment, while specific IgG levels declined 4 years post-treatment [212], suggesting the treatment could have influence on the levels of antibodies in study subjects.

More interestingly, it was observed within this work, that both total and filarial-specific IgA was elevated in EN normals compared to MF- and MF+. This is in line with a study in India, where a similar trend was observed [107]. Furthermore, IgA has been shown to be protective in mice lacking poly-immunoglobulin receptor in *Giardia* infection [213]. Field studies in Sudan also showed elevated concentration of IgA was observed in sera from patients with *O. volvulus* infection [214]. Whilst the role of IgA awaits to be delineated, it seems to be associated with the clearance of the parasites, an area which warrants further investigation in filarial infections. The mechanism underlying increased IgA in EN groups is not clear, but appears to promote protection against filarial infection. This finding was unexpected, because TGF-β has been shown to enhance switching of IgA in human B cells, in association with Tregs [215], and thus defining the role of IgA in human filarial infections may require further studies.

4.12 Conclusion

The current study aimed to assess the impact of *W. bancrofti* and *O. volvulus* parasites on the host immune response and specifically, to identify hitherto unknown components of the immune response that lead to a protective immune response, where MF are absent from peripheral blood or skin compared to immune response, which permits the development and circulation of

MF. To date, investigations into mechanisms of protective immunity and identification of vaccine candidates largely depend on the assessment of individual components; *i.e.* the effector function of a particular antibody, cell type or cytokine, or the ability of a recombinant antigen to prevent infection or reduce morbidity. On the host side and, in the simplest of accounts*,* activation of a protective immune response is under control of many cell types and surface markers/receptors, secreted cytokines and antibody responses. Therefore, a high through-put microarray and immunological approaches were used to measure immune responses from asymptomatic filarial infected (patent and latent) and uninfected individuals in a host-parasite relationship. In conclusion, while there was a huge overlap in the transcriptomics profile between MF+ and MF- individuals, the results also showed some disparity between patently and latently infected individuals. In particular, the gene expression and immunology of patently-infected individuals are characterised with a weaker and regulated responses (hypo-responsiveness), associated with the presence of circulating MF. This scenario was confirmed by the increased levels of IL-10, CLC/Gal-10, GZMB and IgG4, as well as elevated exhausted T cells markers (CTLA-4 and PD-1), which may provide an environment that, support the transmission stage of the parasite. In contrast, individuals with asymptomatic latent infection (a previously neglected cohort of patients) revealed potent genomic expression, cellular and antibody responses, hence may contribute to MF clearance. Such elevated transcriptomics profile and immune responses in the MF- group (characterised by elevated IL-4, IFN-γ, IL-17A, GZMA and IgE) may provide the key into elucidating alternative therapeutic treatments which would essentially block transmission and consequently eliminate the infection.

5 REFERENCES

1.   Simonsen, P.E., et al., *The Filariases.* 2014: p. 737-765.e5.
2.   Basáñez, M.-G., et al., *River Blindness: A Success Story under Threat?* PLoS Med, 2006. 3(9): p. e371.
3.   Ramaiah, K.D. and E.A. Ottesen, *Progress and impact of 13 years of the global programme to eliminate lymphatic filariasis on reducing the burden of filarial disease.* PLoS Negl Trop Dis, 2014. 8(11): p. e3319.
4.   Basanez, M.G., T.S. Churcher, and M.E. Grillet, *Onchocerca-Simulium interactions and the population and evolutionary biology of Onchocerca volvulus.* Adv Parasitol, 2009. 68: p. 263-313.
5.   Brattig, N.W., *Pathogenesis and host responses in human onchocerciasis: impact of Onchocerca filariae and Wolbachia endobacteria.* Microbes Infect, 2004. 6(1): p. 113-28.
6.   Kaiser, C., S.D. Pion, and M. Boussinesq, *Case-control studies on the relationship between onchocerciasis and epilepsy: systematic review and meta-analysis.* PLoS Negl Trop Dis, 2013. 7(3): p. e2147.
7.   Hotez, P.J. and A. Kamath, *Neglected Tropical Diseases in Sub-Saharan Africa: Review of Their Prevalence, Distribution, and Disease Burden.* PLoS Negl Trop Dis, 2009. 3(8): p. e412.
8.   Guderian, R.H., et al., *Onchocerciasis in Ecuador. III. Clinical manifestations of the disease in the province of Esmeraldas.* Trans R Soc Trop Med Hyg, 1984. 78(1): p. 81-5.
9.   Paily, K.P., S.L. Hoti, and P.K. Das, *A review of the complexity of biology of lymphatic filarial parasites.* J Parasit Dis, 2009. 33(1-2): p. 3-12.
10.   Lawrence, R.A., *Immunity to filarial nematodes.* Vet Parasitol, 2001. 100(1-2): p. 33-44.
11.   Maizels, R.M. and R.A. Lawrence, *Immunological tolerance: The key feature in human filariasis?* Parasitol Today, 1991. 7(10): p. 271-6.
12.   Cuenco, K.T., et al., *Heritable factors play a major role in determining host responses to Wuchereria bancrofti infection in an isolated South Pacific island population.* J Infect Dis, 2009. 200(8): p. 1271-8.
13.   Arndts, K., et al., *Elevated adaptive immune responses are associated with latent infections of Wuchereria bancrofti.* PLoS Negl Trop Dis, 2012. 6(4): p. e1611.
14.   Satapathy, A.K., et al., *Human Bancroftian filariasis: loss of patent microfilaraemia is not associated with production of antibodies to microfilarial sheath.* Parasite Immunol, 2001. 23(3): p. 163-7.
15.   Pfarr, K.M., et al., *Filariasis and lymphoedema.* Parasite Immunol, 2009. 31(11): p. 664-72.
16.   Doetze, A., et al., *Antigen-specific cellular hyporesponsiveness in a chronic human helminth infection is mediated by T(h)3/T(r)1-type cytokines IL-10 and transforming growth factor-beta but not by a T(h)1 to T(h)2 shift.* Int Immunol, 2000. 12(5): p. 623-30.
17.   Katawa, G., et al., *Hyperreactive Onchocerciasis is Characterized by a Combination of Th17-Th2 Immune Responses and Reduced Regulatory T Cells.* PLoS Negl Trop Dis, 2015. 9(1): p. e3414.
18.   Arndts, K., et al., *Immunoepidemiological profiling of onchocerciasis patients reveals associations with microfilaria loads and ivermectin intake on both individual and community levels.* PLoS Negl Trop Dis, 2014. 8(2): p. e2679.
19.   Pearlman, E. and I. Gillette-Ferguson, *Onchocerca volvulus, Wolbachia and river blindness.* Chem Immunol Allergy, 2007. 92: p. 254-65.
20.   Debrah, A.Y., et al., *Doxycycline reduces plasma VEGF-C/sVEGFR-3 and improves pathology in lymphatic filariasis.* PLoS Pathog, 2006. 2(9): p. e92.
21.   Brattig, N.W., et al., *Lipopolysaccharide-like molecules derived from Wolbachia endobacteria of the filaria Onchocerca volvulus are candidate mediators in the sequence of inflammatory and antiinflammatory responses of human monocytes.* Microbes Infect, 2000. 2(10): p. 1147-57.
22.   Suma, T.K., et al., *Estimation of ASO titer as an indicator of streptococcal infection precipitating acute adenolymphangitis in brugian lymphatic filariasis.* Southeast Asian J Trop Med Public Health, 1997. 28(4): p. 826-30.
23.   Dreyer, G., et al., *Acute attacks in the extremities of persons living in an area endemic for bancroftian filariasis: differentiation of two syndromes.* Trans R Soc Trop Med Hyg, 1999. 93(4): p. 413-7.

24.   Debrah, A.Y., et al., *Plasma vascular endothelial growth Factor-A (VEGF-A) and VEGF-A gene polymorphism are associated with hydrocele development in lymphatic filariasis.* Am J Trop Med Hyg, 2007. 77(4): p. 601-8.

25.   Murdoch, M.E., et al., *A clinical classification and grading system of the cutaneous changes in onchocerciasis.* Br J Dermatol, 1993. 129(3): p. 260-9.

26.   Weil, G.J., P.J. Lammie, and N. Weiss, *The ICT Filariasis Test: A rapid-format antigen test for diagnosis of bancroftian filariasis.* Parasitol Today, 1997. 13(10): p. 401-4.

27.   Rocha, A., et al., *Comparison of tests for the detection of circulating filarial antigen (Og4C3-ELISA and AD12-ICT) and ultrasound in diagnosis of lymphatic filariasis in individuals with microfilariae.* Mem Inst Oswaldo Cruz, 2009. 104(4): p. 621-5.

28.   Turner, P., et al., *A comparison of the Og4C3 antigen capture ELISA, the Knott test, an IgG4 assay and clinical signs, in the diagnosis of Bancroftian filariasis.* Trop Med Parasitol, 1993. 44(1): p. 45-8.

29.   Dreyer, G., et al., *Ultrasonographic evidence for stability of adult worm location in bancroftian filariasis.* Trans R Soc Trop Med Hyg, 1994. 88(5): p. 558.

30.   Mand, S., et al., *Animated documentation of the filaria dance sign (FDS) in bancroftian filariasis.* Filaria J, 2003. 2(1): p. 3.

31.   Mand, S., et al., *The role of ultrasonography in the differentiation of the various types of filaricele due to bancroftian filariasis.* Acta Trop, 2011. 120 Suppl 1: p. S23-32.

32.   Pilotte, N., et al., *A TaqMan-based multiplex real-time PCR assay for the simultaneous detection of Wuchereria bancrofti and Brugia malayi.* Mol Biochem Parasitol, 2013. 189(1-2): p. 33-7.

33.   Nutting, C.S., et al., *Analysis of nematode motion using an improved light-scatter based system.* PLoS Negl Trop Dis, 2015. 9(2): p. e0003523.

34.   Ozoh, G., et al., *Evaluation of the diethylcarbamazine patch to evaluate onchocerciasis endemicity in Central Africa.* Trop Med Int Health, 2007. 12(1): p. 123-9.

35.   Kilian, H.D., *The use of a topical Mazzotti test in the diagnosis of onchocerciasis.* Trop Med Parasitol, 1988. 39(3): p. 235-8.

36.   Fischer, P., et al., *Strain differentiation of Onchocerca volvulus from Uganda using DNA probes.* Parasitology, 1996. 112 (Pt 4): p. 401-408.

37.   Casiraghi, M., et al., *A phylogenetic analysis of filarial nematodes: comparison with the phylogeny of Wolbachia endosymbionts.* Parasitology, 2001. 122 Pt 1: p. 93-103.

38.   Werren, J.H., L. Baldo, and M.E. Clark, *Wolbachia: master manipulators of invertebrate biology.* Nat Rev Microbiol, 2008. 6(10): p. 741-51.

39.   Hoerauf, A., et al., *Doxycycline in the treatment of human onchocerciasis: Kinetics of Wolbachia endobacteria reduction and of inhibition of embryogenesis in female Onchocerca worms.* Microbes Infect, 2003. 5(4): p. 261-73.

40.   Kozek, W.J., *Transovarially-transmitted intracellular microorganisms in adult and larval stages of Brugia malayi.* J Parasitol, 1977. 63(6): p. 992-1000.

41.   Taylor, M.J., et al., *16S rDNA phylogeny and ultrastructural characterization of Wolbachia intracellular bacteria of the filarial nematodes Brugia malayi, B. pahangi, and Wuchereria bancrofti.* Exp Parasitol, 1999. 91(4): p. 356-61.

42.   Tamarozzi, F., et al., *Onchocerciasis: the role of Wolbachia bacterial endosymbionts in parasite biology, disease pathogenesis, and treatment.* Clin Microbiol Rev, 2011. 24(3): p. 459-68.

43.   Saint Andre, A., et al., *The role of endosymbiotic Wolbachia bacteria in the pathogenesis of river blindness.* Science, 2002. 295(5561): p. 1892-5.

44.   Taylor, M.J. and A. Hoerauf, *A new approach to the treatment of filariasis.* Curr Opin Infect Dis, 2001. 14(6): p. 727-31.

45.   Geary, T.G. and Y. Moreno, *Macrocyclic lactone anthelmintics: spectrum of activity and mechanism of action.* Curr Pharm Biotechnol, 2012. 13(6): p. 866-72.

46.   Rao, U.R., R. Chandrashekar, and D. Subrahmanyam, *Effect of ivermectin on serum dependent cellular interactions to Dipetalonema viteae microfilariae.* Trop Med Parasitol, 1987. 38(2): p. 123-7.

47.   Horton, J., *Albendazole: a review of anthelmintic efficacy and safety in humans.* Parasitology, 2000. 121 Suppl: p. S113-32.

48.   Addiss, D., et al., *Albendazole for lymphatic filariasis.* Cochrane Database Syst Rev, 2004(1): p. CD003753.

49.   Geary, T.G., et al., *Unresolved issues in anthelmintic pharmacology for helminthiases of humans.* Int J Parasitol, 2010. 40(1): p. 1-13.

50.   Taylor, M.J., A. Hoerauf, and M. Bockarie, *Lymphatic filariasis and onchocerciasis.* Lancet, 2010. 376(9747): p. 1175-85.

51.   Fernando, S.D., C. Rodrigo, and S. Rajapakse, *Current evidence on the use of antifilarial agents in the management of bancroftian filariasis.* J Trop Med, 2011. 2011: p. 175941.

52.   Osei-Atweneboana, M.Y., et al., *Prevalence and intensity of Onchocerca volvulus infection and efficacy of ivermectin in endemic communities in Ghana: a two-phase epidemiological study.* Lancet, 2007. 369(9578): p. 2021-9.

53.   Hoerauf, A., et al., *Doxycycline as a novel strategy against bancroftian filariasis-depletion of Wolbachia endosymbionts from Wuchereria bancrofti and stop of microfilaria production.* Med Microbiol Immunol, 2003. 192(4): p. 211-6.

54.   Hoerauf, A., et al., *Wolbachia endobacteria depletion by doxycycline as antifilarial therapy has macrofilaricidal activity in onchocerciasis: a randomized placebo-controlled study.* Med Microbiol Immunol, 2008. 197(3): p. 295-311.

55.   Specht, S., et al., *Efficacy of 2- and 4-week rifampicin treatment on the Wolbachia of Onchocerca volvulus.* Parasitol Res, 2008. 103(6): p. 1303-9.

56.   Mand, S., et al., *Doxycycline improves filarial lymphedema independent of active filarial infection: a randomized controlled trial.* Clin Infect Dis, 2012. 55(5): p. 621-30.

57.   Hoerauf, A., et al., *Filariasis in Africa--treatment challenges and prospects.* Clin Microbiol Infect, 2011. 17(7): p. 977-85.

58.   Hoerauf, A., *Filariasis: new drugs and new opportunities for lymphatic filariasis and onchocerciasis.* Curr Opin Infect Dis, 2008. 21(6): p. 673-81.

59.   Osei-Atweneboana, M.Y., et al., *Phenotypic evidence of emerging ivermectin resistance in Onchocerca volvulus.* PLoS Negl Trop Dis, 2011. 5(3): p. e998.

60.   Serruto, D. and R. Rappuoli, *Post-genomic vaccine development.* FEBS Lett, 2006. 580(12): p. 2985-92.

61.   Turner, J.D., et al., *Wolbachia lipoprotein stimulates innate and adaptive immunity through Toll-like receptors 2 and 6 to induce disease manifestations of filariasis.* J Biol Chem, 2009. 284(33): p. 22364-78.

62.   Babu, S., V. Kumaraswami, and T.B. Nutman, *Alternatively activated and immunoregulatory monocytes in human filarial infections.* J Infect Dis, 2009. 199(12): p. 1827-37.

63.   Hansen, R.D., et al., *A worm's best friend: recruitment of neutrophils by Wolbachia confounds eosinophil degranulation against the filarial nematode Onchocerca ochengi.* Proc Biol Sci, 2011. 278(1716): p. 2293-302.

64.   Capron, M., et al., *Eosinophil-dependent cytotoxicity in rat schistosomiasis. Involvement of IgG2a antibody and role of mast cells.* Eur J Immunol, 1978. 8(2): p. 127-33.

65.   Specht, S., et al., *Lack of eosinophil peroxidase or major basic protein impairs defense against murine filarial infection.* Infect Immun, 2006. 74(9): p. 5236-43.

66.   Babayan, S.A., et al., *Filarial parasites develop faster and reproduce earlier in response to host immune effectors that determine filarial life expectancy.* PLoS Biol, 2010. 8(10): p. e1000525.

67.   Liu, F.T., R.J. Patterson, and J.L. Wang, *Intracellular functions of galectins.* Biochim Biophys Acta, 2002. 1572(2-3): p. 263-73.

68.   Yang, R.Y., G.A. Rabinovich, and F.T. Liu, *Galectins: structure, function and therapeutic potential.* Expert Rev Mol Med, 2008. 10: p. e17.

69.   Kubach, J., et al., *Human CD4+CD25+ regulatory T cells: proteome analysis identifies galectin-10 as a novel marker essential for their anergy and suppressive function.* Blood, 2007. 110(5): p. 1550-8.

70.   Wildenburg, G., M. Kromer, and D.W. Buttner, *Dependence of eosinophil granulocyte infiltration into nodules on the presence of microfilariae producing Onchocerca volvulus.* Parasitol Res, 1996. 82(2): p. 117-24.

71.   Korten, S., et al., *Mast cells in onchocercomas from patients with hyperreactive onchocerciasis (sowda).* Acta Trop, 1998. 70(2): p. 217-31.

72.   Al-Qaoud, K.M., et al., *A new mechanism for IL-5-dependent helminth control: neutrophil accumulation and neutrophil-mediated worm encapsulation in murine filariasis are abolished in the absence of IL-5.* Int Immunol, 2000. 12(6): p. 899-908.

73.   Torrero, M.N., et al., *Basophils amplify type 2 immune responses, but do not serve a protective role, during chronic infection of mice with the filarial nematode Litomosoides sigmodontis.* J Immunol, 2010. 185(12): p. 7426-34.

74.   Kara, E.E., et al., *Tailored immune responses: novel effector helper T cell subsets in protective immunity.* PLoS Pathog, 2014. 10(2): p. e1003905.

75.   Semnani, R.T. and T.B. Nutman, *Toward an understanding of the interaction between filarial parasites and host antigen-presenting cells.* Immunol Rev, 2004. 201: p. 127-38.

76.   King, C.L. and T.B. Nutman, *Regulation of the immune response in lymphatic filariasis and onchocerciasis.* Immunol Today, 1991. 12(3): p. A54-8.

77.   Mahanty, S., et al., *High levels of spontaneous and parasite antigen-driven interleukin-10 production are associated with antigen-specific hyporesponsiveness in human lymphatic filariasis.* J Infect Dis, 1996. 173(3): p. 769-73.

78.   Mitre, E., D. Chien, and T.B. Nutman, *CD4(+) (and not CD25+) T cells are the predominant interleukin-10-producing cells in the circulation of filaria-infected patients.* J Infect Dis, 2008. 197(1): p. 94-101.

79.   Korten, S., et al., *Low levels of transforming growth factor-beta (TGF-beta) and reduced suppression of Th2-mediated inflammation in hyperreactive human onchocerciasis.* Parasitology, 2011. 138(1): p. 35-45.

80.   Mai, C.S., et al., *Onchocerca volvulus-specific antibody and cytokine responses in onchocerciasis patients after 16 years of repeated ivermectin therapy.* Clin Exp Immunol, 2007. 147(3): p. 504-12.

81.   Babu, S. and T.B. Nutman, *Immunopathogenesis of lymphatic filarial disease.* Semin Immunopathol, 2012. 34(6): p. 847-61.

82.   Babu, S., et al., *Filarial lymphedema is characterized by antigen-specific Th1 and th17 proinflammatory responses and a lack of regulatory T cells.* PLoS Negl Trop Dis, 2009. 3(4): p. e420.

83.   Brattig, N.W., et al., *The major surface protein of Wolbachia endosymbionts in filarial nematodes elicits immune responses through TLR2 and TLR4.* J Immunol, 2004. 173(1): p. 437-45.

84.   Debrah, A.Y., et al., *Reduction in levels of plasma vascular endothelial growth factor-A and improvement in hydrocele patients by targeting endosymbiotic Wolbachia sp. in Wuchereria bancrofti with doxycycline.* Am J Trop Med Hyg, 2009. 80(6): p. 956-63.

85.   Hoerauf, A., et al., *Immunomodulation by filarial nematodes.* Parasite Immunol, 2005. 27(10-11): p. 417-29.

86.   Taylor, M.D., N. van der Werf, and R.M. Maizels, *T cells in helminth infection: the regulators and the regulated.* Trends Immunol, 2012. 33(4): p. 181-9.

87.   Satoguina, J.S., et al., *T regulatory-1 cells induce IgG4 production by B cells: role of IL-10.* J Immunol, 2005. 174(8): p. 4718-26.

88.   Satoguina, J.S., et al., *Tr1 and naturally occurring regulatory T cells induce IgG4 in B cells through GITR/GITR-L interaction, IL-10 and TGF-beta.* Eur J Immunol, 2008. 38(11): p. 3101-13.

89.   Adjobimey, T. and A. Hoerauf, *Induction of immunoglobulin G4 in human filariasis: an indicator of immunoregulation.* Ann Trop Med Parasitol, 2010. 104(6): p. 455-64.

90.   Korten, S., et al., *Transforming growth factor-beta expression by host cells is elicited locally by the filarial nematode Onchocerca volvulus in hyporeactive patients independently from Wolbachia.* Microbes Infect, 2010. 12(7): p. 555-64.

91.   Bovenschen, N. and J.A. Kummer, *Orphan granzymes find a home.* Immunol Rev, 2010. 235(1): p. 117-27.

92.   Wensink, A.C., C.E. Hack, and N. Bovenschen, *Granzymes regulate proinflammatory cytokine responses.* J Immunol, 2015. 194(2): p. 491-7.

93.   Kim, W.J., et al., *Macrophages express granzyme B in the lesion areas of atherosclerosis and rheumatoid arthritis.* Immunol Lett, 2007. 111(1): p. 57-65.

94.   Cao, X., et al., *Granzyme B and perforin are important for regulatory T cell-mediated suppression of tumor clearance.* Immunity, 2007. 27(4): p. 635-46.

95.   Salti, S.M., et al., *Granzyme B regulates antiviral CD8+ T cell responses.* J Immunol, 2011. 187(12): p. 6301-9.

96.   Hartmann, W., et al., *A novel and divergent role of granzyme A and B in resistance to helminth infection.* J Immunol, 2011. 186(4): p. 2472-81.

97.   Jordan, K.A. and C.A. Hunter, *Regulation of CD8+ T cell responses to infection with parasitic protozoa.* Exp Parasitol, 2010. 126(3): p. 318-25.

98.   Lal, R.B., et al., *Lymphocyte subpopulations in Bancroftian filariasis: activated (DR+) CD8+ T cells in patients with chronic lymphatic obstruction.* Clin Exp Immunol, 1989. 77(1): p. 77-82.

99.   Freedman, D.O., et al., *Predominant CD8+ infiltrate in limb biopsies of individuals with filarial lymphedema and elephantiasis.* Am J Trop Med Hyg, 1995. 53(6): p. 633-8.

100.   Shin, H. and E.J. Wherry, *CD8 T cell dysfunction during chronic viral infection.* Curr Opin Immunol, 2007. 19(4): p. 408-15.

101.   Wherry, E.J., et al., *Molecular signature of CD8+ T cell exhaustion during chronic viral infection.* Immunity, 2007. 27(4): p. 670-84.

102.   Loffredo-Verde, E., et al., *Schistosome infection aggravates HCV-related liver disease and induces changes in the regulatory T-cell phenotype.* Parasite Immunol, 2015. 37(2): p. 97-104.

103.   Maizels, R.M. and M. Yazdanbakhsh, *Immune Regulation by helminth parasites: cellular and molecular mechanisms.* Nature Reviews Immunology, 2003. 3(9): p. 733-744.

104.   Korten, S., et al., *Natural death of adult Onchocerca volvulus and filaricidal effects of doxycycline induce local FOXP3+/CD4+ regulatory T cells and granzyme expression.* Microbes Infect, 2008. 10(3): p. 313-24.

105.   Hussain, R., M. Grogl, and E.A. Ottesen, *IgG antibody subclasses in human filariasis. Differential subclass recognition of parasite antigens correlates with different clinical manifestations of infection.* J Immunol, 1987. 139(8): p. 2794-8.

106.   Steel, C., A. Guinea, and E.A. Ottesen, *Evidence for protective immunity to bancroftian filariasis in the Cook Islands.* J Infect Dis, 1996. 174(3): p. 598-605.

107.   Sahu, B.R., et al., *Protective immunity in human filariasis: a role for parasite-specific IgA responses.* J Infect Dis, 2008. 198(3): p. 434-43.

108.   Maizels, R.M., et al., *Regulation of pathogenesis and immunity in helminth infections.* J Exp Med, 2009. 206(10): p. 2059-66.

109.   Wammes, L.J., et al., *Regulatory T cells in human lymphatic filariasis: stronger functional activity in microfilaremics.* PLoS Negl Trop Dis, 2012. 6(5): p. e1655.

110.   Allen, J.E., R.A. Lawrence, and R.M. Maizels, *APC from mice harbouring the filarial nematode, Brugia malayi, prevent cellular proliferation but not cytokine production.* Int Immunol, 1996. 8(1): p. 143-51.

111.   Semnani, R.T., et al., *Inhibition of TLR3 and TLR4 function and expression in human dendritic cells by helminth parasites.* Blood, 2008. 112(4): p. 1290-8.

112.   Cooper, P.J., *Interactions between helminth parasites and allergy.* Curr Opin Allergy Clin Immunol, 2009. 9(1): p. 29-37.

113.   McKay, D.M., *The beneficial helminth parasite?* Parasitology, 2006. 132(Pt 1): p. 1-12.

114.   Metenou, S. and T.B. Nutman, *Regulatory T Cell Subsets in Filarial Infection and Their Function.* Front Immunol, 2013. 4: p. 305.

115.   Hoerauf, A., et al., *The variant Arg110Gln of human IL-13 is associated with an immunologically hyper-reactive form of onchocerciasis (sowda).* Microbes Infect, 2002. 4(1): p. 37-42.

116.   Debrah, A.Y., et al., *Transforming growth factor-beta1 variant Leu10Pro is associated with both lack of microfilariae and differential microfilarial loads in the blood of persons infected with lymphatic filariasis.* Hum Immunol, 2011. 72(11): p. 1143-8.

117.   Panda, A.K., et al., *Human lymphatic filariasis: genetic polymorphism of endothelin-1 and tumor necrosis factor receptor II correlates with development of chronic disease.* J Infect Dis, 2011. 204(2): p. 315-22.

118.   Bouma, G. and W. Strober, *The immunological and genetic basis of inflammatory bowel disease.* Nat Rev Immunol, 2003. 3(7): p. 521-33.

119.   Dreyer, G., J. Noroes, and J. Figueredo-Silva, *New insights into the natural history and pathology of bancroftian filariasis: implications for clinical management and filariasis control programmes.* Trans R Soc Trop Med Hyg, 2000. 94(6): p. 594-6.

120.   Pertea, M., *The human transcriptome: an unfinished story.* Genes (Basel), 2012. 3(3): p. 344-60.

121.   Maston, G.A., S.K. Evans, and M.R. Green, *Transcriptional regulatory elements in the human genome.* Annu Rev Genomics Hum Genet, 2006. 7: p. 29-59.

122.   Schoolnik, G.K., *Microarray analysis of bacterial pathogenicity.* Adv Microb Physiol, 2002. 46: p. 1-45.

123.   Slobedman, B. and A.K. Cheung, *Microarrays for the study of viral gene expression during human cytomegalovirus latent infection.* Methods Mol Med, 2008. 141: p. 153-75.

124.   Steel, C., S. Varma, and T.B. Nutman, *Regulation of global gene expression in human Loa loa infection is a function of chronicity.* PLoS Negl Trop Dis, 2012. 6(2): p. e1527.

125.   Dunyo, S.K., et al., *Lymphatic filariasis on the coast of Ghana.* Trans R Soc Trop Med Hyg, 1996. 90(6): p. 634-8.

126.   Duerr, H.P., G. Raddatz, and M. Eichner, *Diagnostic value of nodule palpation in onchocerciasis.* Trans R Soc Trop Med Hyg, 2008. 102(2): p. 148-54.

127.   Lin, S.M., et al., *Model-based variance-stabilizing transformation for Illumina microarray data.* Nucleic Acids Res, 2008. 36(2): p. e11.

128.   Pan, W., *A comparative review of statistical methods for discovering differentially expressed genes in replicated microarray experiments.* Bioinformatics, 2002. 18(4): p. 546-54.

129.   McCarthy, D.J. and G.K. Smyth, *Testing significance relative to a fold-change threshold is a TREAT.* Bioinformatics, 2009. 25(6): p. 765-71.

130.   Ramanathan, R., et al., *Microarray-based analysis of differential gene expression between infective and noninfective larvae of Strongyloides stercoralis.* PLoS Negl Trop Dis, 2011. 5(5): p. e1039.

131.   Adjobimey, T., et al., *Co-activation through TLR4 and TLR9 but not TLR2 skews Treg-mediated modulation of Igs and induces IL-17 secretion in Treg: B cell co-cultures.* Innate Immun, 2014. 20(1): p. 12-23.

132.   DeRisi, J., et al., *Use of a cDNA microarray to analyse gene expression patterns in human cancer.* Nat Genet, 1996. 14(4): p. 457-60.

133.   Schena, M., et al., *Parallel human genome analysis: microarray-based expression monitoring of 1000 genes.* Proc Natl Acad Sci U S A, 1996. 93(20): p. 10614-9.

134.   Ackerman, S.J., et al., *Charcot-Leyden crystal protein (galectin-10) is not a dual function galectin with lysophospholipase activity but binds a lysophospholipase inhibitor in a novel structural fashion.* J Biol Chem, 2002. 277(17): p. 14859-68.

135.   Pincus, S.H., A.M. DiNapoli, and W.R. Schooley, *Superoxide production by eosinophils: activation by histamine.* J Invest Dermatol, 1982. 79(1): p. 53-7.

136.   Geest, C.R., et al., *Tight control of MEK-ERK activation is essential in regulating proliferation, survival, and cytokine production of CD34+-derived neutrophil progenitors.* Blood, 2009. 114(16): p. 3402-12.

137.   Berry, M.P., et al., *An interferon-inducible neutrophil-driven blood transcriptional signature in human tuberculosis.* Nature, 2010. 466(7309): p. 973-7.

138.   Abraham, D., et al., *Immunoglobulin E and eosinophil-dependent protective immunity to larval Onchocerca volvulus in mice immunized with irradiated larvae.* Infect Immun, 2004. 72(2): p. 810-7.

139.   Baitsch, L., et al., *Exhaustion of tumor-specific CD8(+) T cells in metastases from melanoma patients.* J Clin Invest, 2011. 121(6): p. 2350-60.

140.   Burkett, M.W., et al., *A novel flow cytometric assay for evaluating cell-mediated cytotoxicity.* J Immunother, 2005. 28(4): p. 396-402.

141.   Stolk, W.A., C. Stone, and S.J. de Vlas, *Modelling lymphatic filariasis transmission and control: modelling frameworks, lessons learned and future directions.* Adv Parasitol, 2015. 87: p. 249-91.

142.   Hotez, P., *A handful of 'antipoverty' vaccines exist for neglected diseases, but the world's poorest billion people need more.* Health Aff (Millwood), 2011. 30(6): p. 1080-7.

143.   Morris, C.P., et al., *A comprehensive, model-based review of vaccine and repeat infection trials for filariasis.* Clin Microbiol Rev, 2013. 26(3): p. 381-421.

144.   Schallig, H.D., M.A. van Leeuwen, and A.W. Cornelissen, *Protective immunity induced by vaccination with two Haemonchus contortus excretory secretory proteins in sheep.* Parasite Immunol, 1997. 19(10): p. 447-53.

145.   Hotez, P.J., et al., *The Human Hookworm Vaccine.* Vaccine, 2013. 31 Suppl 2: p. B227-32.

146.   Altmann, C.R., et al., *Microarray-based analysis of early development in Xenopus laevis.* Dev Biol, 2001. 236(1): p. 64-75.

147.   Feezor, R.J., et al., *Whole blood and leukocyte RNA isolation for gene expression analyses.* Physiol Genomics, 2004. 19(3): p. 247-54.

148.   Liu, J., et al., *Effects of globin mRNA reduction methods on gene expression profiles from whole blood.* J Mol Diagn, 2006. 8(5): p. 551-8.

149.   Batliwalla, F.M., et al., *Microarray analyses of peripheral blood cells identifies unique gene expression signature in psoriatic arthritis.* Mol Med, 2005. 11(1-12): p. 21-9.

150.   He, G., et al., *The protein Zfand5 binds and stabilizes mRNAs with AU-rich elements in their 3'-untranslated regions.* J Biol Chem, 2012. 287(30): p. 24967-77.

151.   Petit, G., et al., *Maturation of the filaria Litomosoides sigmodontis in BALB/c mice; comparative susceptibility of nine other inbred strains.* Ann Parasitol Hum Comp, 1992. 67(5): p. 144-50.

152.   Le Goff, L., et al., *IL-4 is required to prevent filarial nematode development in resistant but not susceptible strains of mice.* Int J Parasitol, 2002. 32(10): p. 1277-84.

153.   Freedman, D.O., *Immune dynamics in the pathogenesis of human lymphatic filariasis.* Parasitol Today, 1998. 14(6): p. 229-34.

154.   Luster, A.D., R. Alon, and U.H. von Andrian, *Immune cell migration in inflammation: present and future therapeutic targets.* Nat Immunol, 2005. 6(12): p. 1182-90.

155.   Li, R.W. and L.C. Gasbarre, *A temporal shift in regulatory networks and pathways in the bovine small intestine during Cooperia oncophora infection.* Int J Parasitol, 2009. 39(7): p. 813-24.

156.   Hemsath, L., et al., *An electrostatic steering mechanism of Cdc42 recognition by Wiskott-Aldrich syndrome proteins.* Mol Cell, 2005. 20(2): p. 313-24.

157.   Lee, K., et al., *Cdc42 Promotes Host Defenses against Fatal Infection.* Infect Immun, 2013. 81(8): p. 2714-23.

158.   Cau, J. and A. Hall, *Cdc42 controls the polarity of the actin and microtubule cytoskeletons through two distinct signal transduction pathways.* J Cell Sci, 2005. 118(Pt 12): p. 2579-87.

159.   Schroeder, J.H., et al., *Live Brugia malayi microfilariae inhibit transendothelial migration of neutrophils and monocytes.* PLoS Negl Trop Dis, 2012. 6(11): p. e1914.

160.   Gibson, K.D., W.G. Laver, and A. Neuberger, *Initial stages in the biosynthesis of porphyrins. 2. The formation of delta-aminolaevulic acid from glycine and succinyl-coenzyme A by particles from chicken erythrocytes.* Biochem J, 1958. 70(1): p. 71-81.

161.   Shemin, D. and G. Kikuchi, *Enzymatic synthesis of sigma-aminolevulinic acid.* Ann N Y Acad Sci, 1958. 75(1): p. 122-8.

162.   Kumar, S. and U. Bandyopadhyay, *Free heme toxicity and its detoxification systems in human.* Toxicol Lett, 2005. 157(3): p. 175-88.

163.   Foster, J., et al., *The Wolbachia genome of Brugia malayi: endosymbiont evolution within a human pathogenic nematode.* PLoS Biol, 2005. 3(4): p. e121.

164.   Wu, B., et al., *The heme biosynthetic pathway of the obligate Wolbachia endosymbiont of Brugia malayi as a potential anti-filarial drug target.* PLoS Negl Trop Dis, 2009. 3(7): p. e475.

165.   Lentz, C.S., et al., *A selective inhibitor of heme biosynthesis in endosymbiotic bacteria elicits antifilarial activity in vitro.* Chem Biol, 2013. 20(2): p. 177-87.

166.   Desjardins, C.A., et al., *Genomics of Loa loa, a Wolbachia-free filarial parasite of humans.* Nat Genet, 2013. 45(5): p. 495-500.

167.   Nagaraj, V.A., et al., *Malaria parasite-synthesized heme is essential in the mosquito and liver stages and complements host heme in the blood stages of infection.* PLoS Pathog, 2013. 9(8): p. e1003522.

168.   Supuran, C.T., *Carbonic anhydrases: novel therapeutic applications for inhibitors and activators.* Nat Rev Drug Discov, 2008. 7(2): p. 168-81.

169.   Hawking, F. and J.B. Clark, *The periodicity of microfilariae. 13. Movements of Dipetalonema witei microfilariae in the lungs.* Trans R Soc Trop Med Hyg, 1967. 61(6): p. 817-26.

170.   Michael, E., et al., *Transmission intensity and the immunoepidemiology of bancroftian filariasis in East Africa.* Parasite Immunol, 2001. 23(7): p. 373-88.

171.   Simonsen, P.E., et al., *Bancroftian filariasis infection, disease, and specific antibody response patterns in a high and a low endemicity community in East Africa.* Am J Trop Med Hyg, 2002. 66(5): p. 550-9.

172.   Jorgenson, E., et al., *Ethnicity and human genetic linkage maps.* Am J Hum Genet, 2005. 76(2): p. 276-90.

173.   Tang, H., et al., *Genetic structure, self-identified race/ethnicity, and confounding in case-control association studies.* Am J Hum Genet, 2005. 76(2): p. 268-75.

174.   Ye, Q.S., et al., *Population genetics for six STR loci in the population from southern China.* J Forensic Sci, 2005. 50(3): p. 730-1.

175.   Gurish, M.F., et al., *CCR3 is required for tissue eosinophilia and larval cytotoxicity after infection with Trichinella spiralis.* J Immunol, 2002. 168(11): p. 5730-6.

176.   Bonecchi, R., et al., *Up-regulation of CCR1 and CCR3 and induction of chemotaxis to CC chemokines by IFN-gamma in human neutrophils.* J Immunol, 1999. 162(1): p. 474-9.

177.   Uguccioni, M., et al., *High expression of the chemokine receptor CCR3 in human blood basophils. Role in activation by eotaxin, MCP-4, and other chemokines.* J Clin Invest, 1997. 100(5): p. 1137-43.

178.   Gentil, K., et al., *Eotaxin-1 is involved in parasite clearance during chronic filarial infection.* Parasite Immunol, 2014. 36(2): p. 60-77.

179.   Ackerman, S.J., et al., *Eosinophilia and elevated serum levels of eosinophil major basic protein and Charcot-Leyden crystal protein (lysophospholipase) after treatment of patients with Bancroft's filariasis.* J Immunol, 1981. 127(3): p. 1093-8.

180.   Ackerman, S.J., et al., *Molecular cloning and characterization of human eosinophil Charcot-Leyden crystal protein (lysophospholipase). Similarities to IgE binding proteins and the S-type animal lectin superfamily.* J Immunol, 1993. 150(2): p. 456-68.

181.   Metenou, S., et al., *Patent Filarial Infection Modulates Malaria-Specific Type 1 Cytokine Responses in an IL-10-Dependent Manner in a Filaria/Malaria-Coinfected Population.* The Journal of Immunology, 2009. 183(2): p. 916-924.

182.   Kim, J.Y., et al., *Inhibition of dextran sulfate sodium (DSS)-induced intestinal inflammation via enhanced IL-10 and TGF-beta production by galectin-9 homologues isolated from intestinal parasites.* Mol Biochem Parasitol, 2010. 174(1): p. 53-61.

183.   Gandhi, M.K., et al., *Galectin-1 mediated suppression of Epstein-Barr virus specific T-cell immunity in classic Hodgkin lymphoma.* Blood, 2007. 110(4): p. 1326-9.

184.   Seki, M., et al., *Galectin-9 suppresses the generation of Th17, promotes the induction of regulatory T cells, and regulates experimental autoimmune arthritis.* Clin Immunol, 2008. 127(1): p. 78-88.

185.   Blois, S.M., et al., *A pivotal role for galectin-1 in fetomaternal tolerance.* Nat Med, 2007. 13(12): p. 1450-7.

186.   Afonina, I.S., S.P. Cullen, and S.J. Martin, *Cytotoxic and non-cytotoxic roles of the CTL/NK protease granzyme B.* Immunol Rev, 2010. 235(1): p. 105-16.

187.   Gondek, D.C., et al., *Cutting edge: contact-mediated suppression by CD4+CD25+ regulatory cells involves a granzyme B-dependent, perforin-independent mechanism.* J Immunol, 2005. 174(4): p. 1783-6.

188.   Bian, G., et al., *Granzyme B-mediated damage of CD8+ T cells impairs graft-versus-tumor effect.* J Immunol, 2013. 190(3): p. 1341-50.

189.   Irmler, M., et al., *Granzyme A is an interleukin 1 beta-converting enzyme.* J Exp Med, 1995. 181(5): p. 1917-22.

190.   Hendel, A., I. Hsu, and D.J. Granville, *Granzyme B releases vascular endothelial growth factor from extracellular matrix and induces vascular permeability.* Lab Invest, 2014. 94(7): p. 716-25.

191.   Hendel, A. and D.J. Granville, *Granzyme B cleavage of fibronectin disrupts endothelial cell adhesion, migration and capillary tube formation.* Matrix Biol, 2013. 32(1): p. 14-22.

192.   Anuradha, R., et al., *Interleukin-10- and transforming growth factor beta-independent regulation of CD8(+) T cells expressing type 1 and type 2 cytokines in human lymphatic filariasis.* Clin Vaccine Immunol, 2014. 21(12): p. 1620-7.

193.   Fernández Ruiz, D., et al., *Filarial infection induces protection against P. berghei liver stages in mice.* Microbes and Infection, 2009. 11(2): p. 172-180.

194.   Burgdorf, S., et al., *Distinct pathways of antigen uptake and intracellular routing in CD4 and CD8 T cell activation.* Science, 2007. 316(5824): p. 612-6.

195.   Zehner, M., et al., *The translocon protein Sec61 mediates antigen transport from endosomes in the cytosol for cross-presentation to CD8(+) T cells.* Immunity, 2015. 42(5): p. 850-63.

196.   Diaz, A. and J.E. Allen, *Mapping immune response profiles: the emerging scenario from helminth immunology.* Eur J Immunol, 2007. 37(12): p. 3319-26.

197.   Furze, R.C., F.J. Culley, and M.E. Selkirk, *Differential roles of the co-stimulatory molecules GITR and CTLA-4 in the immune response to Trichinella spiralis.* Microbes Infect, 2006. 8(12-13): p. 2803-10.
198.   Steel, C. and T.B. Nutman, *CTLA-4 in filarial infections: implications for a role in diminished T cell reactivity.* J Immunol, 2003. 170(4): p. 1930-8.
199.   Taylor, M.D., et al., *CTLA-4 and CD4+ CD25+ regulatory T cells inhibit protective immunity to filarial parasites in vivo.* J Immunol, 2007. 179(7): p. 4626-34.
200.   Taylor, M.D., et al., *Removal of regulatory T cell activity reverses hyporesponsiveness and leads to filarial parasite clearance in vivo.* J Immunol, 2005. 174: p. 4924-4933.
201.   Doetze, A., et al., *Antigen-specific cellular hyporesponsiveness in generalized onchocerciasis is mediated by Th3/Tr1- type cytokines IL-10 and TGF-beta but not by a Th1 to Th2 shift.* Int. Immunol., 2000. 12: p. 623-30.
202.   Satoguina, J., et al., *Antigen-specific T regulatory-1 cells are associated with immunosuppression in a chronic helminth infection (onchocerciasis).* Microbes Infect., 2002. 4(13): p. 1291-300.
203.   Babu, S., et al., *Regulatory T cells modulate Th17 responses in patients with positive tuberculin skin test results.* J Infect Dis, 2010. 201(1): p. 20-31.
204.   Barber, D.L., et al., *Restoring function in exhausted CD8 T cells during chronic viral infection.* Nature, 2006. 439(7077): p. 682-7.
205.   McKay, J.T., et al., *PD-1 suppresses protective immunity to Streptococcus pneumoniae through a B cell-intrinsic mechanism.* J Immunol, 2015. 194(5): p. 2289-99.
206.   Gros, A., et al., *PD-1 identifies the patient-specific CD8(+) tumor-reactive repertoire infiltrating human tumors.* J Clin Invest, 2014. 124(5): p. 2246-59.
207.   Jin, H.T., et al., *Cooperation of Tim-3 and PD-1 in CD8 T-cell exhaustion during chronic viral infection.* Proc Natl Acad Sci U S A, 2010. 107(33): p. 14733-8.
208.   Kwan-Lim, G.E., K.P. Forsyth, and R.M. Maizels, *Filarial-specific IgG4 response correlates with active Wuchereria bancrofti infection.* J Immunol, 1990. 145(12): p. 4298-305.
209.   Mohanty, M.C., et al., *Human bancroftian filariasis - a role for antibodies to parasite carbohydrates.* Clin Exp Immunol, 2001. 124(1): p. 54-61.
210.   Mpagi, J.L., et al., *Use of the recombinant Onchocerca volvulus protein Ov20/OvS1 for the immunodiagnostic differentiation between onchocerciasis and mansonelliasis and for the characterization of hyperreactive onchocerciasis (sowda).* Trop Med Int Health, 2000. 5(12): p. 891-7.
211.   Petersen, H.H., et al., *The effect of HIV on filarial-specific antibody response before and after treatment with diethylcarbamazine in Wuchereria bancrofti infected individuals.* Parasitol Int, 2009. 58(2): p. 141-4.
212.   Elefant, G.R., et al., *A serological follow-up of toxocariasis patients after chemotherapy based on the detection of IgG, IgA, and IgE antibodies by enzyme-linked immunosorbent assay.* J Clin Lab Anal, 2006. 20(4): p. 164-72.
213.   Davids, B.J., et al., *Polymeric immunoglobulin receptor in intestinal immune defense against the lumen-dwelling protozoan parasite Giardia.* J Immunol, 2006. 177(9): p. 6281-90.
214.   Williams, J.F., et al., *Onchocerciasis in Sudan: the Abu Hamed focus.* Trans R Soc Trop Med Hyg, 1985. 79(4): p. 464-8.
215.   van Vlasselaer, P., J. Punnonen, and J.E. de Vries, *Transforming growth factor-beta directs IgA switching in human B cells.* J Immunol, 1992. 148(7): p. 2062-7

6   APPENDICES
6.1   APPENDIX I: EQUIPMENTS

Instrument	Supplier
Analytical scale	Sartorius AG, Göttingen, Germany
Centrifuge (Eppendorf 5415 R)	Eppendorf AG, Hamburg, Germany
Centrifuge (Multifuge 4KR)	Heraeus Holding GmbH, Hanau, Germany
Counting chamber (Neubauer)	LO Laboroptik GmbH, Bad Homburg, Germany
ELISA plate reader	Molecular Devices, Sunnyvale, USA
DM-RD Fluorescence microscope	Leica, Wetzlar, Germany
FACSCanto flow cytometer™	Becton-Dickinson, Heidelberg , Germany
HumanHT-12 version 4 Expression Bead Chips	Illumina, San Diego, CA, USA
Incubator	Binder GmbH, Tuttlingen, Germany
Filter (Whatman Nucleopore, 5 μm)	Carl Roth, Karlsruhe, Germany
Freezer (-20°C)	Bosch GmbH, Stuttgart, Germany
Freezer (-80°C)	Heraeus Holding GmbH, Hanau, Germany
Fridge	Bosch GmbH, Stuttgart, Germany
Glass mortar	VWR, Langenfeld, Germany
Ice machine (Scotsman AF 80)	Gastro Handel GmbH, Wien, Austria
Microscope (Light)	Leica Microsystems GmbH, Wetzlar, Germany
Microscope (Light)	Zeiss, Germany
pH-meter	Mettler Toledo GmbH, Giessen, Germany
Pipet boy (pipetus®-akku)	Hirschmann Laborgeräte, Eberstadt, Germany
Punch (Holth corneoscleral punch 2mm)	Koch, Hamburg, Germany
Reflotron ® Plus	Roche Diagnostics, Mannheim, German
Sedgewick rafter chamber	VWR, Langenfeld, Germany
Tally Counter	Denominator, Connecticut, USA
Vortex mixer	IKA® GmbH & Co.KG, Staufen, Germany
Water bath	VWR, Langenfeld, Germany

6.2   APPENDIX II: CHEMICALS AND REAGENTS

Chemical	Supplier
Advanced Protein Assay™	Cytoskeleton, Inc., Denver, USA
Coomassie blue G	Cytoskeleton, Inc., Denver, USA
Dimethyl sulfoxide (DMSO)	Sigma-Aldrich GmbH, Munich, Germany
Disodium hydrogen phosphate (Na2HPO4)	Sigma-Aldrich GmbH, Munich, Germany
Giemsa	Merck KGAA, Darmstadt, Germany
Gentamicin	PAA Laboratories GmbH, Pasching, Austria
L-glutamine	PAA Laboratories GmbH, Pasching, Austria
Hydrochloric acid (HCl)	Merck KGAA, Darmstadt, Germany
Methanol	Merck KGAA, Darmstadt, Germany
May-Grünwald	Carl Roth, Karlsruhe, Germany
Paraformaldehyde	Merck KGAA, Darmstadt, Germany
Penicillin /Streptomycin 100 ml	PAA Laboratories GmbH, Pasching, Austria
Tween-20	Merck KGAA, Darmstadt, Germany
TMB	Sigma-Aldrich GmbH, Munich, Germany
Stop solution 2N H2SO4	Merck KGAA, Darmstadt, Germany
Streptavidin-Peroxidase (HRP)	eBioscience, Frankfurt, Germany

6.3   APPENDIX III: CONSUMABLES

Plastic and glass wares	Supplier
Cell culture plates 96 well	Greiner, Frickenhausen, Germany
Cover slip (24 x 32 mm)	Marienfeld, Lauda-Konigshofen, Germany
Cryo tubes (2 ml), Nunc	Nunc, Roskilde, Denmark
Eppendorf tubes (0.5,1.5, 2 ml)	Sarstedt, Germany
FACS tubes	BD Pharmingen, Germany
Falcon sterile centrifuge tubes (15 and 50 ml)	Greiner, Frickenhausen, Germany
Glass pipettes (3,10, 25,50 ml)	Greiner, Frickenhausen, Germany
Microscope slide (75 x 25 x 1mm)	Marienfeld, Lauda-Konigshofen, Germany
Parafilm	VWR, Langenfeld, Germany
Pasteur pipettes	Brand
Pipette tips (10 µl, 200 µl and 1000 µl)	Greiner, Frickenhausen, Germany
PAXgene™ blood RNA tube	PreAnalytiX, Switzerland

6.4   APPENDIX IV: BUFFER AND MEDIA

Buffer or media	Ingredient/Supplier
Bovine serum albumin (BSA)	PAA Laboratories GmbH, Pasching, Austria
Fetal calf serum (FCS)	PAA Laboratories GmbH, Pasching, Austria
Ficoll	Sigma-Aldrich GmbH, Munich, Germany
Leucosep tubes	Greiner Frickenhausen, Germany
Phosphate buffered saline (PBS)	PAA Laboratories GmbH, Pasching, Austria
Normal Rat serum	eBioscience, San Diego, USA
Roswell Park Memorial Institute (RPMI 1640)	PAA Laboratories GmbH, Pasching, Austria
Trypan Blue	Sigma-Aldrich GmbH, Munich, Germany

6.5   APPENDIX V: ELISA KITS

Commercially available kits and Reagents	Supplier
BinaxNow® Filariasis	Alere, Sinnamon Park, Australia
ELISA kit Charcot Leyden Crystal (Human)	Cloud clone Corp, Huston, USA
ELISA kits Ready-SET-Go	eBioscience, San Diego, USA
Cell Fixation/Permealibization Kits for Intracellular Cytokine Analysis	eBioscience, San Diego, USA
Concentrate and Diluent, Permealibization Buffer (10X)	eBioscience, San Diego, USA
Malaria test (Nadal® Malaria test 4species)	Nal von Minden, Moers, Germany
Monoclonal Igs (IgG1-4 and IgA)	Sigma-Aldrich GmbH, Munich, Germany
Monoclonal IgE	Southern Biotechnology, AL, USA
Pierce Limulus amoebocyte lysate (LAL) Chromogenic quantification kit (88282)	Thermo Fisher Scientific, Schwerte, Germany
Soluble CD8 high platinum ELISA kit (Human)	eBioscience, Frankfurt, Germany
Total Igs (IgA, IgM, IgE and IgG1-IgG4)	eBioscience, Frankfurt, Germany

6.6   APPENDIX VI: FACS STAINING ANTIBODIES

Antibody	Marker	Type (clone)	Supplier
αCD3/αCD28	microbeads		Invitrogen, Carlsbad, USA
CD4	APC	OKT-4	ImmunoTools, Friesoythe, Germany
CD4	PECy7	RPA-T4	eBioscience, San Diego, USA
CD8	APC	SK1	
CD8	PECy7	RPA-T8	eBioscience, San Diego, USA
CD25	PE	TB-30	ImmunoTools, Friesoythe, Germany
CD25	APC	HI25a	ImmunoTools, Friesoythe, Germany
CD69	APC	FN50	ImmunoTools, Friesoythe, Germany
CD107	FITC	eBioH4A3	eBioscience, San Diego, USA
CD244	APC	eBioDM244	eBioscience, San Diego, USA
CTLA-4	PE	I4D3	eBioscience, San Diego, USA
PD-1	FITC	MHA	eBioscience, San Diego, USA
IFN-γ	FITC	4S.B3	eBioscience, San Diego, USA
IL-4	APC	B-S4	eBioscience, San Diego, USA
IL-10	PE	JES3-9D7	eBioscience, San Diego, USA
IL-17A	PE	eBio64DEC17	eBioscience, San Diego, USA
IL-17A	FITC		eBioscience, San Diego, USA
T-bet	PE	eBio4B10	eBioscience, San Diego, USA
Eomes	FITC		eBioscience, San Diego, USA
GATA-3	PE	TWAJ	eBioscience, San Diego, USA
RORC2		AFKJS-9	eBioscience, San Diego, USA
FOXP3	FITC	236A/E7	eBioscience, San Diego, USA
Anti-human Galectin-10 (1° Ab)			R&D Systems, Minneapolis, USA
Donkey anti-goat Galectin-10 (2° Ab)	Fluorescein	F0109	R&D Systems, Minneapolis, USA
GZMA	FITC	BD Pharmingin 558905	R&D Systems, Abingdon Science Park, UK
GZMA	PeCy7	CB9	eBioscience, San Diego, USA
GZMB	PE	GB11	R&D Systems, Abingdon Science Park, UK

6.7   APENDIX VII: SOFTWARES

Program (Software)	Supplier
Adobe illustrator 6	Adobe Systems, New York, USA
BD FACSDiva software 3.0	BD™ Biosciences, Heidelberg, Germany
Bio-conductor	Seattle, WA, USA
Endnote 4	Thomson Reuters, Philadelphia, USA
Gene Expression Module (1.8.0)	Genome Studio, USA
Prism 5.02	GraphPad Software, Inc., La Jolla, USA
Ingenuity Pathway Analysis	IPA, Redwood City, USA
PrimoPDF	Nitro PDF, Software , Microsoft, USA
SoftMax Pro	Molecular Devices, Sunnyvale, USA
Diskus microscope software	Carls Hilger Technisches Buro Konigswinter, Germany

6.8   APPENDIX VIII: MEDIA AND SOLUTION

Fetal calf serum

FCS used to supplement medium
was heated for 30 minutes at 56°C
to inactivate the complement factors.
Aliquots were then stored at -20°C until
required.

Flow cytometry
FACS Buffer
1XPBS
1%FCS
Fixation Buffer
1%PBS
4% paraformaldehyde

Cell culture reagents
Complete medium
RPMI 1640
2 mM L-glutamine
50µg/ml penicillin/streptomycin
50µg/ml gentamicin

Cell culture medium
RPMI 1640
2 mM L-glutamine
50 µg/ml penicillin/streptomycin
50 µg/ml gentamicin
10% FCS

Freezing medium
80% FCS
20% Dimethyl sulfoxide (DMSO)

ELISA:
Coating solution
0.1 M NaHCO3, pH 9.6

Washing buffer
1x PBS
0.05% Tween 20

Blocking solution
1x PBS
1% BSA

Substrate buffer
0.1 M $NaH_2PO4.2H_2O$, pH 5.5

Substrate
3,3',5,5' Tetramethylbenzidine,
 dissolved to a concentration of
 6 mg/ml in DMSO.

Substrate solution
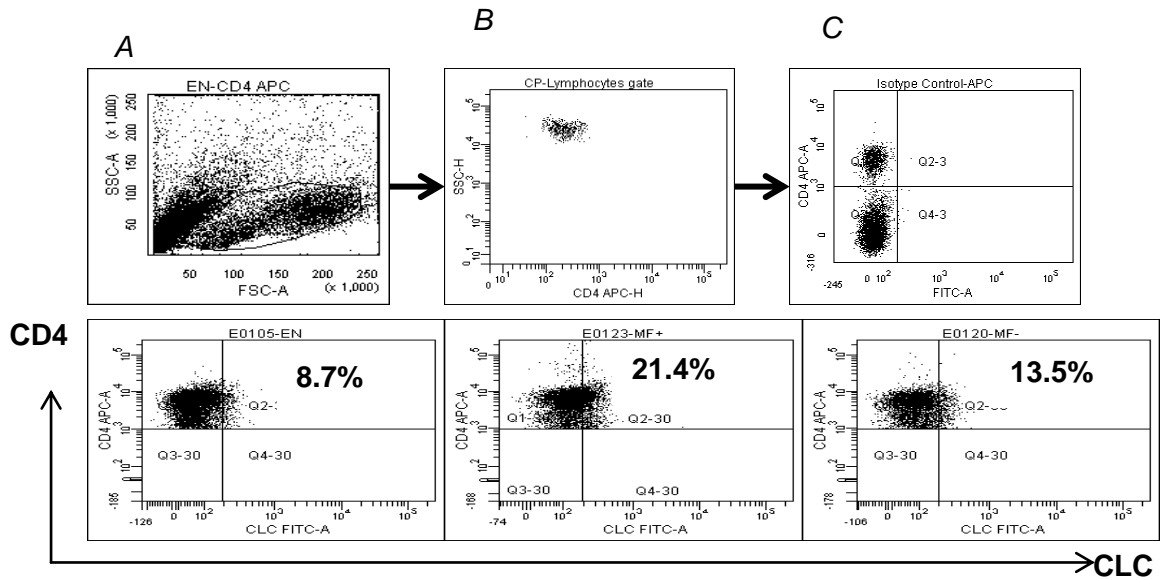12 ml substrate buffer
200 µl substrate
1.2 µl 30% H2O2

Stop solution
2N H_2SO4

6.9   Supplementary Data

Supplementary Figure 1: Increase frequencies of CD4$^+$ T cells expressing CLC in MF+ infected individuals.
Gating strategy *(A)* lymphocytes gate and *(B)* CD4$^+$ T cell gate from total lymphocytes (*C)* isotype control for FITC staining. Cells were stained with anti-CD4 APC antibody and CLC-FITC conjugated antibodies. A-C show gating strategy. The bottom dot plots show representative image for each study group. Flow cytometry was performed using a BD FACSCanto and analyzed using FACSDiva 5.2 software.
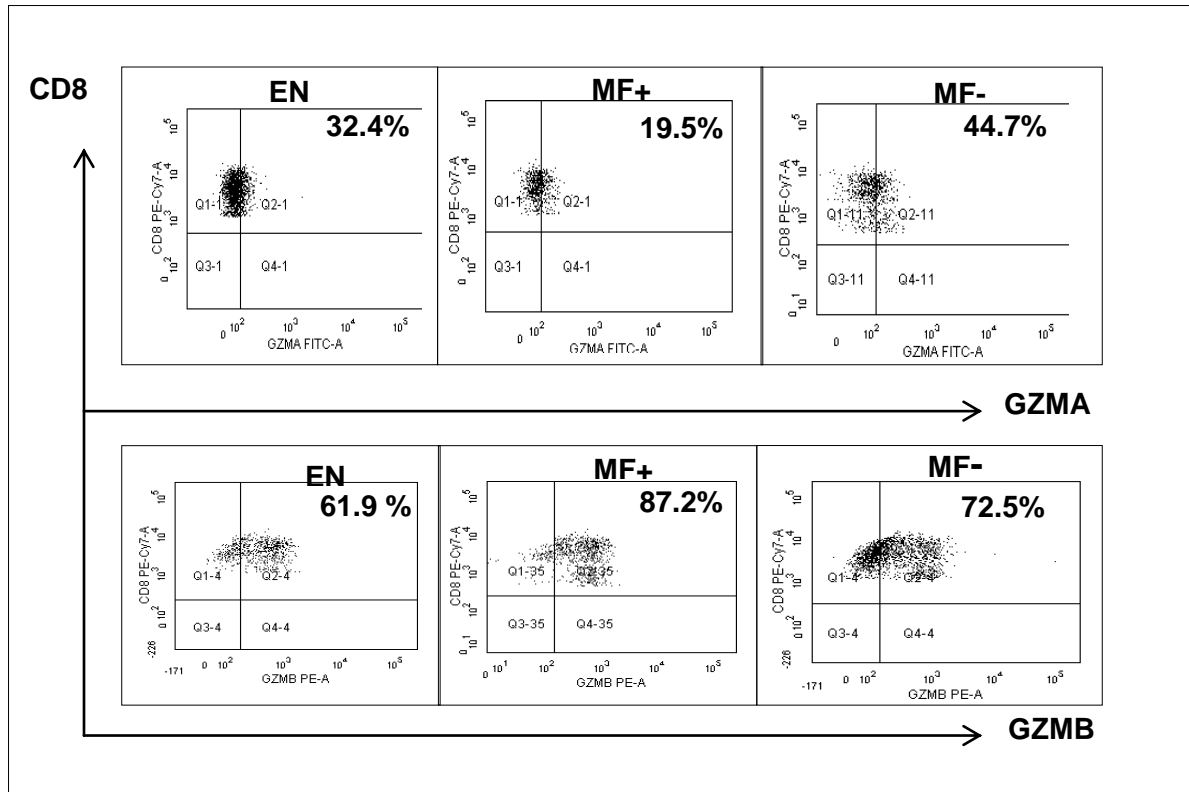
Supplementary Figure 2: Increased frequencies of CD8$^+$ T cells expressing GZMA in latent infected individuals, whilst GZMB was elevated in microfilaremic subjects.
PBMCs from study subjects were assessed with FACS. Cells were stained with anti-CD8 PeCy7 antibody and either GZMA-FITC or GZMB-PE conjugated antibodies. Each dot blot is a representative image showing the frequency of cells in subjects from the EN (left panel), MF+ (middle) and the MF- (right) groups. Flow cytometry was performed using a BD FACSCanto and analyzed using FACSDiva.

6.10 Supplementary Tables

Supplementary Table1: List of regulated genes in *W. bancrofti*-infected individuals vs EN

Group	Gene ID	Gene Description	FC	adj.*p*<0.05
Infected vs EN	CLC	Charcot-Leyden crystal protein	1.46	0.19
	HLA-DRB1	major histocompatibility complex, class II, DR beta 1	1.45	0.16
	RPS4Y1	ribosomal protein S4, Y-linked 1	1.44	0.22
	RNASE2	ribonuclease, RNase A family, 2 (liver, eosinophil-derived neurotoxin)	1.41	0.2
	ADD3	adducin 3 (gamma)	1.39	0.014
	ARGLU1	arginine and glutamate rich 1	1.39	0.024
	ZFAND5	zinc finger, AN1-type domain 5	1.37	0.024
	CAB39	calcium binding protein 39	1.36	0.024
	CTSZ	cathepsin Z	1.33	0.014
	ITGB1	integrin, beta 1 (fibronectin receptor, beta polypeptide, antigen CD29 includes MDF2, MSK12)	1.33	0.024
	DDX5	DEAD (Asp-Glu-Ala-Asp) box polypeptide 5	1.33	0.049
	TMEM66	transmembrane protein 66	1.32	0.036
	UBE2D3	ubiquitin-conjugating enzyme E2D 3 (UBC4/5 homolog, yeast)	1.31	0.024
	OGT	O-linked N-acetylglucosamine (GlcNAc) transferase (UDP-N-acetylglucosamine:polypeptide-N-acetylglucosaminyl transferase)	1.31	0.036
	ARPC3	actin related protein 2/3 complex, subunit 3, 21kDa	1.3	0.03
	RPL17	ribosomal protein L17	1.3	0.17
	NBPF10	neuroblastoma breakpoint family, member 10	1.3	0.18
	RPL17	ribosomal protein L17	1.3	0.19

Supplementary Table2: List of regulated genes in patent infected individuals vs EN

Group	Gene ID	Gene description	FC
Patent vs EN	RPS4Y1	ribosomal protein S4, Y-linked 1	1.73
	HLA-DRB1	major histocompatibility complex, class II, DR beta 1	1.49
	ARGLU1	arginine and glutamate rich 1	1.39
	NBPF10	neuroblastoma breakpoint family, member 10	1.39
	ADD3	adducin 3 (gamma)	1.38
	HLA-H	major histocompatibility complex, class I, H (pseudogene)	1.38
	ITGB1	integrin, beta 1 (fibronectin receptor, beta polypeptide, antigen CD29 includes MDF2, MSK12)	1.37
	ZFAND5	zinc finger, AN1-type domain 5	1.37
	CTSZ	cathepsin Z	1.36
	CAB39	calcium binding protein 39	1.34
	NBPF9	neuroblastoma breakpoint family, member 9	1.33
	STAT1	signal transducer and activator of transcription 1, 91kDa	1.32
	MATR3	matrin 3	1.3

	LOC100133678	similar to hCG2042724	1.3
	PI3	peptidase inhibitor 3, skin-derived	-1.31
	CDC34	cell division cycle 34 homolog (S. cerevisiae)	-1.33
	FAM46C	family with sequence similarity 46, member C	-1.34
	AHSP	alpha hemoglobin stabilizing protein	-1.35
	IFI27	interferon, alpha-inducible protein 27	-1.35
	EPB42	erythrocyte membrane protein band 4.2	-1.38
	BLVRB	biliverdin reductase B (flavin reductase (NADPH))	-1.39
	SELENBP1	selenium binding protein 1	-1.43
	CA1	carbonic anhydrase I	-1.45
	ALAS2	aminolevulinate, delta-, synthase 2	-1.48

Supplementary Table3: List of regulated genes in latent infected individuals vs EN

Group	Gene ID	Description	FC	adj.*p*<0.05
Latent vs EN	*CLC*	Charcot-Leyden crystal protein	1.58	0.11
	RNASE2	ribonuclease, RNase A family, 2 (liver, eosinophil-derived neurotoxin)	1.49	0.15
	HLA-DRB1	major histocompatibility complex, class II, DR beta 1	1.43	0.28
	ADD3	adducin 3 (gamma)	1.40	0.027
	ARGLU1	arginine and glutamate rich 1	1.39	0.034
	ZFAND5	zinc finger, AN1-type domain 5	1.37	0.032
	CAB39	calcium binding protein 39	1.37	0.034
	DDX5	DEAD (Asp-Glu-Ala-Asp) box polypeptide 5	1.36	0.063
	TMEM66	transmembrane protein 66	1.34	0.05
	OGT	O-linked N-acetylglucosamine (GlcNAc) transferase (UDP-N-acetylglucosamine:polypeptide-N-acetylglucosaminyl transferase)	1.33	0.051
	UBE2D3	ubiquitin-conjugating enzyme E2D 3 (UBC4/5 homolog, yeast)	1.32	0.031
	TMEM123	transmembrane protein 123	1.32	0.033
	ARPC3	actin related protein 2/3 complex, subunit 3, 21kDa	1.32	0.039
	CAT	catalase	1.32	0.076
	RPL17	ribosomal protein L17	1.32	0.21
	CTSZ	cathepsin Z	1.31	0.027
	CAT	catalase	1.31	0.034
	LOC729841	hypothetical LOC729841	1.31	0.034
	ITGB1	integrin, beta 1 (fibronectin receptor, beta polypeptide, antigen CD29 includes MDF2, MSK12)	1.31	0.045
	ATP6AP2	ATPase, H+ transporting, lysosomal accessory protein 2	1.31	0.051
	RPL17	ribosomal protein L17	1.30	0.25

Supplementary Table 4: List of regulated genes in Ahanta West samples vs Nzema East samples

Group	Gene ID	Gene Description	FC	adj.*p*<0.05
AW vs NE	*SNAPC1*	small nuclear RNA activating complex, polypeptide 1, 43kDa	1.46	0.041
	BLZF1	basic leucine zipper nuclear factor 1	1.45	0.029
	LOC100128510	hypothetical protein LOC100128510	1.44	0.023
	SEMA3E	sema domain, immunoglobulin domain (Ig), short basic domain, secreted, (semaphorin) 3E	1.44	0.026
	CHRNA5	cholinergic receptor, nicotinic, alpha 5	1.44	0.03
	C11orf63	chromosome 11 open reading frame 63	1.44	0.041
	LOC100130276	hypothetical protein LOC100130276	1.44	0.044
	PLIN5	perilipin 5	1.43	0.027
	FAM73A	family with sequence similarity 73, member A	1.42	0.024
	LMOD3	leiomodin 3 (fetal)	1.42	0.033
	GDPD1	glycerophosphodiester phosphodiesterase domain containing 1	1.42	0.035
	ZNF577	zinc finger protein 577	1.42	0.038
	RHBDL2	rhomboid, veinlet-like 2 (Drosophila)	1.42	0.041
	RNF213	ring finger protein 213	1.41	0.034
	PATE2	prostate and testis expressed 2	1.41	0.039
	LOC730060	hypothetical LOC730060	1.41	0.046
	ZNF557	zinc finger protein 557	1.41	0.052
	C6orf170	chromosome 6 open reading frame 170	1.41	0.056
	SLC5A8	solute carrier family 5 (iodide transporter), member 8	1.41	0.062
	QRFPR	pyroglutamylated RFamide peptide receptor	1.4	0.024
	LOC100131096	hypothetical LOC100131096	1.4	0.025
	PLDN	pallidin homolog (mouse)	1.4	0.032
	GPR1	G protein-coupled receptor 1	1.4	0.042
	PLA2G2D	phospholipase A2, group IID	1.4	0.045
	PCDHB9	protocadherin beta 9	1.4	0.048
	BMP8B	bone morphogenetic protein 8b	1.4	0.05
	TMEM106A	transmembrane protein 106A	1.4	0.052
	C7orf55	chromosome 7 open reading frame 55	1.4	0.057
	PTGR2	prostaglandin reductase 2	1.4	0.07
	TNFSF15	tumor necrosis factor (ligand) superfamily, member 15	1.4	0.074
	LOC100128460	similar to hCG1793472	1.4	0.087
	DOPEY2	dopey family member 2	1.39	0.015
	ZNF223	zinc finger protein 223	1.39	0.016
	HAUS2	HAUS augmin-like complex, subunit 2	1.39	0.017
	C4orf34	chromosome 4 open reading frame 34	1.39	0.017
	XRCC2	X-ray repair complementing defective repair in Chinese	1.39	0.019

		hamster cells 2		
	MBD4	methyl-CpG binding domain protein 4	1.39	0.024
	DENR	density-regulated protein	1.39	0.025
	LOC440704	hypothetical LOC440704	1.39	0.033
	FAM40B	family with sequence similarity 40, member B	1.39	0.035
	RAD51	RAD51 homolog (RecA homolog, E. coli) (S. cerevisiae)	1.39	0.038
	LOC100134868	hypothetical LOC100134868	1.39	0.04
	SSTR2	somatostatin receptor 2	1.39	0.045
	LOC100129269	hypothetical LOC100129269	1.39	0.046
	GCLM	glutamate-cysteine ligase, modifier subunit	1.39	0.056
	ADAM17	ADAM metallopeptidase domain 17	1.39	0.058
	TDRD1	tudor domain containing 1	1.39	0.058
	ZNF860	zinc finger protein 860	1.39	0.068
	PCYOX1	prenylcysteine oxidase 1	1.39	0.068
	MRP63	mitochondrial ribosomal protein 63	1.39	0.07
	LEP	leptin	1.39	0.073
	GSTTP2	glutathione S-transferase theta pseudogene 2	1.39	0.074
	C2orf56	chromosome 2 open reading frame 56	1.39	0.09
	SLC4A5	solute carrier family 4, sodium bicarbonate cotransporter, member 5	1.38	0.016
	LOC728903	hypothetical LOC728903	1.38	0.025
	LOC100132585	similar to speedy homolog A	1.38	0.028
	SLC35E1	solute carrier family 35, member E1	1.38	0.031
	EVI5	ecotropic viral integration site 5	1.38	0.032
	TDP1	tyrosyl-DNA phosphodiesterase 1	1.38	0.036
	EIF2AK4	eukaryotic translation initiation factor 2 alpha kinase 4	1.38	0.036
	VPS41	vacuolar protein sorting 41 homolog (S. cerevisiae)	1.38	0.038
	ICA1L	islet cell autoantigen 1,69kDa-like	1.38	0.039
	LOC391169	hCG2040210	1.38	0.044
	TRIM13	tripartite motif-containing 13	1.38	0.044
	LOC100128274	putative p150	1.38	0.053
	RASSF6	Ras association (RalGDS/AF-6) domain family member 6	1.38	0.064
	C14orf82	chromosome 14 open reading frame 82	1.38	0.085
	FAM175A	family with sequence similarity 175, member A	1.37	0.016
	RAX2	retina and anterior neural fold homeobox 2	1.37	0.026
	SHROOM4	shroom family member 4	1.37	0.031
	MBTD1	mbt domain containing 1	1.37	0.046
	TDRD1	tudor domain containing 1	1.37	0.049
	TNFSF14	tumor necrosis factor (ligand) superfamily, member 14	1.36	0.016

	ZNF682	zinc finger protein 682	1.36	0.018
	PTPLAD2	protein tyrosine phosphatase-like A domain containing 2	1.36	0.021
	GRIPAP1	GRIP1 associated protein 1	1.36	0.024
	KIAA1751	KIAA1751	1.36	0.027
	LOC100129502	hypothetical protein LOC100129502	1.36	0.03
	FAM153B	family with sequence similarity 153, member B	1.36	0.04
	CCBE1	collagen and calcium binding EGF domains 1	1.36	0.043
	ZNF320	zinc finger protein 320	1.36	0.053
	LOC100131541	hypothetical LOC100131541	1.36	0.057
	FAM63A	family with sequence similarity 63, member A	1.36	0.077
	MYO3B	myosin IIIB	1.36	0.088
	CES2	carboxylesterase 2 (intestine, liver)	1.36	0.094
	LOC100128288	hypothetical protein LOC100128288	1.35	0.024
	DEM1	defects in morphology 1 homolog (S. cerevisiae)	1.35	0.026
	LOC401098	hypothetical LOC401098	1.35	0.028
	TMEM156	transmembrane protein 156	1.35	0.036
	SYAP1	synapse associated protein 1	1.35	0.042
	ZNF626	zinc finger protein 626	1.35	0.074
			1.35	0.079
	LLPH	LLP homolog, long-term synaptic facilitation (Aplysia)	1.34	0.027
	ZNF786	zinc finger protein 786	1.34	0.034
	HNRNPU	heterogeneous nuclear ribonucleoprotein U (scaffold attachment factor A)	1.34	0.035
	BIRC3	baculoviral IAP repeat-containing 3	1.34	0.035
	DCLRE1C	DNA cross-link repair 1C	1.34	0.037
	ZNF483	zinc finger protein 483	1.34	0.046
	FCAR	Fc fragment of IgA, receptor for	1.34	0.051
	KLHL28	kelch-like 28 (Drosophila)	1.34	0.074
	C14orf153	chromosome 14 open reading frame 153	1.33	0.028
	MFSD11	major facilitator superfamily domain containing 11	1.33	0.045
	PPP2R3A	protein phosphatase 2, regulatory subunit B", alpha	1.33	0.071
	LOC100129055	cyclin Y-like pseudogene	1.33	0.076
	WDR74	WD repeat domain 74	1.33	0.087
	MAFF	v-maf musculoaponeurotic fibrosarcoma oncogene homolog F (avian)	1.33	0.1
	ZNF600	zinc finger protein 600	1.32	0.067
	AGPHD1	aminoglycoside phosphotransferase domain containing 1	1.32	0.068
	ATG10	ATG10 autophagy related 10 homolog (S. cerevisiae)	1.32	0.068
	HSCB	HscB iron-sulfur cluster co-chaperone homolog (E. coli)	1.32	0.11
	ZNF69	zinc finger protein 69	1.31	0.022

	CD68	CD68 molecule	1.31	0.022
	CREB1	cAMP responsive element binding protein 1	1.31	0.024
	C15orf63	chromosome 15 open reading frame 63	1.31	0.024
	CATSPER2	cation channel, sperm associated 2	1.31	0.026
	NLRP8	NLR family, pyrin domain containing 8	1.31	0.031
	USP49	ubiquitin specific peptidase 49	1.31	0.035
	CCDC125	coiled-coil domain containing 125	1.31	0.036
	UBXN2A	UBX domain protein 2A	1.31	0.042
	NUBPL	nucleotide binding protein-like	1.31	0.046
	PRRG4	proline rich Gla (G-carboxyglutamic acid) 4 (transmembrane)	1.31	0.048
	GALNT3	UDP-N-acetyl-alpha-D-galactosamine:polypeptide N-acetylgalactosaminyltransferase 3 (GalNAc-T3)	1.31	0.085
	FKBP14	FK506 binding protein 14, 22 kDa	1.3	0.025
	ZNF652	zinc finger protein 652	1.3	0.031
	LRRFIP1	leucine rich repeat (in FLII) interacting protein 1	1.3	0.031
	N4BP2	NEDD4 binding protein 2	1.3	0.039
	RUNDC2C	RUN domain containing 2C	1.3	0.086
	SPN	sialophorin	1.3	0.089
	LOC730202	hypothetical protein LOC730202	1.3	0.09
	LOC644949	hypothetical LOC644949	1.3	0.09
	IPP	intracisternal A particle-promoted polypeptide	1.3	0.096
	CGGBP1	CGG triplet repeat binding protein 1	-1.3	2.30E-05
	PIGY	phosphatidylinositol glycan anchor biosynthesis, class Y	-1.3	7.00E-05
	C6orf62	chromosome 6 open reading frame 62	-1.3	0.00026
	ROD1	ROD1 regulator of differentiation 1 (S. pombe)	-1.3	0.00027
	TGFBR2	transforming growth factor, beta receptor II (70/80kDa)	-1.3	0.00032
	ARHGEF3	Rho guanine nucleotide exchange factor (GEF) 3	-1.3	9.00E-04
	TGFBR2	transforming growth factor, beta receptor II (70/80kDa)	-1.3	0.00098
	MATR3	matrin 3	-1.3	0.0014
	RPL9	ribosomal protein L9	-1.3	0.025
	IFIT2	interferon-induced protein with tetratricopeptide repeats 2	-1.3	0.028
	RAB8B	RAB8B, member RAS oncogene family	-1.31	0.00018
	IFNGR1	interferon gamma receptor 1	-1.31	0.00022
	MAT2B	methionine adenosyltransferase II, beta	-1.31	0.00033
	RPL15	ribosomal protein L15	-1.31	0.00071
	GOLGA8B	golgin A8 family, member B	-1.31	0.00071
	XBP1	X-box binding protein 1	-1.31	0.001
	NSA2	NSA2 ribosome biogenesis homolog (S. cerevisiae)	-1.31	0.0022
	ATP6AP2	ATPase, H+ transporting, lysosomal accessory protein 2	-1.31	0.0026

SF3B1	splicing factor 3b, subunit 1, 155kDa	-1.32	1.90E-05
SET	SET nuclear oncogene	-1.32	0.00018
MS4A6A	membrane-spanning 4-domains, subfamily A, member 6A	-1.32	0.00018
CD44	CD44 molecule (Indian blood group)	-1.32	0.00023
MBNL1	muscleblind-like (Drosophila)	-1.32	0.00026
RPL5	ribosomal protein L5	-1.32	0.00028
PRKAR1A	protein kinase, cAMP-dependent, regulatory, type I, alpha (tissue specific extinguisher 1)	-1.32	0.00041
ROD1	ROD1 regulator of differentiation 1 (S. pombe)	-1.33	3.00E-04
FAM120A	family with sequence similarity 120A	-1.33	0.00032
PJA2	praja ring finger 2	-1.33	0.00037
YWHAQ	tyrosine 3-monooxygenase/tryptophan 5-monooxygenase activation protein, theta polypeptide	-1.33	8.00E-04
ITGB1	integrin, beta 1 (fibronectin receptor, beta polypeptide, antigen CD29 includes MDF2, MSK12)	-1.33	0.0012
ETS1	v-ets erythroblastosis virus E26 oncogene homolog 1 (avian)	-1.33	0.0014
GCA	grancalcin, EF-hand calcium binding protein	-1.33	0.011
PAIP2	poly(A) binding protein interacting protein 2	-1.34	1.90E-05
TRAM1	translocation associated membrane protein 1	-1.34	0.00097
RTN4	reticulon 4	-1.34	0.0011
RPS3A	ribosomal protein S3A	-1.34	0.0089
SUZ12	suppressor of zeste 12 homolog (Drosophila)	-1.35	0.00017
SRSF2	serine/arginine-rich splicing factor 2	-1.35	0.00019
ACTR2	ARP2 actin-related protein 2 homolog (yeast)	-1.35	0.00028
AP1S2	adaptor-related protein complex 1, sigma 2 subunit	-1.35	0.00055
MGEA5	meningioma expressed antigen 5 (hyaluronidase)	-1.35	0.0018
DDX5	DEAD (Asp-Glu-Ala-Asp) box polypeptide 5	-1.35	0.0054
TMEM123	transmembrane protein 123	-1.36	0.00023
RPS3A	ribosomal protein S3A	-1.36	0.013
PPP1CC	protein phosphatase 1, catalytic subunit, gamma isozyme	-1.37	0.00053
EIF4A2	eukaryotic translation initiation factor 4A2	-1.37	0.00062
ARL6IP5	ADP-ribosylation-like factor 6 interacting protein 5	-1.37	0.0012
CDC42SE2	CDC42 small effector 2	-1.38	9.60E-05
SELENBP1	selenoprotein	-1.38	0.00016
RAB10	RAB10, member RAS oncogene family	-1.38	0.00018
RPL17	ribosomal protein L17	-1.38	0.011
SRP9	signal recognition particle 9kDa	-1.39	4.90E-05
CHURC1	churchill domain containing 1	-1.39	0.00026

	Gene ID	Gene Description	FC	p-value
	ZFAND5	zinc finger, AN1-type domain 5	-1.39	0.00032
	AP1S2	adaptor-related protein complex 1, sigma 2 subunit	-1.39	0.00041
	PRKAR1A	protein kinase, cAMP-dependent, regulatory, type I, alpha (tissue specific extinguisher 1)	-1.4	1.90E-05
	RPL17	ribosomal protein L17	-1.4	0.0073
	UBE2D3	ubiquitin-conjugating enzyme E2D 3 (UBC4/5 homolog, yeast)	-1.41	1.90E-05
	TMEM66	transmembrane protein 66	-1.43	0.00018
	ADD3	adducin 3 (gamma)	-1.45	4.00E-05
	OGT	O-linked N-acetylglucosamine (GlcNAc) transferase (UDP-N-acetylglucosamine:polypeptide-N-acetylglucosaminyl transferase)	-1.45	6.40E-05
	CAB39	calcium binding protein 39	-1.46	6.40E-05
	ARGLU1	arginine and glutamate rich 1	-1.53	2.30E-05
	RPS4Y1	ribosomal protein S4, Y-linked 1	-1.54	0.022

Supplementary Table 5: List of regulated genes in *O. volvulus*-infected individuals vs EN

Group	Gene ID	Gene Description	FC
Infected (MF+ vs EN)	CLC	Charcot-Leyden crystal protein	1.89
	RNASE2	Ribonuclease, RNase A family, 2 (liver, eosinophil-derived neurotoxin)	1.68
	RPS4Y1	ribosomal protein S4, Y-linked 1	1.65
	DEFA1	defensin, alpha 1	1.55
	RNASE3	ribonuclease, RNase A family, 3	1.47
	CAT	catalase	1.40
	CCR3	chemokine (C-C motif) receptor 3	1.37
	CD24	CD24 molecule	1.36
	CAMP	cathelicidin antimicrobial peptide	1.34
	DEFB1	defensin, beta 1	1.33

ACKNOWLEDGEMENTS

I cannot quantify the emotional support from my parents, my dearest Efiba Vidda Senkyire Kwarteng, Phebe Adutwumwaa Senkyire Kwarteng, Sarah Yaa Adutwumwaa Kwarteng, Triscia Maame Ama Afihene and Trischelle Nana Ama Afihene and Doris Glenda Schmeer. Special thanks go to my friends Yarhands Dissou-Arthur, Alex Aboagye, Kenneth Fletcher and Samuel Terkper Ahuno for their morale support during my studies.